The Influence of Dislocations on Ultrasonic Waves in Single Crystals.

A thesis submitted to the University of London for the degree of Ph.D. by:

Clive Reed Scorey.

February, 1969.

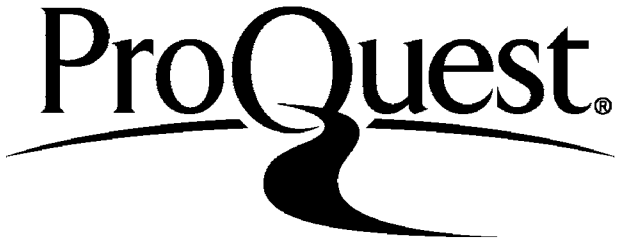

Abstract

Some properties of dislocations in aluminium and sodium chloride single crystals have been investigated by observing the generation of harmonics in an ultrasonic pulse travelling through a crystal. Pulses of 10 MHz longitudinal waves were generated at one end of a crystal with a quartz transducer and either 20 MHz or 30 MHz waves were detected at the opposite end of the crystal. The harmonic waves were detected either with a quartz transducer or a capacitative detector.

Experiments on the generation of second harmonics due to dislocations were carried out on aluminium crystals. No dislocation contribution to the second harmonic was detected in NaCl crystals, and this was attributed to a lack of purity in the crystals. However, experiments on third harmonic generation due to dislocations were performed on both aluminium and NaCl crystals. The amplitude of the third harmonics and the attenuation of the fundamental wave were measured as a function of impurity content, static bias stress, plastic deformation, temperature, the amplitude of the fundamental wave and, in the case of NaCl, X-irradiation also. The results of these experiments are compared with the behaviour predicted by the theory of Hikata and Elbaum (1966). Many of the results are found to be in good qualitative agreement with this theory.

During the course of some third harmonic measurements in NaCl evidence was found of internal stresses

remaining after plastic deformation. Compressive internal stresses were found after a plastic deformation in tension, and tensile internal stresses were found after further plastic deformation in compression.

A previously unreported time dependence of the second harmonic and third harmonic amplitudes was noted in some crystals after a bias stress was applied. Thermal activation energies associated with the time dependent behaviour were measured. Such measurements provide a useful method of studying strain-ageing properties in crystals.

Acknowledgements

The author wishes to express his sincere thanks to Dr. W. G. B. Britton for his continued guidance and encouragement during the course of this work.

He would also like to thank both Dr. E.L. James, under whose guidance this work was started, and Chelsea College of Science and Technology for the provision of a grant.

CONTENTS

CHAPTER 1.

Introduction

The anharmonicity of interatomic forces is a well known characteristic of all solids. One consequence of this anharmonicity is that a sinusoidal ultrasonic wave of given frequency distorts as it propagates so that the second, third and higher harmonics of the fundamental frequency are generated. Much of the recent interest in harmonic generation arises because it is possible to determine third order elastic constants from measurements of the amplitude of a second harmonic wave. In practice, the second harmonic wave is normally expected to have a much larger amplitude than the higher harmonics.

The generation of harmonics in an ultrasonic stress wave will take place even in a perfectly ordered lattice. However, in an imperfect lattice there may be a contribution to the harmonic generation from the imperfections themselves. The purpose of the present work is the study of harmonic generation due to dislocations in the lattice. This harmonic generation arises because the nonlinear nature of the stress-strain relation governing dislocation motion leads to an equation of particle motion in the lattice which does not permit a simple harmonic solution. Since both the lattice and dislocations give rise to harmonic generation, a way of separating these two contributions is needed before dislocation properties may be studied in terms of harmonic generation.

In the case of the second harmonic an external static stress is found to influence the dislocation contribution. The magnitude of the dislocation contribution to the second harmonic in fact increases as the rest position of a dislocation deviates further from the straight line configuration in a stress-free crystal. However, a theoretical analysis of second harmonic generation shows that in general it is difficult to separate the two contributions to the harmonic generation.

In the case of the third harmonic it is found that the lattice contribution may be sufficiently small to be negligible in comparison with the dislocation contribution. Thus dislocation properties are more easily studied in terms of third harmonics than second harmonics. The dislocation third harmonic amplitude is also sensitive to a static bias stress. However, this stress must be sufficient to cause changes in dislocation loop length rather than changes in the degree of bowing out of dislocations as for the second harmonic.

The procedure adopted in the present work was first to repeat some published measurements of second and third harmonic generation due to dislocations in aluminium single crystals. This was done primarily to check that the experimental set-up was functioning correctly. In fact these measurements not only confirmed many of the already published results, but also led to the discovery of hitherto unreported effects (see below). Secondly, experiments were performed using NaCl crystals. Detailed studies of dislocation harmonic generation had previously been reported in metallic crystals but not in ionic

crystals. NaCl was chosen because dislocation pinning points in the form of colour centres may easily be produced by X-irradiation. This provides a convenient way of studying dislocation-point defect interactions. A disadvantage of using NaCl was that crystals could not be obtained with the high purity possible with metal crystals. This meant that dislocation loop lengths were short in comparison with those possible in metal crystals.

Fundamental waves were observed which contained typically 1% of the second harmonic and 1/3% of the third harmonic. The experimental technique used for the observation of second and third harmonic generation was similar to that used by, for example, Hikata, Sewell and Elbaum (1966). This was a modification of the well known ultrasonic pulse-echo technique. An ultrasonic pulse was generated at one end of a crystal specimen using a quartz transducer. At the other end of the sample was either a second quartz transducer or a capacitative detector (see Section 4.40) with which the ultrasonic pulse could be monitored each time it was reflected at this end of the specimen. Using a filter and amplifying system the harmonic content of a pulse could be observed. Static bias stresses were normally applied to a specimen simply by attaching weights to one end of a specimen and suspending it from the other. A slight modification of this arrangement enabled compressive stresses to be applied instead.

An estimate of the relative purity of the aluminium single crystals used was obtained by measuring the ratio

of the electrical resistivity of the crystals at room temperature to that at 4.2°K, (see Section 5.1). These measurements also permitted a comparison of the purities of the crystals used in the present work with those of the crystals used by Hikata, Sewell and Elbaum (1966).

The results of the experiments with aluminium crystals were generally in good agreement with the measurements reported by Hikata, Chick and Elbaum (1965) and Hikata, Sewell and Elbaum (1966). Many of the results were also in agreement with the predictions of the Hikata and Elbaum (1966) theory of dislocation harmonic generation.

It has already been remarked that some previously unreported effects were also found. In particular, a time dependence of the second harmonic amplitude in an aluminium crystal after applying a static stress was found. A thermal activation energy has been calculated from measurements of this time dependence, and a model of dislocation-point defect behaviour is proposed to account for this. A rather similar time dependence was also found with the third harmonic amplitude in a sodium chloride crystal. A thermal activation energy was again determined and a model of dislocation-point defect behaviour proposed.

Some other measurements of the third harmonic in an NaCl crystal revealed the presence of internal stresses remaining after plastic deformation. Compressive internal stresses were found after a plastic deformation in tension, and tensile internal stresses after a plastic deformation

in compression. Internal stresses after plastic deformation have also been reported by Hikata, Chick and Elbaum (1965) in measurements of the second harmonic in an aluminium crystal. However, whereas these measurements in aluminium require the internal stresses to produce a bowing out of dislocations only, it is argued that the present measurements require an actual unpinning of dislocations by the internal stresses.

In Chapter 2 of this work a brief summary of lattice harmonic generation is given. Then, in Chapter 3, the theory of Hikata and Elbaum (1966) for dislocation harmonic generation is discussed in some detail. Chapters 4 and 5 are concerned with the experimental techniques and the preparation of the specimens used in this work. The experimental measurements which were made and an interpretation of the results are presented in Chapters 6,7,8 and 9. Finally, Chapter 10 contains a conclusion to the present work.

CHAPTER 2.

Harmonic Generation due to Lattice Anharmonicity

2.1. Theoretical Considerations

The purpose of the present work is to investigate the effect of dislocations on the generation of harmonics when an ultrasonic wave propagates in a crystal. However, the lattice itself also contributes to the harmonic generation and in the present chapter a brief discussion of the way in which this arises is given. This discussion is not detailed but is included so that the importance of lattice harmonic generation in relation to the dislocation harmonic generation discussed in succeeding chapters may be appreciated.

In a dissipationless solid for small displacements stress is a linear function of strain, i.e. Hooke's Law applies. In such a solid a sinusoidal stress wave of small amplitude may propagate without loss of energy or change in waveform. When large displacements are considered, the interatomic forces are such that stress is no longer linearly related to strain and linear elasticity theory no longer applies. In order to discover what effect this non-linearity has on a finite amplitude sinusoidal stress wave we consider the general equation of motion of a particle in a three dimensional configuration, following the treatment of Thurston and Shapiro (1967).

If x_i denotes the cartesian coordinates of a particle in the unstressed reference configuration and y_i the coordinates of the same particle in the stressed configuration, then the equation of particle motion may be written as

$$\rho_o \ddot{u}_r = \frac{\partial}{\partial x_p}\left[\frac{\partial y_r}{\partial x_q}\left(\frac{\partial U}{\partial \eta_{pq}}\right)_S\right], \qquad (2.1)$$

where u_i are the displacement components and η_{ij} the Lagrangian strain components, ρ_o is the mass density in the unstressed state, s is the entropy and U the internal energy per unit volume. Summation is understood to be carried out over repeated subscripts. When the configuration is stressed at constant entropy, the internal energy change (or strain energy) per unit of original unstressed volume can be expressed as

$$\Delta U = \tfrac{1}{2} c_{ijkm}\, \eta_{ij}\, \eta_{km} + 1/6 c_{ijkmpq}\, \eta_{ij}\, \eta_{km}\, \eta_{pq} + \ldots \qquad (2.2)$$

where c_{ijkm} and c_{ijkmpq} are respectively second and third order adiabatic elastic coefficients, in full tensor notation. [See Brugger (1964)]

Considering the special case of one dimensional motion in a solid, the equation of motion (2.1), reduces upon substitution of expression (2.2), to the form

$$\rho_o \ddot{u} = \frac{\partial^2 u}{\partial x^2}\left[M_2 + M_3 \frac{\partial u}{\partial x} + M_4 \left(\frac{\partial u}{\partial x}\right)^2 + \ldots\right], \qquad (2.3)$$

where x is the coordinate in the direction of particle motion and u is the particle displacement. M_2 is a linear combination of second order elastic coefficients, M_3 is a linear combination of second and third order coefficients, and M_4 is a linear combination of second, third and fourth order coefficients.

It will be seen that, when only the term in M_2 is retained on the R.H.S. of equation (2.3), the equation of motion reduces to that for a linear solid for which Hooke's Law applies. In this case the velocity of a stress wave is dependent on M_2 only. However when the term in M_3 is included also, as it must be when large particle displacements are considered, then the equation of motion becomes non-linear. Solution of this non-linear equation reveals that, as a finite amplitude sinusoidal stress wave with pulsatance ω propagates, a second harmonic wave with pulsatance 2ω is

generated. The amount of energy transferred to this second harmonic wave depends on the second and third order elastic coefficients. Similarly a solution of equation (2.3) when terms up to M_4 are included shows that both a second and third harmonic wave are generated. The amplitude of the third harmonic wave depends on elastic coefficients of second, third and fourth order. In general the greater the particle displacement of the fundamental wave, the more terms must be considered in equation (2.3)

We now consider analytical expressions for the amplitude of second and third harmonic waves, starting with the second harmonic. Several authors have analysed the growth of the second harmonic in an initially sinusoidal wave; a partial list of references follows. Gedroits and Krasil'nikov(1963); Melngailis, Maradudin and Seeger (1963); Buck and Thompson (1966); Thurston and Shapiro (1967); Holt and Ford (1967); Stanford and Zehner (1967); Gauster and Breazeale (1968); Carr (1968). For example, Buck and Thompson (1966) consider a longitudinal wave propagating in a <100> direction in a cubic material. This case is particularly interesting since it represents the situation in the experiments with aluminium and NaCl crystals which are discussed in Chapters 6-9 of the present work. A second harmonic wave is found with a stress amplitude of the form

$$A_2 = \tfrac{3}{4}\rho_o c_{11}^2 \left(1 + \frac{c_{111}}{3c_{11}}\right)\frac{\omega^2}{k} \times A_{10}^2 \quad , \qquad (2.4)$$

where ρ_o is the density of the unstressed medium, c_{11} is a second order elastic coefficient, c_{111} is a third order elastic coefficient (in contracted tensor notation), ω is the pulsatance of the fundamental wave, k is the wave constant, x is the distance the wave has propagated, and A_{10} is the stress amplitude of the fundamental wave at x = 0. Expression (2.4), which applies to a dissipationless medium, shows that the amplitude of the second harmonic wave

increases linearly with distance of propagation. The second harmonic amplitude is also seen to be proportional to the square of the fundamental wave amplitude and proportional to the square of the pulsatance of the fundamental wave.

Considering next the case of third harmonic generation, an expression for the amplitude of a third harmonic wave has been derived by Peters and Breazeale (1968) using the theory developed by Thurston and Shapiro (1967). This expression for the stress amplitude of the third harmonic is of the form

$$A_3 = \frac{6k^2x^2}{c_{11}^2} \cdot A_1^3 \left(\frac{c_{111} + 3c_{11}}{8c_{11}}\right)^2 \left\{1 + \frac{16}{9k^2x^2}\left[1 - \frac{c_{11}(\frac{1}{2}c_{1111} + 3c_{111} + 3/2c_{11})}{(c_{111} + 3c_{11})^2}\right]^2\right\}^{\frac{1}{2}} \tag{2.5}$$

where c_{1111} is a fourth order elastic coefficient, in contracted tensor notation.

The third harmonic amplitude is seen to be proportional to the cube of the fundamental wave amplitude. For the frequencies used in the present measurements on aluminium and NaCl the second term in expression (2.5) is expected to be much smaller than the first. The third harmonic amplitude will therefore be influenced only slightly by the fourth order elastic coefficient.

The third harmonic amplitude is expected, for normally encountered fundamental wave amplitudes, to be very much smaller than the corresponding second harmonic amplitude. Since the second and third harmonic wave amplitudes, due to dislocations, are expected to be of similar magnitude (see § 3.1), it follows that a study of dislocation third harmonic generation will be less influenced by lattice harmonic generation than will be the case with the second harmonic.

The interest in lattice harmonic generation arises mainly because higher order elastic coefficients may be determined from harmonic measurements. Similar experimental techniques (see § 2.2) are used in such measurements as are used in the present work on dislocation harmonic generation. In particular, the pulse-echo technique is used. The use of this technique raises certain points which have been discussed in the literature for lattice harmonic generation. These points will be mentioned here also, because of their relevance to dislocation harmonic generation in the same experimental situation.

It is of interest to consider the effect of successive reflections at the boundary of a medium upon the relative amplitudes of the fundamental and harmonic waves; for example, the effect of (a) phase changes of the fundamental and harmonic wave on reflection, (b) overlap of a foreward travelling wave and a reflected wave near the reflecting boundary, and (c) generation of harmonics at the reflecting surface.

The analysis of second harmonic generation by Buck and Thompson (1966) considers reflection from a stress-free boundary. Neglecting surface generation of harmonics and the effect of pulse overlap, the displacement of the second harmonic wave during reflection from a surface at a distance L from the driving face at x = 0 is found to be

$$u_2 = \left(\frac{3c_{11} + c_{111}}{8c_{11}}\right)k^2 u_{10}^2 x\{\cos 2(\omega t - kx) + \cos 2\left[\omega t - k(2L - x)\right]\}, \qquad (2.6)$$

where u_{10} is the displacement of the fundamental wave at x = 0. The displacement at x = L is seen to be consistent with the condition of a free boundary. After reflection the second harmonic displacement is

$$v_2^1 = \left(\frac{3c_{II} + c_{III}}{8c_{II}}\right)k^2 \, v_{10}^2 \, x \cos 2\left[\omega t - k(2L - x)\right] . \qquad (2.7)$$

This is the equation of a wave travelling in the -x direction with an amplitude proportional to x. Thus as the wave returns to the driven face at x = 0 energy is transferred back from the second harmonic wave to the fundamental, and at x = 0 the amplitude of the second harmonic wave becomes zero. After reflection at the driven face of the fundamental wave, a new second harmonic wave is generated as $x \to L$, and the cycle repeats.

Thompson, Tennison and Buck (1968) have observed the reflection of second harmonic pulses from a stress free boundary using a capacitative detector (see § 2.2) and found agreement with the above predictions. Some similar experiments have been carried out by Carr (1968) in which the effect of transducer thickness on the reflection of harmonic waves is investigated. The measurements were made at frequencies of about 9 GHz using CdS transducers. These measurements show that the energy flow from the fundamental to the second harmonic wave is reversed after longitudinal waves are reflected from a stress free surface or from a half wave-length thick transducer whose outer surface is stress free. It is also shown that for transverse waves (in AC-cut quartz) there is no phase shift of the fundamental with respect to the second harmonic and the energy flow is not reversed. These results are strictly true only in a dissipationless material (see § 3.2).

Buck and Thompson (1966) also consider effects (b) and (c) above. It is shown that a harmonic wave is generated at a stress free boundary during reflection, but that this

wave has an amplitude of typically only 10^{-3} that of the main harmonic component. In addition, Buck and Thompson (1966) consider the effect of pulse overlap during reflection. The importance of pulse overlap effects in the present work is minimised by using specimens which are as long as possible and pulses which are as short as possible (see § 4.4).

Several authors have pointed out that the amount of energy transferred from a fundamental wave to a second harmonic wave owing to lattice anharmonicity may be minimised by suitable choice of wave polarisation and propagation direction [Buck and Thompson (1966); Krasil'nikov and Zarembo (1967)]. For example, a transverse wave propagating in a ‹100› direction in a cubic lattice is not expected to generate a transverse second harmonic. This result may be attributed physically to the lack of dilation associated with a transverse wave, since it is the anharmonicity of the lattice forces which leads to the generation of harmonics. It also provides a way of studying dislocation harmonics without a large lattice harmonic being present. In the present work only longitudinal waves have been used.

2.2. Experimental Studies of Lattice Second Harmonic Generation.

It is seen from expression (2.4) that, if the absolute values of the fundamental and second harmonic wave amplitudes are measured at a particular distance of propagation, then the third order elastic constant c_{111} may be calculated very easily. Similar measurements with waves travelling in other crystal directions would give values for other third order elastic constants.

Absolute strain amplitudes of ultrasonic waves may be determined using a capacitative detector, after Gauster and Breazeale (1966). This type of detector is used in the present work also (see § 4.40). To determine strain amplitudes in this way a sinusoidal stress wave is generated at one end of a sample of the material to be investigated and the displacement of the opposite end of the sample when the wave undergoes reflection is measured with the capacitative detector. The displacement amplitude of the end surface of the sample is twice the displacement amplitude of the stress wave as seen from expressions (2.6) and (2.7).

With experiments such as these third order elastic constants have been measured in KCl and NaCl [Stanford and Zehner (1967); Gedroits and Krasil'nikov (1963)], copper [Gauster and Breazeale (1968)], quartz and sapphire [Carr (1968)].

The analyses of harmonic generation mentioned in § 2.1 from which the elastic constants are calculated assume a non-dissipative medium for wave propagation i.e. no energy is lost from the fundamental wave, except that transferred to the second harmonic. However, Gauster and Breazeale(1968) show that in practice when, for example, thermal attenuation and dislocation attenuation are present, the effect of this attenuation on the fundamental and second harmonic waves may be neglected when other experimental errors are considered. These authors irradiate their samples with fast neutrons to reduce the dislocation contribution to the attenuation.

CHAPTER 3

Second and Third Harmonic Generation due to Dislocations

3.0. Introduction

In this chapter a review is first given of a theory of dislocation second and third harmonic generation due to Hikata and Elbaum (1966). Some important features of the dislocation second and third harmonics predicted by this theory are then discussed. Finally, a brief review of some published measurements of dislocation second and third harmonic generation is presented.

3.1. Review of Theoretical Analyses

An analysis of the generation of ultrasonic second harmonics due to dislocations has been given by Suzuki, Hikata and Elbaum (1964). This theory assumed the harmonic generation to result from nonlinearities in the stress-strain relation governing the displacement of a dislocation loop length under the influence of an applied stress under conditions in which the stress is considered insufficient to produce unpinning of dislocations.

In a later paper [Hikata, Chick and Elbaum (1965)], experimental results were compared with predictions of a simplified theory in which the damping due to dislocation motion was not directly taken into account. The agreement between experiment and theory was good in many respects.

The analysis of Suzuki, Hikata and Elbaum (1964) has

been further refined and extended to include the generation of dislocation third harmonics by Hikata and Elbaum (1966). The analysis of Hikata and Elbaum will be considered here in some detail.

(i) The Equation of Motion

The analysis considers the simplified case of one dimensional wave propagation. Let υ be the longitudinal displacement of an infinitesimal element of a solid in the x-direction when a stress wave is propagated, then

$$\upsilon = \upsilon_{\ell} + \upsilon_{d} \ , \tag{3.1}$$

where υ_{ℓ} is the lattice displacement and υ_{d} the dislocation displacement. The one-dimensional equation of motion for the displacement υ in the x-direction is

$$\rho_o \frac{\partial^2 \upsilon}{\partial t^2} = \rho_o \frac{\partial^2}{\partial t^2}(\upsilon_{\ell} + \upsilon_{d}) = \frac{\partial \sigma}{\partial x} \ , \tag{3.2}$$

where ρ_o is the density of the undeformed material, σ is the applied stress and t represents time. Differentiating with respect to x, equation (3.2) becomes

$$\rho_o \frac{\partial^2}{\partial t^2}\left(\frac{\partial \upsilon_{\ell}}{\partial x} + \frac{\partial \upsilon_{d}}{\partial x}\right) = \frac{\partial^2 \sigma}{\partial x^2} \tag{3.3}$$

When a sinusoidal wave of frequency ω is introduced at one end of a specimen at $x = 0$, the problem is to solve equation (3.3) for σ at some distance x. In terms of the harmonics of the fundamental wave σ should be of the form

$$\sigma = A_o + A_1 \cos(\omega t - kx) + A_2 \cos 2(\omega t - kx - \delta_2) + A_3 \cos 3(\omega t - kx - \delta_3) + \ldots \tag{3.4}$$

where A_0 is a static bias stress, A_1, A_2 and A_3 are the stress amplitudes of respectively the fundamental, second harmonic and third harmonic, $2\delta_2$ and $3\delta_3$ are the phase angles of the second and third harmonics, respectively, to the fundamental wave, and k is the wave vector. It is assumed that dispersion is negligible and one value of k is used. The first step in the calculation is to find expressions for $\frac{\partial u_\ell}{\partial x}$ and $\frac{\partial u_d}{\partial x}$ as a function of stress.

(ii) The Expression for $\frac{\partial u_\ell}{\partial x}$

The one-dimensional relation between stress, σ, and displacement gradient $\frac{\partial u_\ell}{\partial x}$ of a solid correct to the second order terms in displacement gradient is [Landau and Lifshitz (1959)]

$$\sigma = E_1 \frac{\partial u_\ell}{\partial x} + a\left(\frac{\partial u_\ell}{\partial x}\right)^2 + \ldots \qquad (3.5)$$

where E_1 represents second order elastic constants and a is a combination of second and third order elastic constants.

The case of longitudinal wave propagation in a <100> direction of a cubic lattice is of particular interest since it applies to the measurements which have been made in the present work with aluminium and NaCl. In this case E_1 becomes c_{11} and a takes the form $\frac{3c_{11}+c_{111}}{2}$

Neglecting terms in a^3, expression (3.5) may be written

$$\frac{\partial u_\ell}{\partial x} = \frac{\sigma}{E_1} - \frac{a}{E_1^3}\sigma^2 + \ldots \qquad (3.6)$$

Substitution of equation (3.4) in expression (3.6) then yields an expression for $\frac{\partial u_\ell}{\partial x}$ as required.

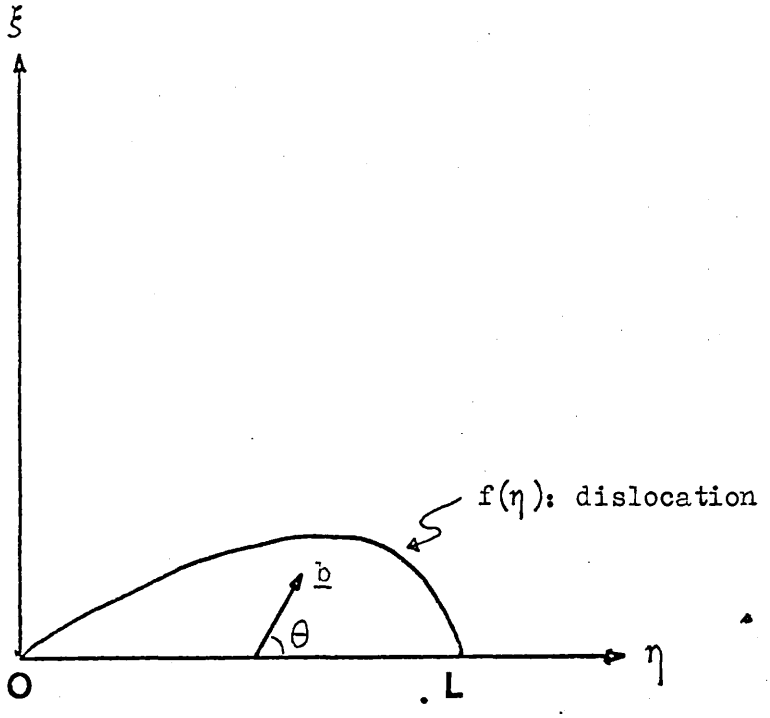

Fig. 3.1. A bowed out dislocation $\xi = f(\eta)$ The η axis coincides with the straight line configuration of the dislocation before bowing out. $\underline{b}$ is the Burgers vector.

(iii) The Expression for $\frac{\partial v_d}{\partial x}$

In order to calculate an expression for $\frac{\partial v_d}{\partial x}$ Hikata and Elbaum first derive a nonlinear relation between a static stress and the displacement of a pinned dislocation line, using the string analogy of Koehler(1952). Fig.3.1. shows a bowed out dislocation loop of length L pinned at each end. (ξ, η) are the coordinates of a point on the bowed out dislocation. The η-axis coincides with the straight line configuration of the dislocation before bowing out. $\underline{b}$ is the Burgers vector, which makes an angle θ to the η-axis. A relation is found of the form

$$\tau b = - \frac{\partial^2 \xi}{\partial \eta^2} C + C C^1 \frac{\partial^2 \xi}{\partial \eta^2} \left(\frac{\partial \xi}{\partial \eta}\right)^2, \qquad (3.7)$$

where τ is the resolved shear stress in the glide plane and in the slip direction, and

$$C = W_e (1 + m \cos^2 \theta - 2 m \sin^2 \theta), \qquad (3.8)$$

$$C^1 = 3/2 \frac{(1 + 3 m \cos^2 \theta - 4 m \sin^2 \theta)}{(1 + m \cos^2 \theta - 2 m \sin^2 \theta)} , \qquad (3.9)$$

with

$$m = \frac{W_e - W_s}{W_e} , \qquad (3.10)$$

where W_e is the line energy of an edge dislocation per unit length in an isotropic medium and W_s is the corresponding line energy of a screw dislocation.

In the linear approximation of a small dislocation displacement, such as is considered in the Granato-Lücke (1956) theory of dislocation damping, only the first term on the R.H.S. of equation (3.7) is retained. The second

term on the R.H.S. of equation (3.7) is the term which makes the dislocation stress-displacement relation non-linear and which is responsible, therefore, for the appearance of harmonics. This non-linear term arises because the line energy of the dislocation loop (see Fig. 3.1.) is considered dependent upon the position and orientation of the dislocation; in deriving equation (3.7) account is taken of the variation in line energy along the dislocation loop, and higher order terms of $\frac{\partial \xi}{\partial \eta}$ are retained in the expression for the total line energy of the dislocation loop.

When a dislocation segment, as shown in Fig.3.1., is subjected to a combined static and oscillatory stress equation (3.7) gives the restoring force on the segment, due to the dislocation line energy, which tends to return the dislocation to its equilibrium position. The equation of motion of the dislocation segment then becomes [Koehler (1952)]

$$A\frac{\partial^2 \xi}{\partial t^2} + B\frac{\partial \xi}{\partial t} - C\left[\frac{\partial^2 \xi}{\partial \eta^2} - C^1\left(\frac{\partial \xi}{\partial \eta}\right)^2\left(\frac{\partial^2 \xi}{\partial \eta^2}\right)\right] = \sigma b R, \qquad (3.11)$$

where R is a resolving shear factor converting an axial stress to a shear stress in the slip plane and in the slip direction, $A = \pi \rho_o b^2$ is the effective mass of dislocation per unit length [see Koehler (1952)], and B is the damping coefficient. The terms $A\frac{\partial^2 \xi}{\partial t^2}$ and $B\frac{\partial \xi}{\partial t}$ represent, respectively, the inertia force and frictional force of a dislocation, per unit length. Hikata and Elbaum then solve equation (3.11) for ξ in terms of η and calculate $\frac{\partial v_d}{\partial x}$ from the relation

$$\frac{\partial v_d}{\partial x} = \frac{Nbq}{L_o}\int_o^{L_o} \xi . d\eta \, , \qquad (3.12)$$

where N is the dislocation density, q is a factor converting shear strain to longitudinal strain and L_o is the effective dislocation loop length. Equation (3.12) follows from the usual definition of dislocation strain [see Cottrell (1961)].

(iv) The Second and Third Harmonic Amplitudes

Inserting the expressions (3.4),(3.6) and (3.12) into equation (3.3) leads to expressions for A_2, A_3, α_1, α_2 and α_3, where α_1, α_2 and α_3 are respectively the attenuation of the fundamental, second harmonic and third harmonic waves. Neglecting A_2 in comparison with A_1, and A_1^3 in comparison with A_1 the expression for A_2 may be written

$$A_2 = \frac{\rho_o \omega^2}{k}\left[X^2 + Y^2 - 2XY\cos 2(\delta_{10} + \delta_{20})\right]^{\frac{1}{2}} \cdot A_{10}^2 \frac{e^{-2\alpha_1 x} - e^{-\alpha_2 x}}{\alpha_2 - 2\alpha_1}, \quad (3.13)$$

where A_{10} is the stress amplitude of the fundamental wave at x = 0, and

$$X = \frac{a}{2E_1^3} \quad (3.14)$$

$$Y = \frac{48Nb^4R^3q\,C^{\frac{1}{2}}A_o}{\pi^2A^3S_oM_o^{1/2}L_o^{\frac{1}{2}}}, \quad (3.15)$$

in which

$$S_o = (\omega_o^2 - \omega^2)^2 + (\omega d)^2, \quad (3.16)$$

$$M = (\omega_o^2 - 4\omega^2)^2 + 4(\omega d)^2, \quad (3.17)$$

with

$$\omega_o = \pi/L_o\left(\frac{C}{A}\right)^{1/2}, \quad (3.18)$$

and the phase angles $2\delta_{10}$ and $2\delta_{20}$ are defined by

$$\tan \delta_{10} = \frac{\omega d}{\omega_o^2 - \omega^2} \quad , \tag{3.19}$$

and

$$\tan 2\delta_{20} = \frac{2\omega d}{\omega_o^2 - (2\omega)^2} \quad . \tag{3.20}$$

The quantity X represents the lattice contribution and Y the dislocation contribution. If the dislocation contribution is ignored and wave propagation in a <100> direction of a cubic material for which both α_1 and α_3 tend to zero is considered, then

$$\frac{a}{2E_1^3} = \frac{3c_{11} + c_{111}}{4c_{11}^3}$$

and

$$\frac{e^{-2\alpha_1 x} - e^{-\alpha_2 x}}{\alpha_2 - 2\alpha_1} \rightarrow x.$$

Expression (3.13) then reduces to

$$A_2 = \tfrac{3}{4} \frac{\rho\omega}{c_{11}^2} \left(1 + \frac{c_{111}}{3c_{11}}\right) \frac{\omega^2}{k} \times A_{10}^2 \quad . \tag{3.21}$$

This is identical to expression (2.4) which was derived by Buck and Thompson (1966) for the second harmonic in a dissipationless medium.

In the case where $\omega_o >> 4\omega$ the factor $\cos 2(\delta_{10} + \delta_{20})$ can be replaced by $\frac{\omega_o^2}{S_o M_o^{1/2}} (\omega_o^4 - 5\omega^2 d^2)$.

The third harmonic stress amplitude is found to a good approximation to be of the form

$$A_3 = \frac{12\rho\omega^2 Nb^4 qR^3 CC^1}{kA^4 S_o^{3/2} T_o^{1/2} L_o^4} \cdot A_{10}^3 \cdot \frac{e^{-3\alpha_1 x} - e^{-\alpha_3 x}}{\alpha_3 - 3\alpha_1} \quad . \tag{3.22}$$

The expression for α agrees with that obtained by Granato and Lücke (1956) in their theory of dislocation damping. The expressions for α_2 and α_3 are of the same form as that for α_1 when the harmonic waves are considered to be independent waves propagating with pulsatance 2ω and 3ω respectively.

3.2. Discussion of the Theory

Some important consequences of the expressions for the second and third harmonic stress wave amplitudes are listed below.

(a) There are two contributions to the second harmonic, one arising from the lattice anharmonicity, the other arising from the non-linear dislocation motion. In addition, the existence of the phase angle $2(\delta_{10} + \delta_{20})$ between the lattice and dislocation contributions leads to a cross-term in expression (3.13). Because of this cross-term it is difficult to distinguish experimentally between the contributions, unless $2(\delta_{10} + \delta_{20}) \simeq \pi/2$ [δ_{10} and δ_{20} depend on dislocation loop length]. The quantity X is considered to be independent of bias stress in the range used in the present measurements. The factor Y is a function of dislocation density, loop length and bias stress.

An important consequence of the factor A_0 , the static stress, in expression (3.15) is that the dislocation contribution becomes zero for zero static bias stress

(internal or external). This implies that the dislocation stress-strain relation must be asymmetric as well as non-linear for second harmonic generation.

The bias stress dependence of the third harmonic should be contrasted with that of the second harmonic. Expression (3.22) indicates that a third harmonic due to dislocations may arise even when the static bias stress is zero. Thus while a static bias stress is needed before any dislocation second harmonics are generated, a static bias stress influences the generation of dislocation third harmonics only by, for example, changing dislocation loop lengths by unpinning.

In the expression for the third harmonic amplitude the lattice contribution does not appear because the terms in powers higher than the square of the displacement gradient are not considered in expression (3.5). The experiments of Peters and Breazeale (1968) indicate that the third harmonic due to lattic anharmonicity is very much less than the second harmonic (see also Chapter 2.1). Since it is also found that the dislocation contribution to both second and third harmonic waves is of a similar magnitude, the assumption of equation (3.5) appears to be justified.

(b) The amplitudes of the second and third harmonic waves are proportional respectively to the square and cube of the amplitude of the fundamental wave, as long as the dislocation loop length remains constant.

(c) Expression (3.13) predicts a second harmonic amplitude

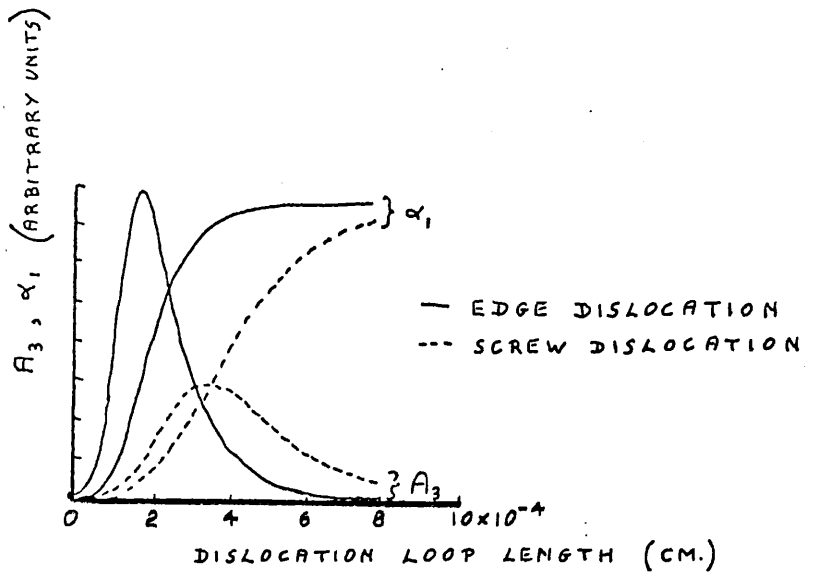

Fig. 3.2. Amplitude of the third harmonic A_3 and attenuation of the fundamental wave α_1 for edge and screw dislocations as a function of loop length. (After Hikata and Elbaum, 1966)

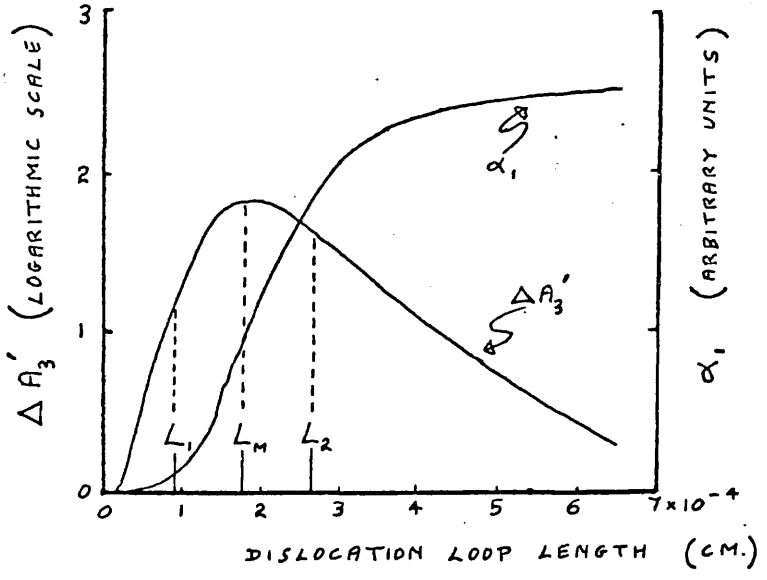

Fig. 3.3. Theoretical curve for the amplitude of the third harmonic and the attenuation of the fundamental wave for edge dislocations as a function of dislocation loop length. (After Hikata, Sewell and Elbaum, 1966)

which is zero at x = 0 and which increases linearly with x in a dissipationless medium. As a result of attenuation the second harmonic amplitude passes through a maximum at a distance

$$x_2 = \frac{\ell n(\frac{2\alpha_1}{\alpha_2})}{2\alpha_1 - \alpha_2} \quad (\text{c m.}) \tag{3.23}$$

Similarly the third harmonic amplitude has a maximum at

$$x_3 = \frac{\ell n(\frac{3\alpha_1}{\alpha_3})}{3\alpha_1 - \alpha_3} \quad (\text{c m.}) \tag{3.24}$$

(d) In the case of the second harmonic the static stress A_o is a parameter indicating the degree of deviation of a bowed out dislocation from its straight line configuration. Therefore, regardless of whether the stress is in tension or compression, the absolute value $|A_o|$ should be used in expression (3.13).

(e) The dependence of both α_1 and A_3 upon dislocation loop length is illustrated in Fig.3.2 for both edge and screw dislocations, using typical values for the parameters involved. In both cases A_3 shows a maximum as a function of loop length. Screw dislocations are seen to generate a smaller harmonic than edge dislocations. It is also seen that the maximum in A_3 occurs approximately where the point of inflection in the α_1 curve appears. The maximum in the A_3 curve therefore corresponds approximately to the transition between underdamped and overdamped behaviour [Granato and Lücke (1956)]. The absolute value of A_3 for both edge and screw dislocations also depends appreciably on the orientation θ (see Fig.3.1). It is expected that some modification of the theory would result if a distribution in loop lengths were to be considered.

The dependence of the third harmonic amplitude upon loop length may be investigated by unpinning dislocations with a static bias stress. This stress is assumed sufficient to unpin dislocations without increasing the dislocation density. The terms in expression (3.22) which involve L_o may be written as $f_1(L_o)$ and $f_2(\alpha,x)$, where

$$f_1(L_o) = \frac{1}{S_o^{3/2} T_o^{1/2} L_o^4}, \tag{3.25}$$

and

$$f_2(\alpha,x) = \frac{e^{-3\alpha_1 x} - e^{-\alpha_3 x}}{\alpha_3 - 3\alpha_1}. \tag{3.26}$$

Thus the change in third harmonic amplitude may be expressed logarithmically as

$$\Delta A_3 = 20 \ell n_{10} \frac{A_3}{A_{30}}, \tag{3.27}$$

$$= 20 \ell n_{10} \frac{f_1(L_o)}{[f_1(L_o)]_o} + 20 \ell n_{10} \frac{f_2(\alpha,x)}{[f_2(\alpha,x)]_o}. \tag{3.28}$$

Here A_{30} and A_3 are the third harmonic amplitudes at, respectively, zero bias stress and a finite bias stress. When $|3\alpha_1 x - \alpha_3 x| \ll 1$ the second term in expression (3.28) can be approximated by $-26\Delta\alpha_1 x$, where $\Delta\alpha_1$ is the measured change in attenuation of the fundamental wave corresponding to the change ΔA_3. Together with Hikata, Sewell and Elbaum (1966) third harmonic amplitude changes in the present work are plotted in the form

$$\Delta A_3' = \Delta A_3 + 26.x.\Delta\alpha_1$$

$$= 20 \ell n_{10} \frac{f_1(L_0)}{[f_1(L_0)]_0}, \tag{3.29}$$

when N remains constant.

Measurements plotted in this way are interpreted in terms of Fig.3.3, which shows both $\Delta A_3'$ and α_1 plotted against loop length for typical values of the dislocation and lattice parameters involved. The curves are of a similar form to those of Fig.3.2.

(f) In the case of longitudinal wave propagation discussed above, it has been pointed out that the lattice and dislocation contributions to the second harmonic are difficult to separate. It therefore appears that dislocation dynamics are more easily studied through the generation of third harmonics.

3.3 Review of some Published Experimental Measurements

A dislocation contribution to second harmonic generation has been noted by Hikata, Chick and Elbaum (1963) and (1965), Breazeale and Ford (1965), and Krasil'nikov and Zarembo (1967). The measurements of Hikata, Chick and Elbaum (1963) were made in an aluminium single crystal using a 10 MHz longitudinal fundamental wave. A second harmonic amplitude dependent upon a tensile bias stress was observed and attributed to an alteration in the dislocation configuration in the crystal. Hikata, Chick and Elbaum (1965) made further measurements in an aluminium crystal, again using a 10 MHz fundamental wave. The measurements are interpreted in terms of a simplified version of the theory discussed in §3.1 above. The measurements are found to reveal the presence of internal stresses remaining after plastic deformation. This effect is considered further in Chapter 8, where somewhat similar

measurements in NaCl using third harmonic generation are discussed. Breazeale and Ford (1965) have made measurements in a copper single crystal using a longitudinal 30 MHz fundamental wave. These authors find a second harmonic wave with an amplitude sensitive to the state of anneal of the specimen and to neutron irradiation, a behaviour which they attribute to the presence of dislocations. This is because neutron irradiation is expected to produce lattice defects which may pin dislocations and so alter the loop lengths. Krasil'nikov and Zarembo (1967) report measurements using a 5 MHz shear wave in NaCl to generate a 10 MHz second harmonic wave which is apparently related to dislocation properties. No detailed study of this effect is given however.

Direct measurements on a dislocation contribution to the third harmonic appear to have been made only by Hikata, Sewell and Elbaum (1966), who interpret their results in terms of the theory set out in § 3.1. The measurements involve a 10 MHz fundamental longitudinal wave propagating along <100>, <110> and <111> directions in aluminium single crystals of various purities. The measurements give good support to the theory of Hikata and Elbaum (1966) and are considered in more detail in Chapter 6. In this chapter the results of some similar measurements made in the course of the present work are presented.

All the authors mentioned here have used the same basic system for observing harmonics, namely a type of pulse-echo measurement in which a specimen has a driving transducer at one end and a receiving transducer at the other connected to a harmonic amplifying system. This is

also the method used in the present work. A slight modification of this system has been employed by Gauster and Breazeale (1967) for observing the lattice contribution to the third harmonic. This involves increasing the ultrasonic pulse length until overlap between successive echoes occurs. An appreciable increase in harmonic signal level occurs in the region of overlap if the frequency of the successive echoes is correctly adjusted. In this way third harmonic echoes may be distinguished from spurious pulses excited in the electronics employed, since there is a random phase relation between such signals. This technique is useful since the lattice third harmonic signal level is very small and the spurious signals can be appreciable. There was found to be no need to use this technique in the present work since the dislocation harmonic signals were easily detectable.

CHAPTER 4

Ultrasonic Measuring Techniques

In this chapter a description is given of the systems and methods used to observe the generation of second and third harmonics of an ultrasonic stress wave. The method used to measure the attenuation of the fundamental ultrasonic wave is also described.

4.0. The Experimental Observation of Second Harmonic Generation

4.1. Introduction

The experimental system was designed to detect the second harmonic content of a 10MHz fundamental ultrasonic wave after propagation in a crystal. Fig.4.1 is a simplified block diagram illustrating the method used. The crystal specimen had a quartz transducer attached to each end. One of these had a fundamental resonant frequency of 10MHz and was used to generate the fundamental ultrasonic wave. The transducer at the other end of the specimen had a fundamental resonant frequency of 20MHz and was used to receive the second harmonic signal generated in the specimen. The filter(1) between the pulsed oscillator and the driving transducer removed unwanted 20MHz signal from the fundamental pulse of 10MHz sinusoidal signal. The filter(2) removed unwanted 10MHz signal from the harmonic amplifying system. The harmonic signal received by the 20MHz transducer was amplified and displayed on an oscilloscope screen. The actual experimental system was more complex than that shown by Fig.4.1 and it is discussed in detail in the following

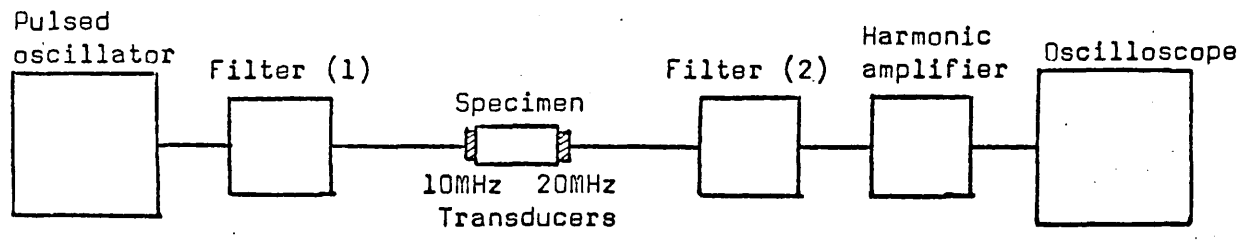

Fig. 4.1. Simplified block diagram of second harmonic system.

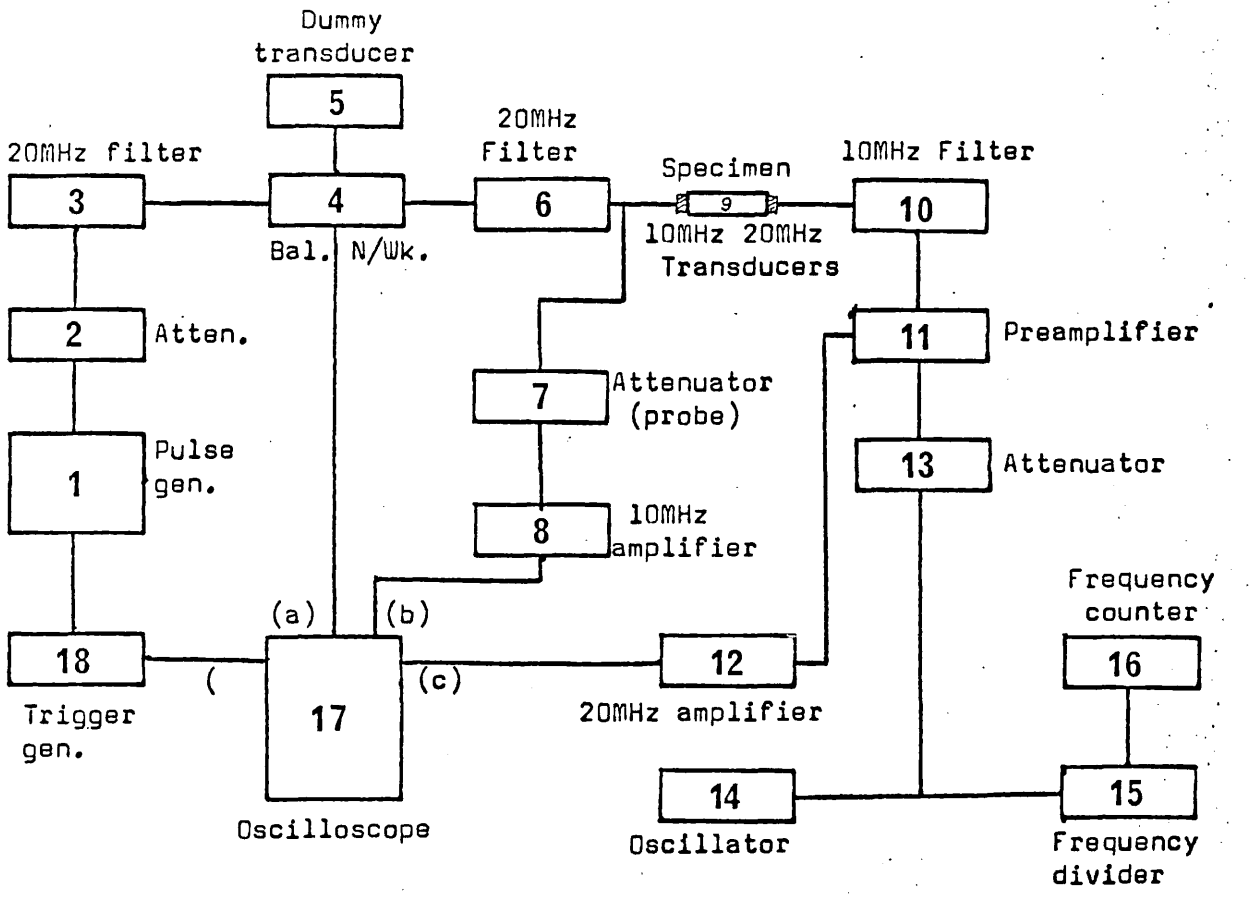

Fig. 4.2. Block diagram of the second harmonic system.

Table 4.1. Details of components appearing in Fig.4.2.

1	Arenberg Pulse Generator, PG-650-C.
2	Arenberg 93 ohm attenuator, ATT-693.
3	Filter, see Fig.4.4.
4	Balancing Network, see Fig.4.7.
5	Dummy 10 MHz transducer.
6	Filter, see Fig.4.5.
7	x10 attenuating probe, Tektronix P-6000.
8	10 MHz amplifier, see Fig.4.9.
9	Specimen.
10	Filter, see Fig.4.6.
11	Arenberg preamplifier, PA-620-B.
12	Tuned 20 MHz amplifier, see Fig.4.8.
13	Solartron 600 ohm attenuator, AT-201.
14	Advance signal generator, SG-62-B.
15	Advance frequency divider, TCD-100-A.
16	Advance frequency counter, TC-4.
17	Tektronix oscilloscope, 555.
(a)	Tektronix plug-in unit, 1A1 (Ch.1).
(b)	Tektronix plug-in unit, L.
(c)	Tektronix plug-in unit, 1A1 (Ch.2).
18	Tektronix time mark generator, 180-A.

paragraphs.

4.2 The Experimental System

Fig.4.2 is a block diagram of the experimental system used. Both the input pulse and the fundamental echoes of this pulse could be monitored as well as the second harmonic content of the echoes. Table 4.1 gives details of the units incorporated in the system.

The pulse generator(1) was capable of giving pulses of sinusoidal signal of a frequency between 360 KHz and 180 MHz with pulse lengths from about 2μ sec. to 100 μsec. and pulse repetition frequencies of up to 3 KHz. In practice, pulses of 10 MHz signal of about 5 μsec. duration were used; these were triggered externally to give a pulse repetition frequency of 100 Hz by a time mark generator(18), which also triggered the time base of an oscilloscope(17). The pulses from the generator passed first through a 93Ω attenuator(2) by means of which signal attenuation in the range 0 to 121 db could be introduced in steps of 1 db. Distortion of the pulses was minimised when the pulse generator was terminated with 93Ω . The filter(3) then attenuated any 20 MHz signal present before the pulse reached the balancing network(4). This network was used simply to increase the signal level, as described in § 4.3(b). The pulse was monitored at this point with the oscilloscope(17) before passing through a second filter(6) which further attenuated any unwanted remaining 20 MHz signal. The pulse was then applied to the 10 MHz quartz transducer attached to the specimen(9). A pulse of up to 1500 volts (peak-to-peak) could be applied to the transducer; at larger

voltages electrical breakdown occurred between the transducer electrodes. Echoes of the driving pulse, picked up by the 10 MHz transducer, were monitored on the oscilloscope screen(17) with the aid of an attenuating probe(7) and a 10 MHz tuned amplifier(8). Diodes were used to prevent saturation of the amplifier by the driving pulse.

20 MHz ultrasonic waves in the specimen were picked up by the receiving transducer which, although it had a fundamental resonant frequency of 20 MHz, also picked up a quite considerable 10 MHz signal corresponding to both the direct signal and echoes from the 10 MHz fundamental pulse. These signals were reduced in amplitude with the filter(10) so that they would not excite the tuned circuits of the amplifiers(11) and (12). After amplification the 20 MHz echoes were displayed on the screen of the oscilloscope (17).

The preamplifier(11) had a mixing stage so that a reference c.w. signal from the oscillator(14) could be superimposed on the 20 MHz echoes. When the two frequencies were similar a beating effect was observed, which disappeared when the two frequencies became identical. The c.w. frequency was then measured with the frequency counter(16) used in conjunction with a frequency divider(15). In this way the frequency of the sinusoidal component of ultrasonic echoes could be determined to $\pm$ 0.05 MHz in 20.00 MHz. The attenuator(13) was included so that the c.w. signal level could be adjusted to the same order of magnitude as the echo amplitude.

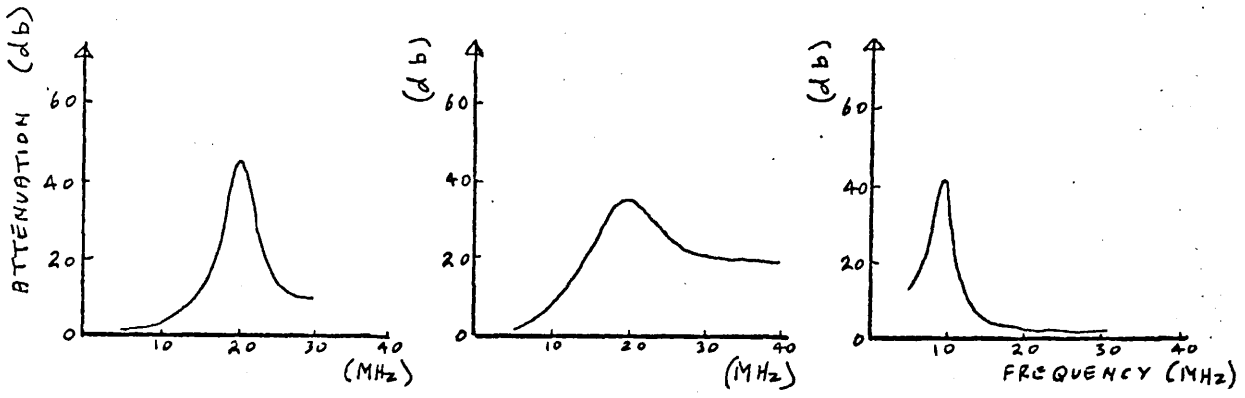

(a) 93ohm filter (b) 500ohm filter (c) 150ohm filter

Fig. 4.3. Filter attenuation as a function of frequency.

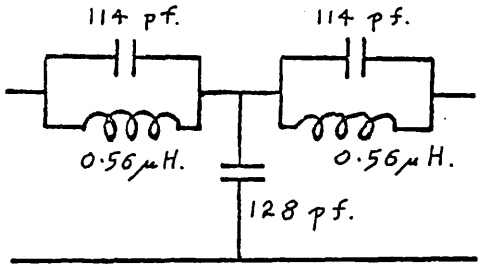

Fig. 4.4. 20MHz filter, 93ohm.

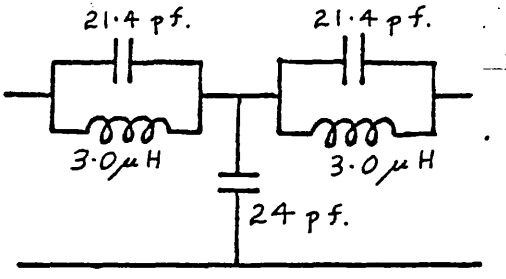

Fig. 4.5. 20MHz filter, 500ohm.

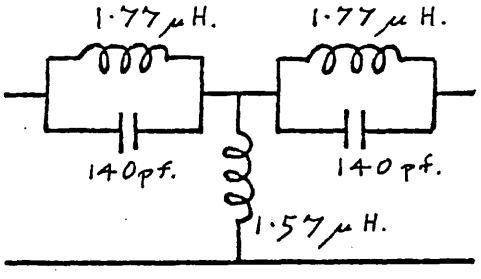

Fig. 4.6. 10MHz filter, 150ohm.

4.3 Description of the Filters, Balancing Network and Tuned Amplifiers.

4.3(a) Filters

The two filters (3) and (6) were designed to pass a frequency of 10 MHz and reject one of 20 MHz, while the filter (10) was designed to reject a frequency of 10 MHz and pass one of 20 MHz. The experimentally determined insertion losses of these filters as a function of frequency are shown in Fig.4.3(a) (b) and (c), and in Figs.4.4, 4.5 and 4.6 the electrical circuits of the filters are shown.

Starting with a constant K π-section [Williams(1963)] as prototype, the corresponding m-derived type was designed. From this a shunt derived T-section was designed and used as the filter, with m = 0.6. For this value of m the characteristic impedance of the filter was an almost constant resistance at frequencies within the pass band. The filter (3) shown in Fig.4.4 was given a characteristic impedance of 93Ω to match the impedance of the pulse generator(1) and attenuator(2). The filter (6) shown in Fig.4.5 was given a higher impedance of 500Ω so that it would not load excessively the high voltage signal from the balancing netowrk(4). The capacitors in this filter were variable air capacitors with high voltage ratings. The filter (10) shown in Fig.4.6 had a characteristic impedance of 150Ω which was calculated to be of the same order as the input impedance of the preamplifier(11).

4.3(b) The Balancing Network

The balancing network (4) was constructed according to the design of a commercially available network (see

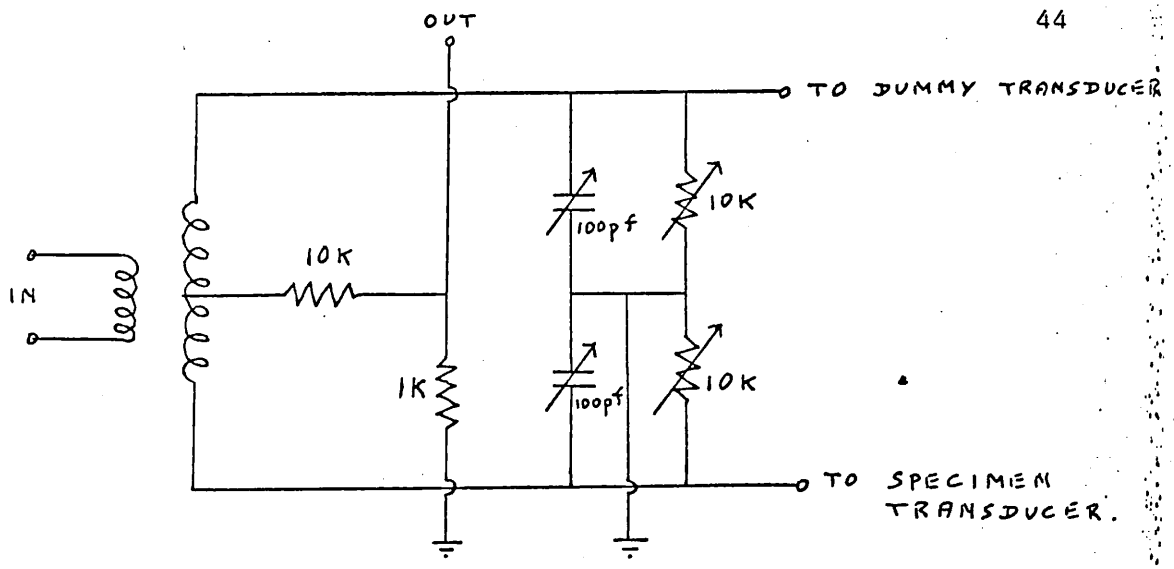

Fig. 4.7. The balancing net-work.

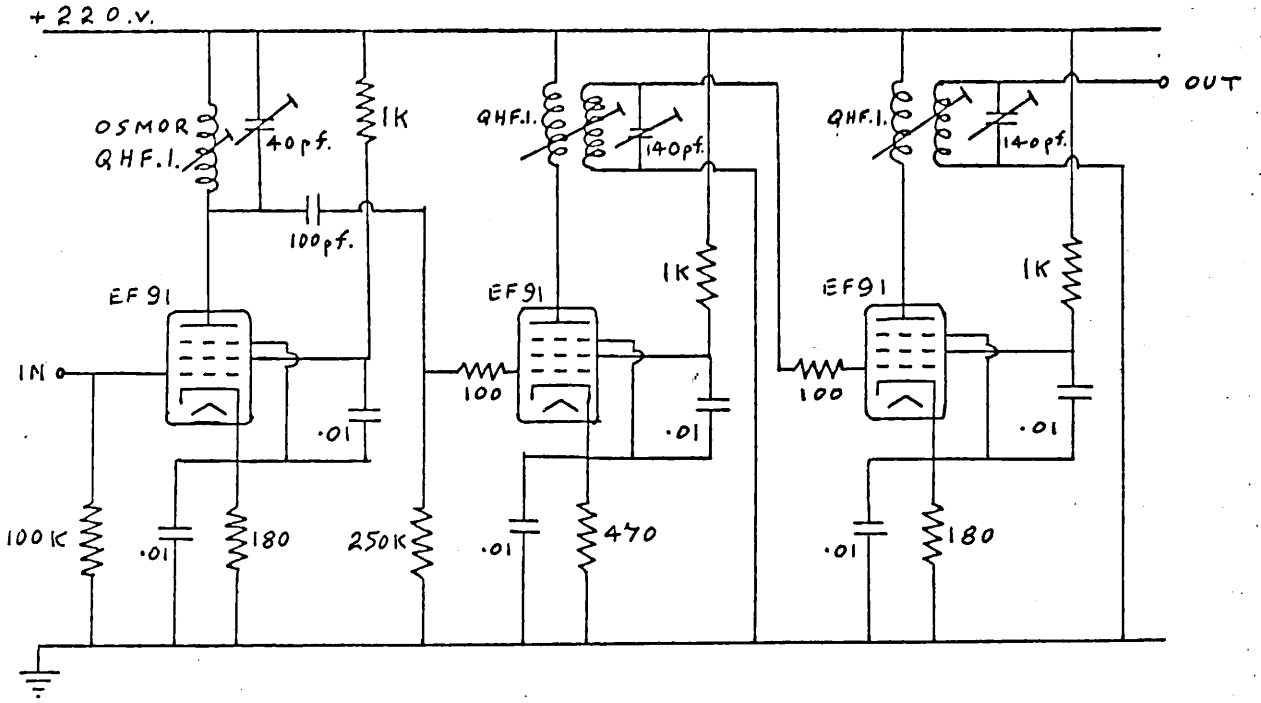

Fig. 4.8. The tuned 20 MHz amplifier.

table 4.1). The commercial network was designed primarily to act as an impedance matching network, but it could also be used simply as a step-up voltage transformer. It was in this latter capacity that it was used in the present work. Fig.4.7 shows the construction of the network. Increases in signal level of up to five times were possible. The capacitors used in the network had high voltage ratings.

4.3(c) The Tuned Amplifiers

The 20 MHz amplifier (12) was designed to use thermionic valves and the circuit diagram is shown in Fig.4.8. Attempts to build a solid state amplifier failed owing to lack of stability at the high voltage gains required. The amplifier had a voltage gain of about 60 db and a band-width of about 0.5 MHz. The tuned circuits were damped with suitable resistors to increase stability. When the out-put of the amplifier was viewed on an oscilloscope, the gain was found to be linear for output signal levels up to 1.0 volt, with the wide-band preamplifier(11) tuned for maximum gain; the noise level was 0.02 volt. The band-width was, of course, greater when the harmonic input level was sufficiently high to require use of the amplifier below maximum gain.

The 10 MHz amplifier(8) was constructed to essentially the same design, and Fig.4.9 shows the circuit diagram. The amplifier had a voltage gain of about 40 db, and diodes were included at the input and output to limit the amplitude of the fundamental driving pulse. These diodes were found not to affect appreciably the linearity of the amplifier gain at the small output signal levels used.

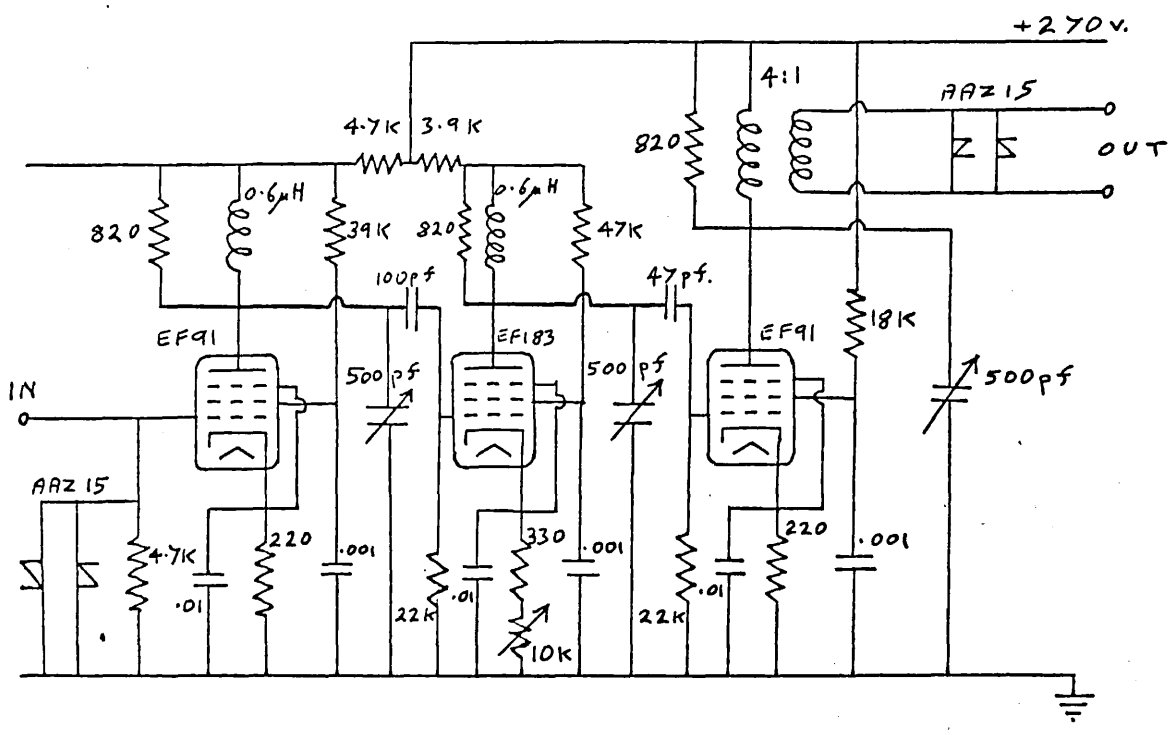

Fig. 4.9. The tuned 10 MHz amplifier.

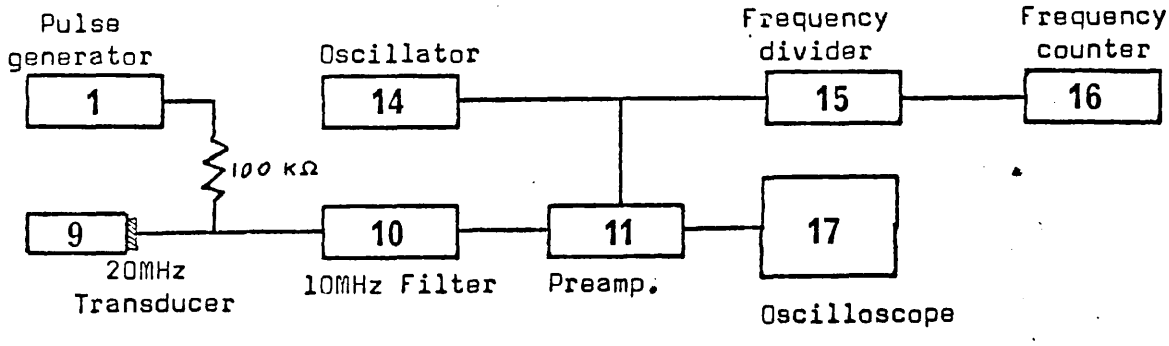

Fig. 4.10. System for alignment of the 10MHz filter. See table 4.1 for details of the apparatus.

4.4. The Alignment Procedure

The tuned circuits of the filters and amplifiers were adjusted approximately before incorporation in the system, but because these elements were sensitive to input and output impedances the following alignment procedure was used.

(a) The 10 MHz filter(10) was first tuned, using the arrangement shown in Fig.4.10.

10 MHz pulses from the pulse generator were fed through a 100 KΩ resistor (so that the low output impedance of the pulse generator did not influence the filter characteristic) to the 20 MHz transducer and filter circuit. The preamplifier was tuned to 10 MHz and the filter was adjusted for maximum attenuation at 10 MHz, as indicated by the signal displayed on the oscilloscope. Frequencies were measured by beating the pulses with a sinusoidal signal from an oscillator as described in § 4.2 above. In actual use the preamplifier was tuned to 20 MHz and hence presented a different impedance to the filter, but the effect on the filter was found to be small.

(b) The tuned circuits of the 20 MHz amplifier(12) and the preamplifier(11) were then adjusted using the arrangement of Fig.4.11. A pulse of 20 MHz signal produced by the pulse generator(1) was used to drive a 20 MHz transducer bonded to one end of a specimen. The 20 MHz transducer at the other end of the specimen was connected to the second harmonic detecting system and frequency measuring system described in § 4.2 above. The attenuator(2) was included because the high voltage gain of the harmonic detecting system meant that only a small ultrasonic pulse was required.

The centre frequency of the amplifier system could be adjusted to within 0.02 MHz by this method, and frequency stability over long periods (~ six hours) was to within 0.1 MHz.

(c) The next step was the adjustment of the balancing network (4). The complete arrangement of Fig.4.2 was assembled, with the 20 MHz filters (3) and (6) approximately tuned. The variable resistors and capacitors of the balancing network were then adjusted to give a pulse of good rectangular shape over the entire voltage range of the generator.

(d) The 20 MHz filters (3) and (6) were then adjusted. 20 MHz pulses were obtained from the pulse generator and passed through both 20 MHz filters and the balancing network to the transducer; these pulses were detected by a pick-up coil placed near to the transducer leads. The signal from this coil was connected to the input of the harmonic amplifying system.

(e) The frequency spectrum of a repeated square wave pulse becomes narrower as the pulse length is increased. If the pulse is very short the band-width of the transducer-specimen coupling may not be large enough for the pulse to be transmitted without distortion. The minimum pulse length necessary for the pulse to build up to its full amplitude is about $\frac{1.3}{B.W}$, where B.W. is the band-width of the transducer coupling to the specimen [Mason (1958)] . This estimate assumes a non- dispersive medium.

The length of the ultrasonic pulse was therefore adjusted in the pulse generator (1) to ensure that it was

great enough for the pulse to build up to its full amplitude.

The pulse generator did not produce good rectangular shaped pulses when the pulse amplitude was low. Consequently, when small amplitude ultrasonic driving pulses were required, a pulse sufficiently large to be without distortion was generated and attenuated with the attenuator (2). This attenuator was therefore adjusted as required.

4.5 Discussion of the System

With the experimental system described above, a 20 MHz signal might be observed on the oscilloscope screen not only as a result of harmonics generated in the sample but for at least three other reasons. These three reasons are (i) 20 MHz signal coming from the pulse generator being incompletely filtered out, (ii) the excitation of the tuned circuits in the detecting amplifiers (11) and (12) by large amplitude 10 MHz signals, and (iii) the generation of harmonics of the fundamental pulse at the specimen surfaces and at electrical impedance mismatches. These three effects will be considered in turn.

The amount of second harmonic signal present in the pulses leaving the pulse generator was found experimentally to be about 5%. Taking into account the insertion losses of the various filters used and the fundamental resonant frequency of the driving transducer, then this unwanted 20 MHz signal is calculated to be only about $\frac{1}{100}$ of the

expected specimen harmonic signal. This is assuming that the second harmonic generated in the sample has an amplitude equal to about 0.1% of the fundamental 10 MHz wave. The effect of (i) above is therefore probably negligible.

Excitation of the tuned circuits of the harmonic detecting amplificrs by a large amplitude 10 MHz signal was made negligible by the use of the 10 MHz filter (10). The use of a wideband preamplifier (11) before the main amplifier (12) also assisted in this.

The generation of harmonics at the surface of a specimen has been considered by Buck and Thompson (1966) and by Carr (1968). These analyses show the effect to be small and no special precautions were taken against it, except that specimens with good flat surfaces for attaching transducers were always used. Electrical impedance mismatches may also lead to distortion of the fundamental pulse and thus to the production of harmonic signals. The driving pulse was monitored at the 10 MHz transducer to check that a good rectangular pulse envelope was obtained and some care was taken in the design of the filter impedances so that serious impedance mismatches were unlikely.

With the experimental system designed and adjusted as described above it was possible to observe second harmonic signals which could be related to the anharmonic strain properties of the particular specimen being used.

4.6 Recording Methods

Two methods were used to record pulse amplitudes.

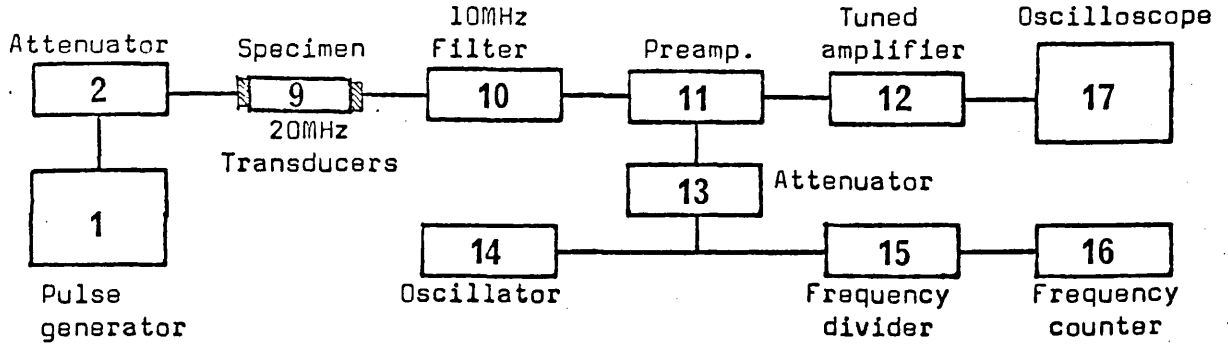

Fig. 4.11. Block diagram of the system for amplifier alignment. See table 4.1 for details of the apparatus.

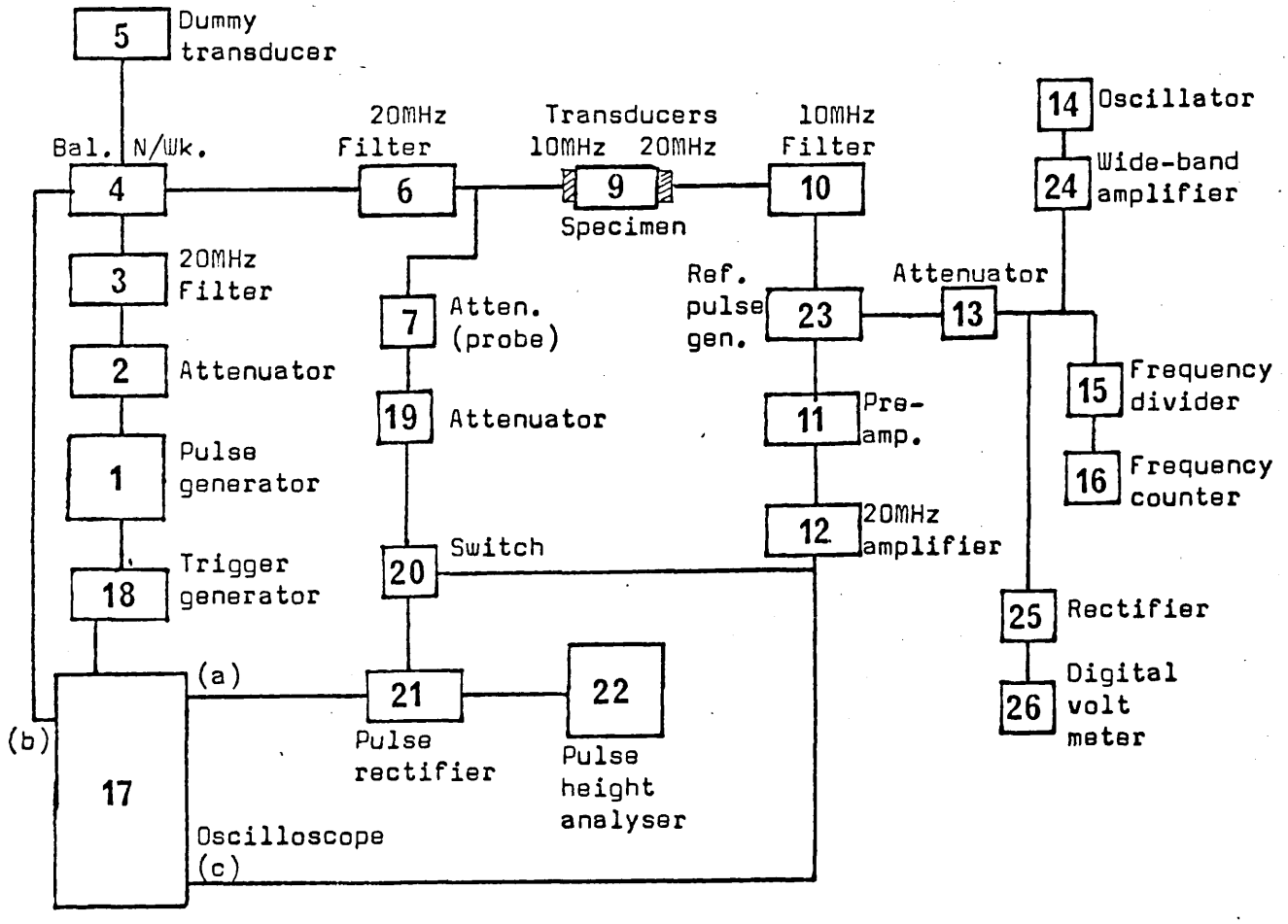

Fig. 4.12. Block diagram of the second harmonic system incorporating the pulse height analyser.

Table 4.2.

1 to 18		See table 4.1.
19	-	Solartron 600Ω attenuator, AT-201.
20	-	Two-way switch.
21	-	Pulse rectifier, see Fig. 4.13.
22	-	Pulse height analyser: Intertechnique SA-40.
23	-	Reference pulse generator, see Fig. 4.14.
24	-	Keithley type 108 wide band amplifier.
25	-	Rectifier, see Fig. 4.15.
26	-	Solartron digital volt meter, LM-1420.2-M.

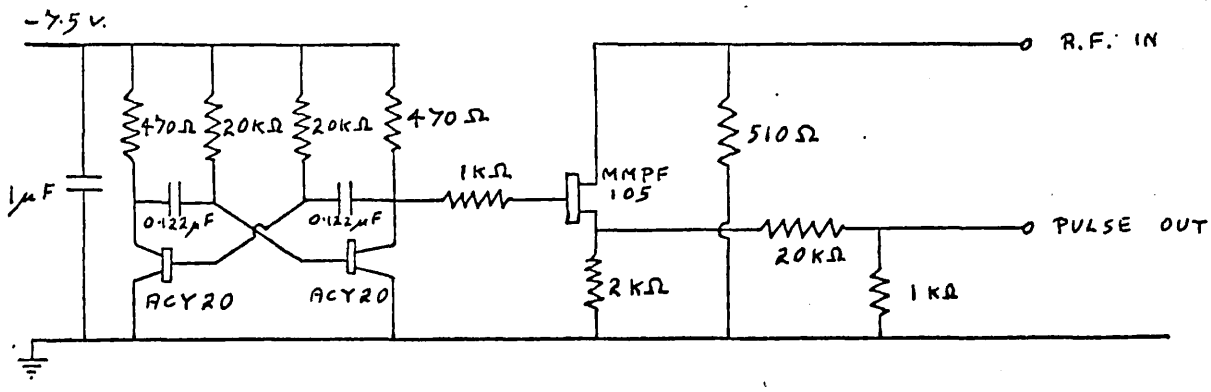

Fig. 4.14. The reference-pulse generator.

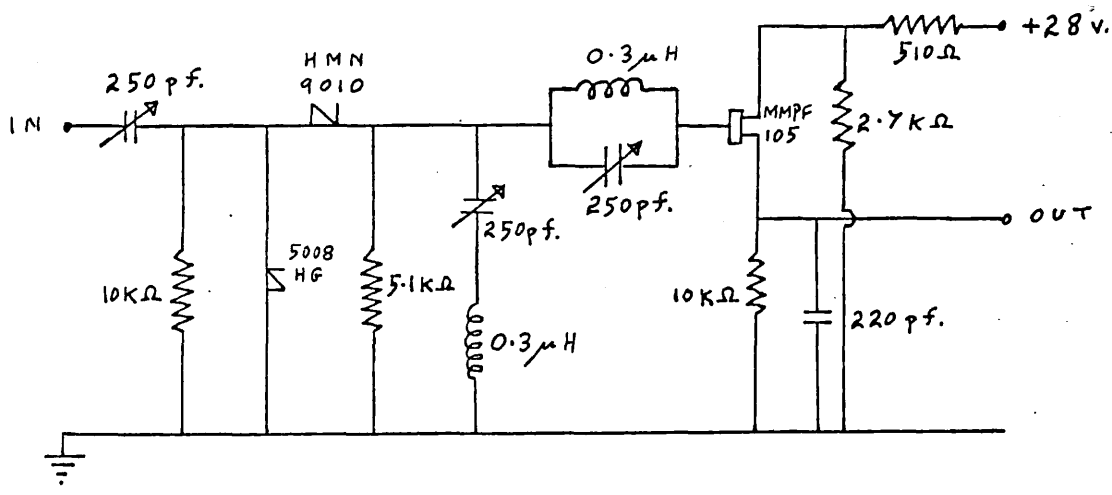

Fig. 4.13. The pulse rectifier.

The normal method involved photographing traces on the oscilloscope screen with a Polaroid Land Camera (Type PLI) and measurement of the recorded pulse amplitudes with a Hilger travelling microscope. In any series of measurements the input pulse was always recorded together with the harmonic signal and a correction made to the harmonic pulse amplitude for fluctuations in input level, assuming a square relationship between the fundamental and harmonic signals. After the apparatus had been allowed to warm up for two hours before use, subsequent fluctuations over a period of some minutes in input signal level were generally less than $\frac{1}{2}\%$. The gain of the harmonic amplifiers was also found to be constant over short periods, although variations of as much as 5% were observed over periods of several hours.

A second method of measuring pulse amplitudes was used in which recordings were made electronically with the aid of a Pulse Height Analyser. This method was found particularly useful when an experimental run required a large number of pulse amplitudes to be recorded, since it eliminated many tedious travelling microscope measurements. It also had the advantage that amplitudes could be determined immediately after measuring without a delay due to photographic processing. The progress of an experiment could then be followed closely. Fig.4.12 shows a block diagram of the system used. Table 4.2 lists the components.

The system is a modification of that already considered. The attenuating probe (7) at the driving transducer is now used for monitoring the driving pulse and not the fundamental echoes. Provision is also made for measuring changes in the gain of the 20 MHz amplifying system over long periods of time. Reference pulses of

20 MHz signal were obtained by using the sinusoidal signal generator (14) in conjunction with the gating circuit(23); the circuit diagram of the gating circuit is shown in Fig.4.14. The amplitude of these pulses was an experimentally determined function of the amplitude of the initial sinusoidal signal. This amplitude was measured by first rectifying the signal with the circuit shown in Fig.4.15 and then measuring the d.c. signal obtained with a digital volt meter (26). The amplifier (24) was included merely to give sufficient signal for the rectifier (25) to operate. The reference pulses were attenuated to a level similar to that of the harmonic echoes by the attenuator (13). These reference pulses could be applied to the input of the amplifier (11) instead of the harmonic pulses. After initially calibrating the reference pulse height against the digital volt meter reading, any changes in measured pulse height not corresponding to a change in digital volt meter reading were attributed to a change in amplifier gain and a correction made accordingly. In this way measurements of pulse height to an accuracy of 2 or 3% could be made over periods of some hours.

Either the pulse from the harmonic amplifiers (11) and (12) or the driving pulse could be selected by switch (20). The selected pulse was then rectified to leave its positive envelope by the circuit (21) of Fig.4.13.

The pulse height analyser (22) was then used to measure the amplitude of the rectified pulse. This instrument sorted pulses into one of 400 channels according to the pulse amplitude, channel number one corresponding to a pulse of zero height while channel number 400 could be set to receive pulses of any fixed voltage between

0.06 volts and 32 volts. In this way channel number is a measure of pulse height, enabling pulse heights to be measured to within about $\pm 1\%$. In addition to distributing pulses into channels according to the pulse height, the instrument also counts the number of pulses put into each channel (up to 10^5 per channel). All this information is displayed on an oscilloscope screen with channel number as abscissa and number of counts as ordinate.

Since the diodes used in the rectifying circuits (21) of Fig.4.13 did not conduct until a voltage of about 0.5 volts appeared across them, it was necessary before using the system of Fig.4.12 to calibrate the channel numbers in terms of true pulse height as determined from photographs taken of the direct unrectified pulse. In order to make a measurement the instrument was set to analyse first the driving pulse, then the harmonic pulse and then the reference pulse for about three seconds each. In the case of pulses from the 20 MHz amplifiers, jitter resulting from the high gain and tuned circuits used led to fluctuations of successive pulse heights about a mean value, and the counts were distributed over ten or fifteen channels. However, because of the method of display on the P.H.A. oscilloscope, the centre channel number was easily determined. In practice, all harmonic echoes except the first were of too low an amplitude to interfere with the readings.

4.10 Experimental Observation of Third Harmonic Generation

4.11 Introduction

The method was essentially similar to that used for

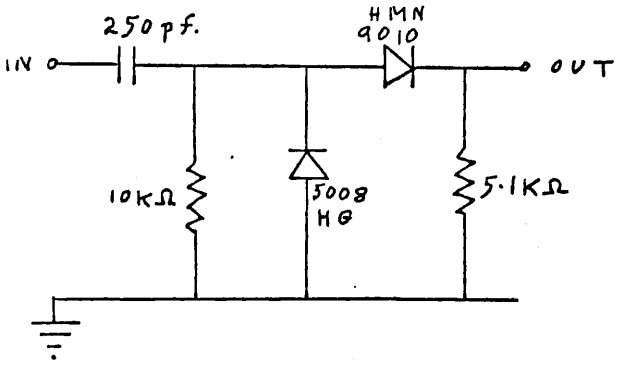

Fig. 4.15. Rectifying circuit.

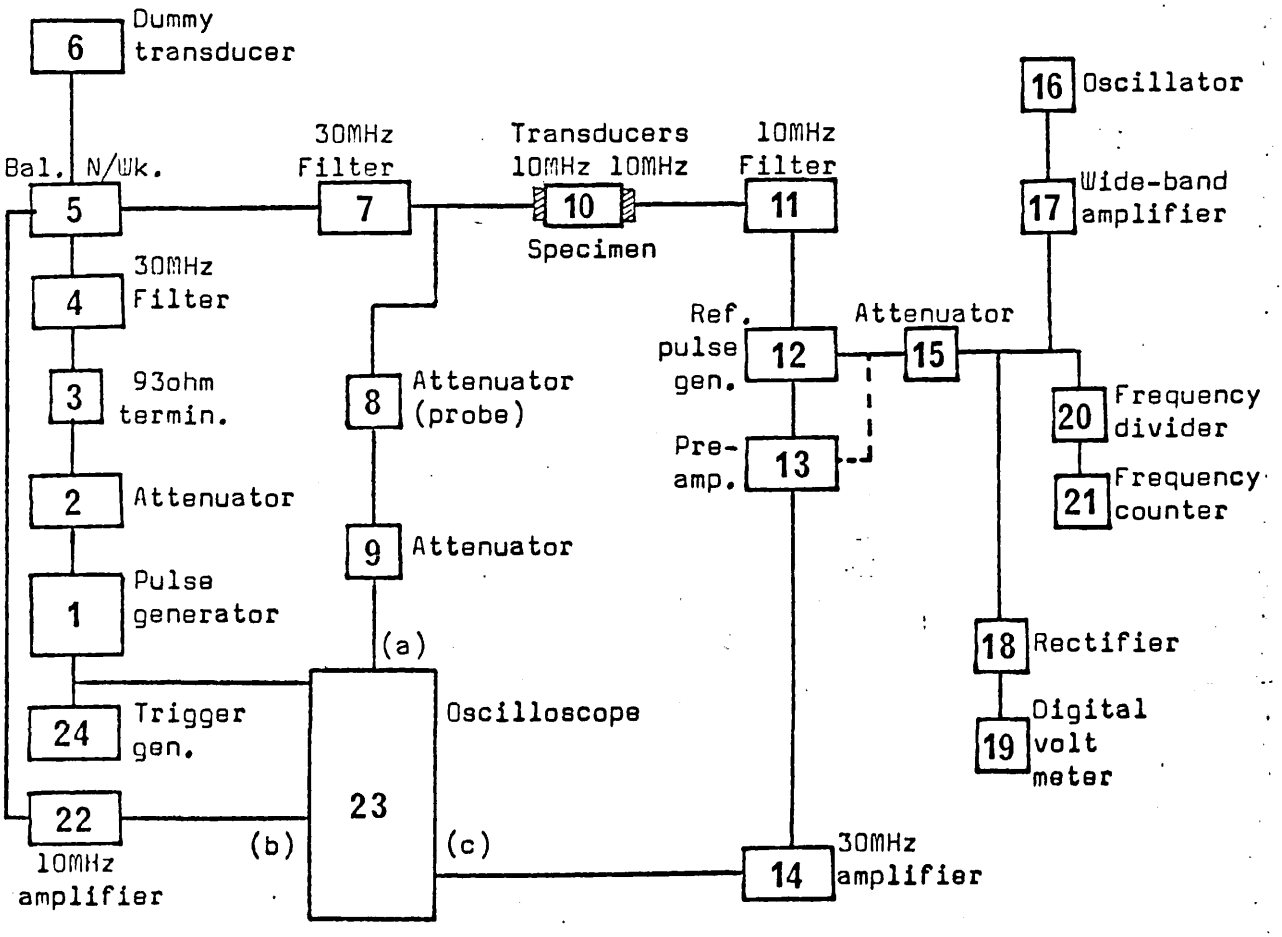

Fig. 4.16. Block diagram of the third harmonic system.

Table 4.3. Details of components appearing in Fig.4.16.

1 Arenberg pulse generator, PG-650-C.
2 Arenberg 93 ohm attenuator, ATT-693.
3 Tektronix 93 ohm termination.
4 Filter, see Fig.4.17.
5 Balancing network, see Fig.4.7.
6 Dummy 10 MHz transducer.
7 Filter, see Fig.4.18.
8 x10 attenuating probe, Tektronix P-6000.
9 Solartron 600 ohm attenuator, AT-201.
10 Specimen.
11 Filter, see Fig.4.19.
12 Reference pulse generator, see Fig.4.14.
13 Arenberg preamplifier, PA-620-B.
14 Tuned 30 MHz amplifier, as in Fig.4.8 with the appropriate tuned circuits.
15 Solartron 600 ohm attenuator, AT-201.
16 Advance signal generator, SG-62-B.
17 Keithley type 108 wide band amplifier.
18 Rectifier, see Fig.4.15.
19 Solartron digital volt meter, LM-1420.2-M.
20 Advance frequency divider, TCD-100-A.
21 Advance frequency counter, TC-4.
22 Tuned 10 MHz amplifier, see Fig.4.9.
23 Tektronix oscilloscope type 555.
(a)Tektronix plug-in unit, 1A1 (Ch.1).
(b)Tektronix plug-in unit, L.
(c)Tektronix plug-in unit, 1A1 (Ch.1).
24 Tektronix time mark generator, 180-A.

the second harmonic, a third harmonic signal level only a little below that of the second harmonic being expected. However, 30 MHz transducers could not be obtained owing to the manufacturers' inability to polish quartz wafers of the required thickness, and two 10 MHz crystals were used with the receiving one being worked at its first odd harmonic.

4.12 The Experimental Arrangement

Fig.4.16 is a block diagram of the experimental system and Table 4.3 gives details of the individual instruments. A signal from the pulse generator(1) passes through an attenuator(2) and a 93Ω termination(3) followed by a 30 MHz filter(4) and then into a balancing network(5). This network was the same as that shown in Fig.4.7. Fundamental echoes returning from the specimen are amplified by the tuned amplifier(22) and displayed on the oscilloscope (23). The input pulse was monitored at the driving transducer with the aid of an attenuating probe(8) and an attenuator(9). The third harmonic signal was detected in the same way as the second harmonic, a reference pulse being obtained to calibrate the harmonic amplifiers as described for the second harmonic system. As in the case of the second harmonic, the frequency of the third harmonic pulses could be measured by comparison with a sinusoidal signal from the oscillator(16) using the mixing facility of the preamplifier(13) [shown as a broken line in Fig.4.16]

Since a 10 MHz transducer is capable of generating a 30 MHz wave the extra attenuation of harmonics from the pulse generator over the fundamental signal does not occur

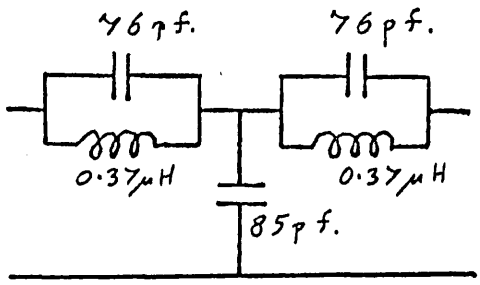

Fig. 4.17. 30MHz filter, 93ohm.

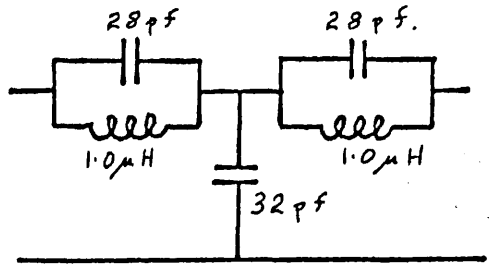

Fig. 4.18. 30MHz filter, 500ohm.

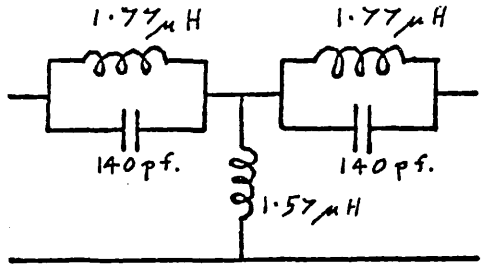

Fig. 4.19. 10MHz filter, 150ohm.

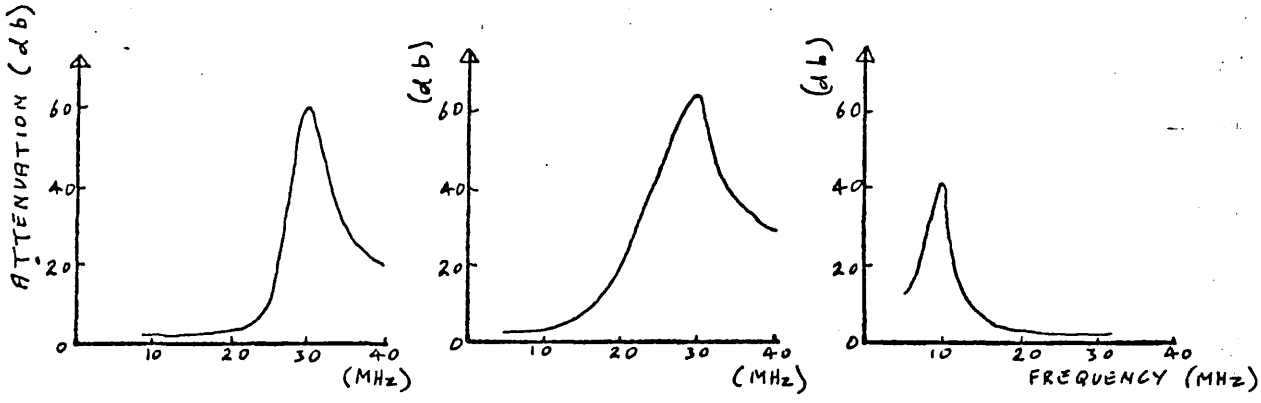

(a) 93ohm filter (b) 500ohm filter (c) 150ohm filter

Fig. 4.20. Filter attenuation as a function of frequency.

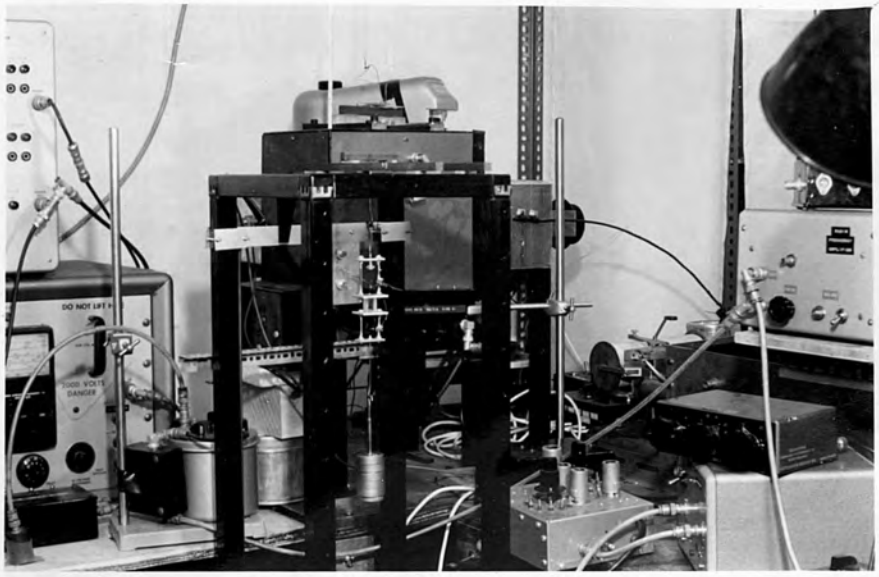

PLATE 1 Part of the 3rd harmonic system

PLATE 2 A mounted NaCl specimen

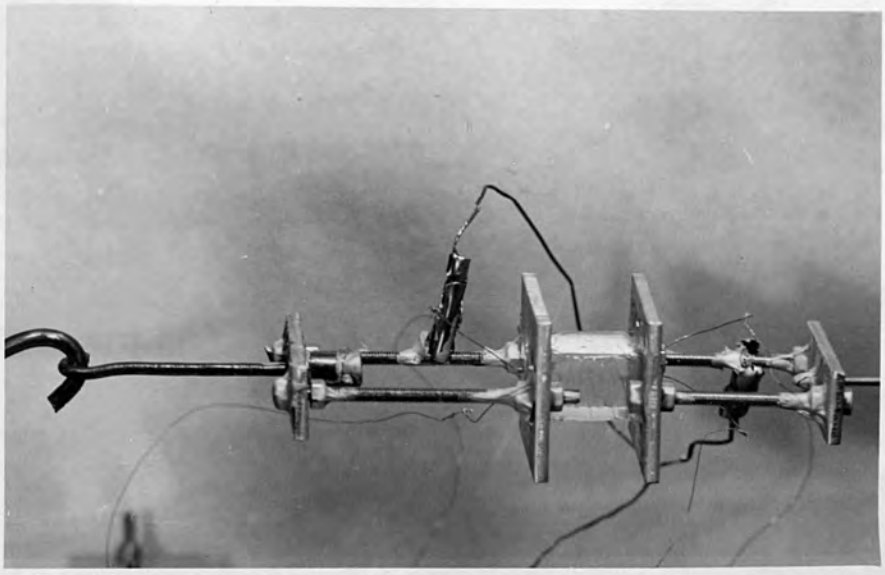

as in the second harmonic system, but the 30 MHz filters were nevertheless found in practice to provide sufficient attenuation. The same consideration applies to the receiving transducer and the 10 MHz filter(11), although again the filter was found in practice to provide sufficient attenuation to prevent excitation of the 30 MHz tuned circuits in the amplifiers(13) and (14). The circuit diagrams of the filters are shown in Figs.4.17, 4.18 and 4.19 while the experimentally determined insertion losses are plotted against frequency in Fig.4.20(a),(b) and (c).

The same alignment procedure was used as for the second harmonic system.

Measurements of pulse amplitude were again made using Polaroid photographs of oscilloscope traces. The pulse height analyser technique was not used since harmonic pulses of sufficient amplitude could only be obtained by driving the 30 MHz amplifiers into a non-linear region.

Plate 1 shows part of the experimental set-up for observing third harmonics in an NaCl specimen. On the left is seen part of the pulse generator, and part of the time mark generator can be seen above it. In the centre foreground is seen a suspended NaCl sample with weights attached to give a bias stress. In the centre rear is seen the constant temperature enclosure (see § 5.7). At centre right is seen the 10 MHz amplifier and below this is the Hounsfield Tensometer (see § 5.6). In the bottom right hand corner are seen the wide-band amplifier and the 30 MHz amplifier. Resting upon the 30 MHz amplifier is a 600Ω attenuator.

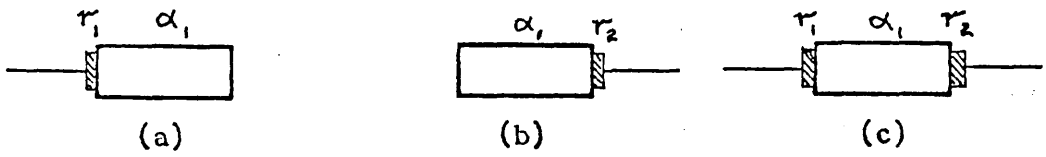

Fig. 4.21. The transducer arrangements for attenuation measurement.

Cut	Thickness	Wave mode	Fundamental frequency	Application
X	0.295mm.	Longitudinal	10 MHz	Generating 10MHz and receiving 30MHz
X	0.145mm.	Longitudinal	20 MHz	Receiving 20 MHz

Table 4.4. Transducer details.

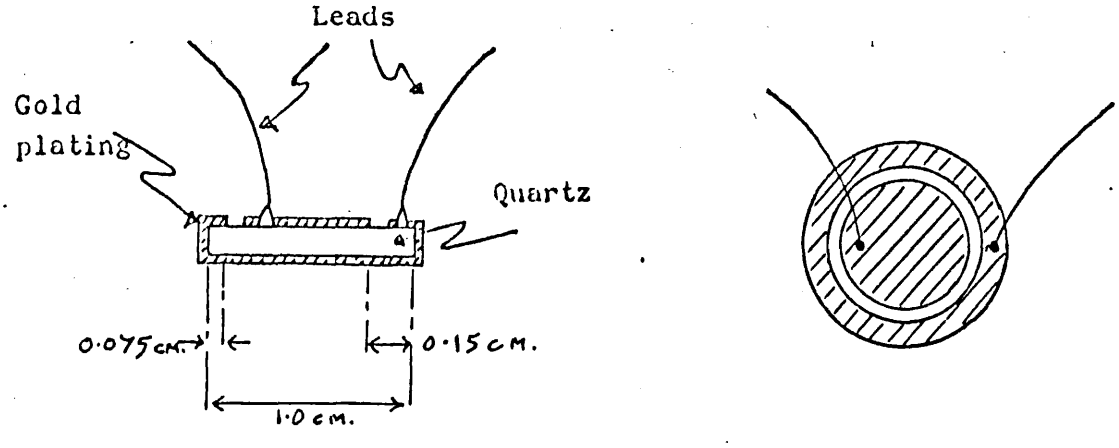

Fig. 4.22. Electrode configuration of the quartz transducers.

4.20 Measurement of Attenuation

The attenuation of a sample was measured with transducers arranged as shown in Fig.4.21. With a transducer at one end as in Fig.4.21(a) the measured attenuation between successive echoes is $\alpha_1 + r_1$, where α_1 is the true absorption and r_1 is that due to the transducer bond. With this transducer removed and a second one attached at the other end as in Fig.4.21(b) the attenuation measured between successive echoes becomes $\alpha_1 + r_2$, r_2 being that due to the second transducer. Finally with both transducers attached as in Fig.4.21(c) the attenuation measured between successive echoes becomes $\alpha_1 + r_1 + r_2$. From these measurements α_1, r_1 and r_2 may be deduced. A typical value found for an NaCl specimen was $r_1 = 0.2$db.

Changes in attenuation could be measured much more accurately and this was the more frequent measurement made. The amplitudes of two echoes A_i and A_j were measured before and after the change occurred, when they became A_i^1 and A_j^1. Equation (4.1) gives the change in attenuation $\delta\alpha$ in db's.

$$\delta\alpha = 20 \ell n_{10} \left[\frac{A_i/A_j}{A_i^1/A_j^1} \right] \quad \text{(db)}. \qquad (4.1)$$

Units of db/μsec were normally used however, when

$$\delta\alpha = \frac{20}{t} \ell n_{10} \left[\frac{A_i/A_j}{A_i^1/A_j^1} \right] \quad \text{(db/μsec.)} \qquad (4.2)$$

where t is the time interval between A_i and A_j.
Changes of about 0.001 db/μsec could normally be measured.

Factors influencing the accuracy of absolute ultrasonic attenuation measurements have been extensively reviewed [Redwood (1964)]. The most important of these are (i) lack of parallelism of end faces, (ii) diffraction effects leading to energy losses from the sides of an ultrasonic wave, (iii) reflection losses at sample ends.

Lack of parallelism of sample end faces between which pulses are being reflected leads to a modulation of the perfect exponential decay, maxima and minima appearing. This is because different ultrasonic path lengths over the area of the transducer give rise to different particle displacements and hence different signals at the transducer, whose output is the sum of all these signals. The effect becomes more important at higher frequencies. Two NaCl crystals had ends professionally polished optically flat and parallel to within a few seconds of arc, when about 50 echoes could be observed at 10 MHz before the first minimum. This was a sufficient number for an attenuation measurement to be made. Other NaCl crystals having cleaved ends were sometimes suitable for absolute attenuation measurements depending on the quality of the cleavage. Aluminium crystals were spark planed flat and parallel to a few minutes of arc only and were not suitable for accurate absolute attenuation measurements.

4.30 Quartz Transducers

The quartz transducers used were thickness mode X cut crystals as listed in Table 4.4. All transducers were 1.0 cm. in diameter and gold plated as shown in

Fig.4.22. The parts of the transducer surface to which leads were attached were first plated with a silver compound using a baking technique to give the leads mechanical strength. Transducers were obtained from The Quartz Crystal Company Limited ready plated and wired, although some crystals were replated with gold at Chelsea after repeated use. The electrode configuration shown in Fig.4.22 was used because it solved the problem of making electrical contact to the face of the crystal in contact with a non-conducting specimen, e.g: NaCl. This method of plating is also reported to influence the energy loss from an ultrasonic wave by diffraction, [Papadakis (1963)]; at certain frequencies and propagation distances this loss may be minimised.

In second harmonic generation measurements care was taken to select a receiving transducer with a fundamental resonant frequency as near as possible twice that of the driving transducer. It was found that most transducers had been manufactured with resonant frequencies within 1% of their nominal values, and matching of transducers was therefore not difficult.

Silicone oil was used as a bonding agent for X-cut transducers. 'Salol', Dow-resin 276-V9, Araldite (resin only) and Araldite (resin + hardener) were investigated but found to have no particular advantage from the point of view of insertion loss or length of service over silicone oil. However, silicone oil bonds were found to deteriorate at temperatures much above 50°C. Transducers were mounted by putting a drop of oil on the underside of the transducer, pressing it onto the sample surface and

then rotating the transducer while applying a slight pressure. The oil then spread out to cover the whole area of the transducer in contact with the specimen and a firm bond was obtained. The amount of oil used was critical, too little giving an incomplete bond and too much causing the transducer to float on a thicker layer of oil. Transducers were unmounted with the aid of carbon tetrachloride.

4.40 The Capacitative Detector

A capacitative detector was constructed for several reasons. Firstly such a detector enables an absolute value of the strain amplitude associated with an ultrasonic wave to be measured. This information is useful in understanding the type of ultrasonic behaviour observed in a specimen. Secondly such a detector may be used to receive harmonic signals, instead of a quartz transducer. This is particularly useful since the detector has a very wide bandwidth, unlike a quartz transducer which must be used at one of its resonant frequencies. Thirdly the specimen surface at which ultrasonic waves are detected is stress free, which makes possible certain experiments concerned with the reflection of ultrasonic harmonic waves, as discussed in § 7.1.

A capacitative detector for the measurement of ultrasonic strain amplitudes as small as 10^{-8} at MHz frequencies in aluminium and NaCl crystals was constructed according to the principles described by Gauster and Breazeale (1966). One surface of the specimen at which

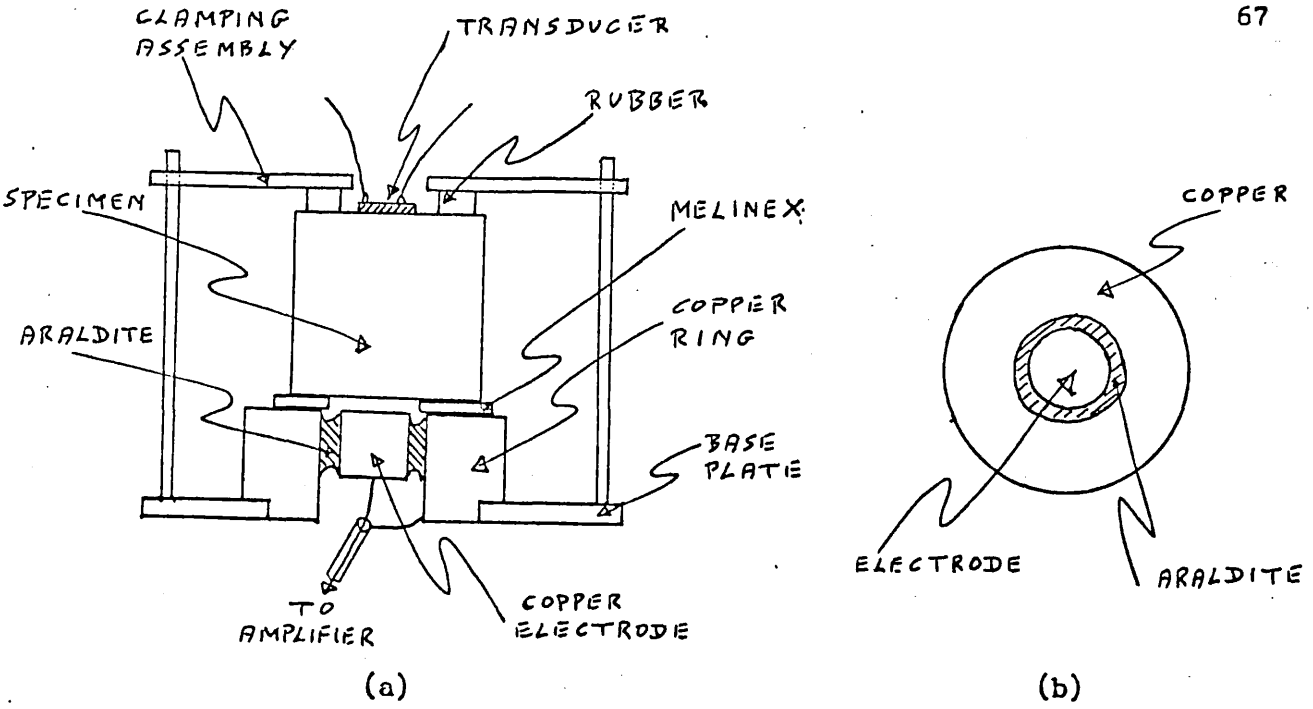

Fig. 4.23. The capacitative detector.

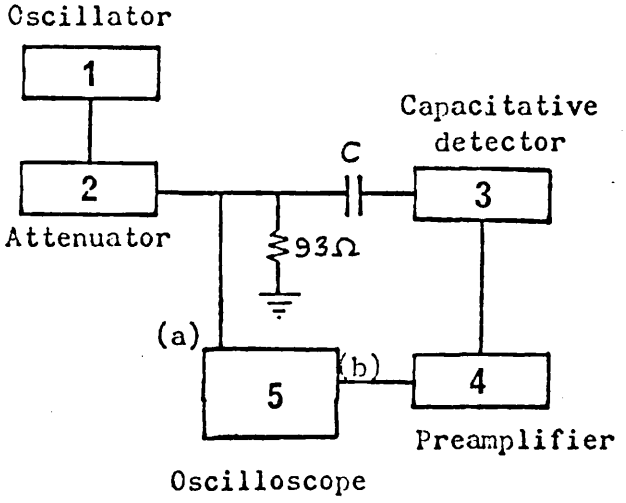

Fig. 4.24. Calibration system for the capacitative detector.

Table 4.5.

1	Advance Oscillator SG-62-B.
2	Arenberg Atten. ATT-693.
3	Capacitative detector.
4	Arenberg pre-amp. PA-620-B.
5	Tektronix oscilloscope 555.
(a)	Plug-in 1-A-1. (channel 1)
(b)	Plug-in 1-A-1. (channel 2)

ultrasonic waves were reflected constituted one "plate" of a parallel plate capacitor, the other plate being an optically polished copper surface. A constant d.c. voltage was maintained across the capacitor and the charge entering and leaving the capacitor as the plate separation was modulated by an ultrasonic wave was amplified and could be related to the amplitude of the ultrasonic wave. The capacitor plate separation was not controlled by an electroplating technique as used by Gauster and Breazeale but by a much simpler method using I.C.I. 'Melinex' sheets. These had thicknesses from 1μ⟶ 100μ and over an area of a few square centimetres were of a uniform thickness to within about 50 optical wavelengths, as determined by an optical interference method. Fig.4.23(a) shows the construction of the detector.

The centre copper electrode of 0.4" diameter, shown from above in Fig.4.23(b), was fixed in the centre of a large copper ring with epoxy resin and the surface of the disc and electrode were polished flat by a hand lapping technique. A disc of Melinex with an 0.5" diameter hole in the centre was placed over the copper electrode and the sample was positioned over this, with a clamping arrangement to ensure that the capacitor gap was determined solely by the Melinex. A quartz transducer was attached to the upper surface of the specimen. In the case of NaCl specimens the surface which was to form part of the capacitor was first optically polished and then given a conducting coating of aluminium. Electrical contact to this surface was made using 'Ag - dag' (a suspension of silver particles in methyl iso-butyl ketone). The capacitor was connected to a

d.c. bias circuit and preamplifier as used by Gauster and Breazeale (1966).

Gauster and Breazeale show that the sinusoidal voltage, V, generated across the capacitor is given approximately by

$$V = V_0 \cdot \frac{u_0}{s_0} , \qquad (4.3)$$

with an error of $\frac{1}{2}\%$, where s_0 is the gap spacing (typically 10 μ), u_0 is the displacement of the crystal end face and V_0 is the d.c. bias voltage (decoupled from the bias power supply with a 1 MΩ resistor). The strain amplitude of the ultrasonic wave is given by $\frac{u_0}{2}$. In practice, the measurement of the gain of the amplifying system, needed for an evaluation of V, limited the accuracy of values obtained for u_0. Changes in capacitor gap spacing as a result of temperature changes experienced by Gauster and Breazeale were to a large extent avoided by the use of Melinex instead of a copper layer to provide the capacitor plate separation. The system used to measure the amplification of the detector is shown in the block diagram of Fig.4.24, with components listed in Table 4.5.

The capacitor C through which the calibration signal is passed to the detector is equivalent to and replaces the gap capacitance. Signal levels before and after amplification were compared using the oscilloscope.

A second capacitative detector was made identical to the one described above except that the electrode diameter was only 0.9 cm. and the preamplifier circuit of Gauster and Breazeale (1966) was not used. This

detector was used to measure the third harmonic content of a 10 MHz fundamental wave in a NaCl crystal. The detector replaced the 10 MHz quartz transducer normally used for observing third harmonic signals. The remainder of the experimental system was as indicated in Fig.4.16. The end face of the NaCl crystal was made conducting by depositing a thin film of aluminium under vacuum. The film was about 500 Å thick.

CHAPTER 5

The Single Crystal Specimens and Ancillary Measurements

5.0 Specimen Preparation

(a) Aluminium Specimens

The aluminium specimens were purchased from Metals Research Limited (Cambridge), and could be obtained with nominal impurity densities of one part in 10^4, 10^5 and 10^6, designated 4N, 5N and 6N respectively. They were single crystals 50 mm. long and 12 mm. in diameter with a ⟨100⟩ direction along the cylindrical axis. The tolerance on the coincidence of the crystallographic and geometric axes was $\pm 3^0$. The cylindrical surfaces were coarse spark planed to give a uniform circular cross-section (for constant force per unit area when the crystal was stressed) while the ends were fine spark planed to give surfaces suitably flat for attaching transducers and sufficiently parallel for reflection of an ultrasonic wave between the crystal ends [Truell and Oates (1963)]. The advantage of spark planing is that little mechanical damage is done to the bulk of the material.

(b) Sodium Chloride Specimens

Sodium chloride crystals were obtained from two sources, Hilger and Watts Limited, and Gulton Industries Limited. Only crystals from the second supplier, which

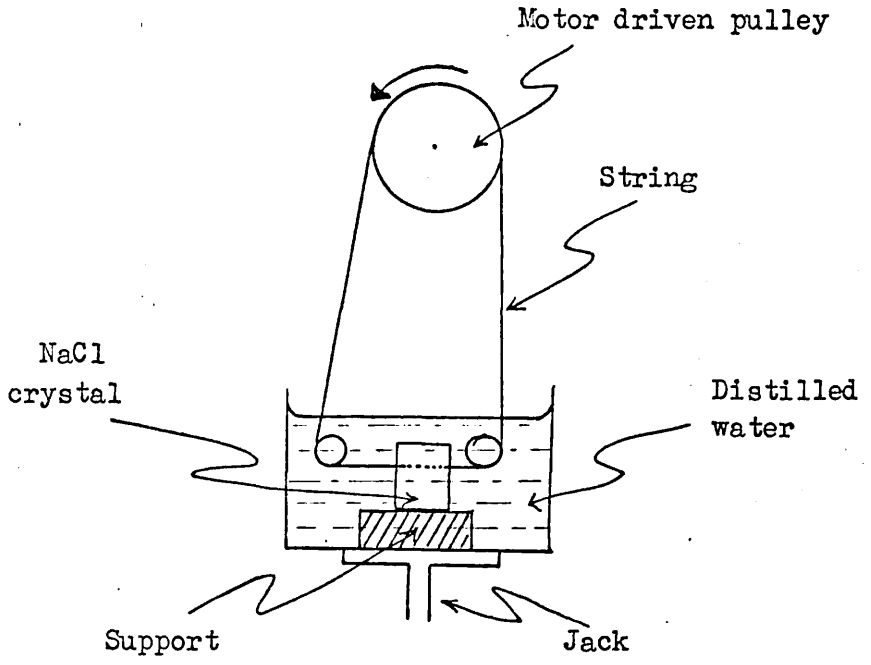

Fig. 5.1. The string saw, (diagrammatical).

Impurity	%	Impurity	%
Lead	5.10^{-6}	Thallium	1.10^{-6}
Copper	5.10^{-6}	Barium	5.10^{-4}
Cobalt	5.10^{-6}	Strontium	3.10^{-4}
Nickel	1.10^{-6}	Calcium	5.10^{-5}
Zinc	1.10^{-6}	Magnesium	1.10^{-5}
Iron	5.10^{-6}	Lithium	4.10^{-5}
Aluminium	1.10^{-6}	Potassium	1.10^{-3}
Manganese	5.10^{-6}	Total (approx.)	2.10^{-3}%

Table 5.1. Impurity content of the specially grown NaCl crystal.

were grown by the Stockbarger-Bridgman technique, showed a detectable dislocation contribution to harmonic generation and they were used for almost all the measurements made. The material was bought in cleaved blocks of approximately 1"x1" cross-section and lengths of between 3" and 5". Some specimens were cut from this material with the aid of a string saw. Specimen sizes varied, some being approximately 1.25cm x 1.25cm x 2.5cm (6 samples) and some approximately 1.25 cm x 1.25cm x 8.0cm (4 samples). The string saw is shown diagrammatically in Fig.5.1. A loop of cotton driven by a pulley was run over the surface of an NaCl block immersed in water. Rapid dissolving of NaCl occurred in the region of the string, which then penetrated the crystal. The crystal was slowly raised to keep pressure on the cotton. The outer surfaces of the crystal were protected from dissolving slowly themselves by a coating of perspex cement. This method of cutting was used rather than cleaving because (a) long thin blocks were difficult to obtain by cleavage, and (b) less mechanical damage was done. However, some further samples were prepared by cleavage alone, these having dimensions 2.5cm x 2.5 cm x 10cm (one sample) and 3cm x 1.25cm x 1.25cm (4 samples).

The ends of the samples were prepared for attaching transducers by cleavage, but because of the difficulty of obtaining surfaces free from cleavage-steps early specimens were short, typically 2.5cm long. Later specimens had end surfaces mechanically polished after cleavage. However, the ends of these crystals were not normally sufficiently parallel for attenuation measurements to be made. Polishing was done on glass lapping blocks by hand using methyl alcohol as a lubricant, with

final polishing on a Selvyt Cloth with jewellers rouge. It was possible to obtain surfaces flat to within a few tens of optical wavelength, as indicated by optical interference fringes produced with the aid of an optical flat.

An especially pure boule of NaCl was also obtained, which had a stated impurity content as set out in Table 5.1.

It was found that cleavage was often more successful if the crystal was first annealed at approximately 650°C (M.P. = 801°C). The annealing procedure is described in § 5.3.

5.1 Estimation of the Relative Purity of Aluminium Crystals

The method used was an adaptation of that due to Bean, De Blois and Nesbitt (1959) in which the electrical resistivity of a crystal is measured at room temperature and at liquid helium temperature by an eddy current technique. The resistivity of a metal at room temperatures is determined primarily by interactions of conduction electrons with lattice vibrations and is largely independent of the purity of the metal. As the temperature is reduced the resistivity decreases approximately as the temperature to some power, until at liquid helium temperature of 4.2°K scattering from impurity centres becomes important in determining the resistivity. The value of the resistivity at 4.2°K is very sensitive to the purity of the metal, and the ratio $\frac{\rho_{300}}{\rho_{4.2}}$ may be used to classify different samples according

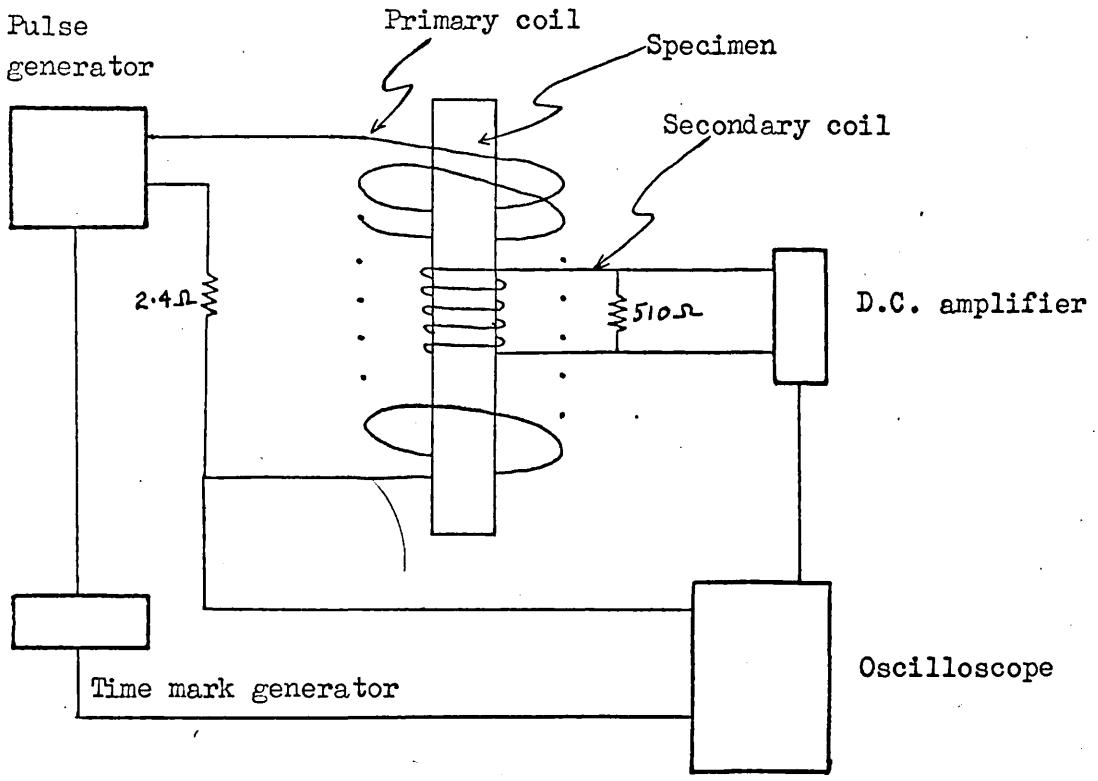

Fig. 5.2. The experimental system for resistivity measurement.

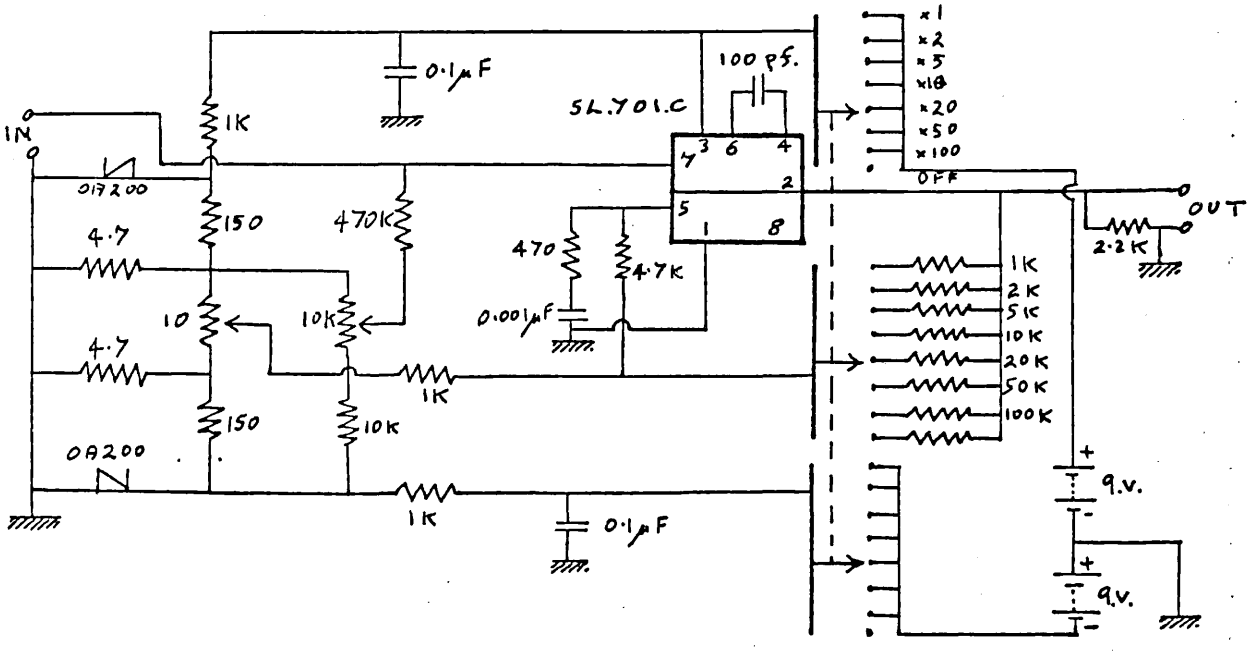

Fig. 5.3. The D.C. amplifier.

to their purity.

The resistivity was determined by noting the rate of decay of magnetic flux in a specimen when an externally applied magnetic field was rapidly reduced to zero. Resistivities in the range $10^{-11} \longrightarrow 10^{-3}$ ohm. cm. could be deduced. Fig.5.2 shows the system used. The pulse generator gave a square pulse of current into a 2.4 Ω resistor and a primary coil wound round a specimen. The changing flux through the specimen was picked up in a secondary coil, which was shunted with 510 Ω, and amplified by a d.c. amplifier (see Fig.5.3), before being displayed on an oscilloscope. The pulse generator was triggered by a signal from the Time Mark Generator which also provided time markers on the oscilloscope screen and the oscilloscope time base was triggered from the pulse generator.

Bean, De Blois and Nesbitt (1959) show that for a specimen of circular cross-section the voltage across the secondary coil after removing the magnetic field approaches a simple exponential, according to

$$V(t) \longrightarrow 10.N.\rho H_o \exp\left(-\frac{t}{\tau_r}\right) \qquad (5.1)$$

after a time of the order of $\tau_r/2$, where

$$\tau_r = 2.17\mu R^2 \frac{10^{-9}}{\rho} \qquad (5.2)$$

Here N is the number of turns in the secondary coil, ρ is the resistivity and μ the permeability of the specimen, H_o is the magnetic field, R is the radius of the sample. Fig.5.4 shows oscilloscope traces of the

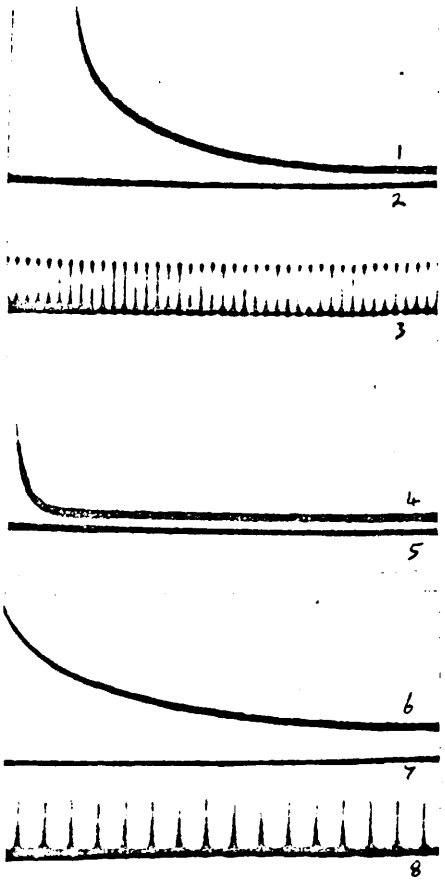

1. V(t) at 300°K, with specimen.
2. Zero signal line.
3. 10 μ sec. time markers.
4. V(t) at 300°K, without specimen.
5. Zero signal line.
6. V(t) at 4.2 K, with specimen.
7. V(t) at 4.2 K, without specimen.
8. 5 msec. time markers.

Fig. 5.4. Records of resistivity measurements in an aluminium rod.

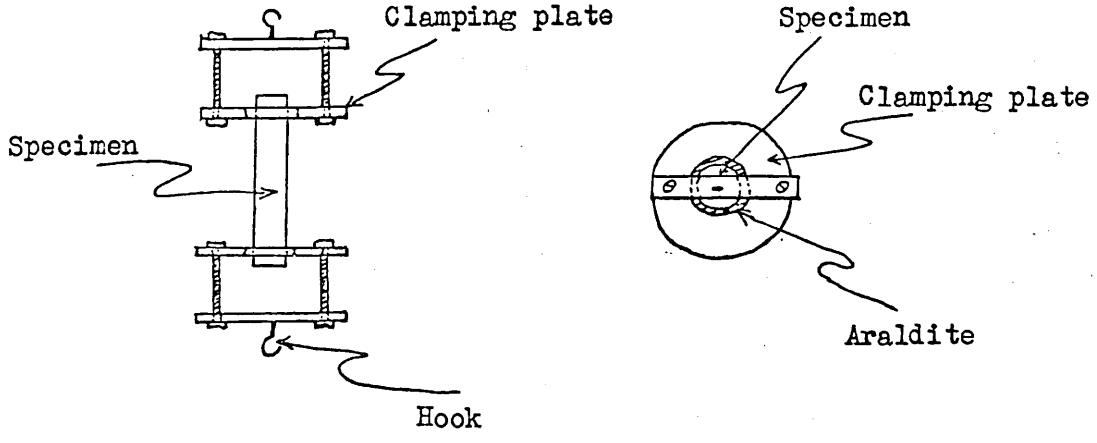

Fig. 5.5. Side and end views of a mounted aluminium specimen.

signal detected by the secondary coil for an aluminium specimen of 6.4 mm. diameter at room temperature and also at 4.2°K. The ratio of τ_r at each temperature gives the resistivity ratio $\frac{\rho_{300}}{\rho_{4.2}}$.

The primary of the coil was designed with sufficient turns to give a suitable value of H_o and this was not found to be very critical. The secondary was designed with sufficient turns to give an observable output signal while at the same time keeping its self-resonant frequency $>> \frac{1}{\tau_r}$. The 510Ω resistor was included to damp out self-resonant oscillations. The coil used at 293°K had a primary of 105 turns and a secondary of 77 turns, while the 4.2°K coil had a primary of 105 turns and a secondary of 5,000 turns.

The advantage of the method is its simplicity, the absence of any need to attach electrical leads to the sample and the ability to use the samples directly without reshaping them. A disadvantage is that the value of τ_r can correspond to frequencies at which "skin depth" effects are appreciable, leading to resistivities of surface material rather than bulk material. This effect was not important in any of the measurements actually made.

5.2 Specimen Mounting

Both the aluminium and the sodium chloride crystal specimens were mounted in a similar way which enabled axial stresses to be applied to them. Metal plates with

suitable holes in the centre to fit a particular specimen were attached at each end of a specimen using 'Araldite'. Fig.5.5 illustrates the mounting method for an aluminium specimen. Plate 2 shows a mounted sodium chloride specimen. Hooks for suspending the specimen and attaching weights were fixed to the metal plates with brass screws. Care was taken to align the specimen and hooks axially and to earth the specimen and all the metallic parts of the attached assemblies. 'Ag-Dag', a suspension of silver particles in methyl iso-butyl ketone, was much used for this latter purpose.

5.3 The Annealing of Specimens

It was usually necessary to anneal the single crystal specimens, and for this purpose an annealing oven was constructed. The annealing oven consisted of a $2\frac{1}{2}$" diameter silica tube 18" long and surrounded by fire brick and sheet asbestos to give outside dimensions of 15" x 15" x 24". A filament was wound round the outside of the silica tube. The ends of the tube were sealed, one end permanently, with fire brick plugs and silica wool. A Pt-Pt/Rh thermocouple was inserted through the centre of the sealed end and the e.m.f. generated between this junction and a similar one at $0^{\circ}C$ was measured with a potentiometer to determine the temperature of the oven. Temperatures of $800^{\circ}C$ could be attained and the temperature gradient over a 3" central region of the furnace tube was not more than $2^{\circ}C$ per inch. The heater current was from a 2 K.W. variac connected to the mains supply. The variac output was mechanically controlled with an

electric motor and a series of reduction gears so that the temperature of the oven could be either raised or lowered between room temperature and ~ 750°C over several days. The speed of the electric motor was also controlled with a variac. The maximum rate of heating or cooling could be restricted to about 10°C per hour. Samples were normally placed on a porcelain slab in the oven. However some Al samples were annealed in vacuo. This was done by sealing the Al sample in a spectrosil silica tube under vacuum, together with a carbon boat for the Al crystal to rest in. This carbon boat, made from spectroscopically pure carbon, was further purified before use by boiling in a mixture of 50% HCl and 50% double distilled water for 48 hours, then boiling in double distilled water for two days changing the water eight times.

5.4 X-irradiation of Sodium Chloride Samples

In order to carry out studies of dislocation-point defect interactions in sodium chloride samples it was decided to introduce colour centres into certain samples. A convenient way of doing this is by X-irradiation, which introduces, amongst other things, F-centres into an NaCl lattice.

A General Electric X-ray machine was used which could give up to 225 Kv X-rays at a tube current of up to 15 mA. Typical dose rates used in these experiments were 10^2 rads/minute. Specimens to be irradiated (usually with grips and transducers mounted) were normally about

3 cm x 1 cm x 1 cm and were placed with the long axis perpendicular to the X-ray beam. Because the density of colour centres produced decreased with X-ray penetration distance, all four sides of a specimen were in turn exposed for equal times to the X-ray beam in order to obtain a more uniform colour centre density. To prevent the F-centres being converted to F_1-centres the samples were irradiated and stored in a black paper box. Measurements were likewise made in a light proof apparatus. The density of F-centres introduced was determined by measuring the absorption as a function of wavelength with an automatically recording spectrophotometer (Unicam SP.800). The absorption peak was centred at 463mμ and from the measured absorbance at this wavelength the F-centre density could be calculated using published tables and Smakula's formula [Markham (1966)].

5.5 Etch Pit Studies of Dislocation Densities in NaCl.

The dislocation densities in the sodium chloride crystals used for ultrasonic harmonic generation experiments were of interest since these densities are an important parameter determining the amount of harmonic generation to be expected. The effect of an anneal on the dislocation density in a crystal may also be evaluated if some method of measuring dislocation density is available. In the present work dislocation densities in NaCl were estimated using a solution etching technique.

Many etchants for NaCl have been reported [Barber(1962)] and the one used in these experiments was ethyl alcohol

saturated with mercuric chloride [Gimpl, Fuschillo and Nelson (1965)]. Etching times of between one and five seconds were employed, followed by rinsing with n-butanol and drying in a current of dried air. The etch-pits could then be viewed with a microscope using oblique illumination and magnifications of about x100. Areas of crystal surface were photographed using a Polaroid Land Camera so that densities of etch pits could be evaluated.

Surfaces to be etched were either cleaved surfaces, which could be etched directly, or surfaces prepared by polishing. A polishing technique was developed in which the surface to be polished was held horizontally about 3 mm above and 8 cm from the centre of a 30 cm diameter turntable electrically driven at about 20 revs./minute. The turntable was covered to a depth of 3 mm with a mixture of 50% glycerol and 50% n-butanol. After polishing the surface was cleaned with pyridine. In this way the surface of the crystal became sufficiently well polished for etch pits to be observed over large areas without any appreciable number of dislocations being introduced by the polishing operation. This latter point was checked by repeated etching and polishing of a crystal.

5.6 Static Stressing of Specimens.

Two methods of subjecting specimens to a static stress were used. When the force required was less than 15×10^6 dynes, suitable weights were simply attached to

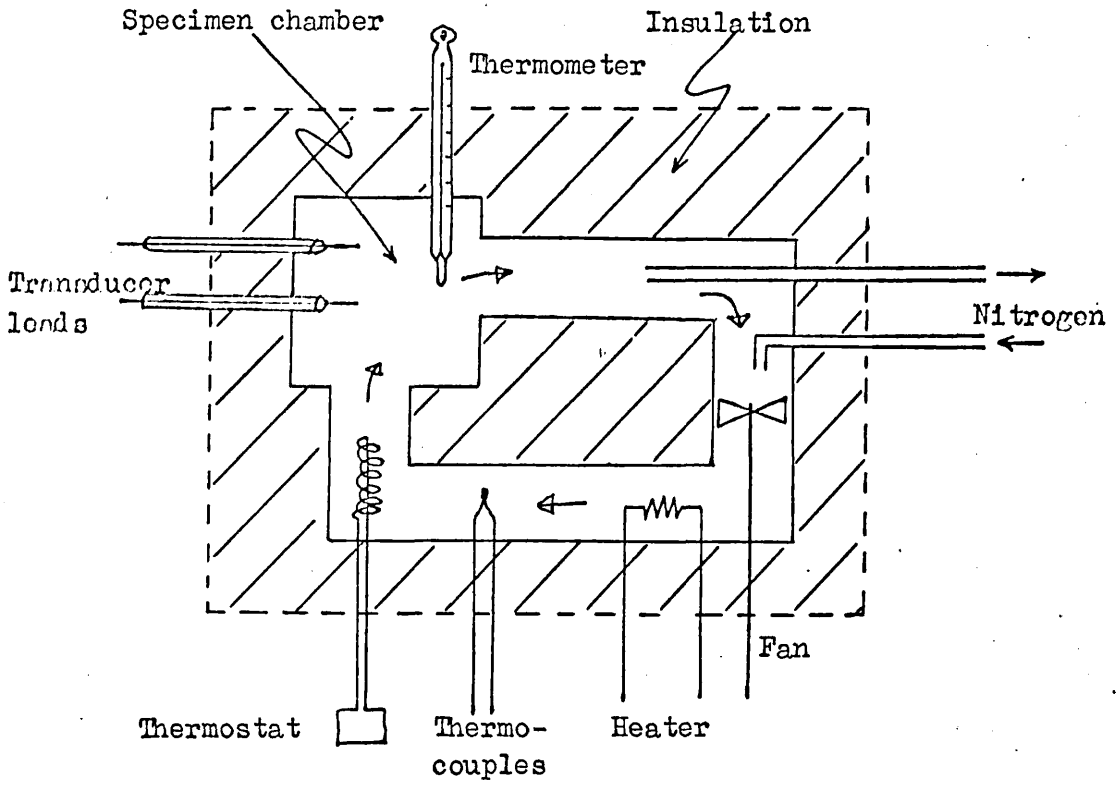

Fig. 5.6. The constant temperature enclosure.

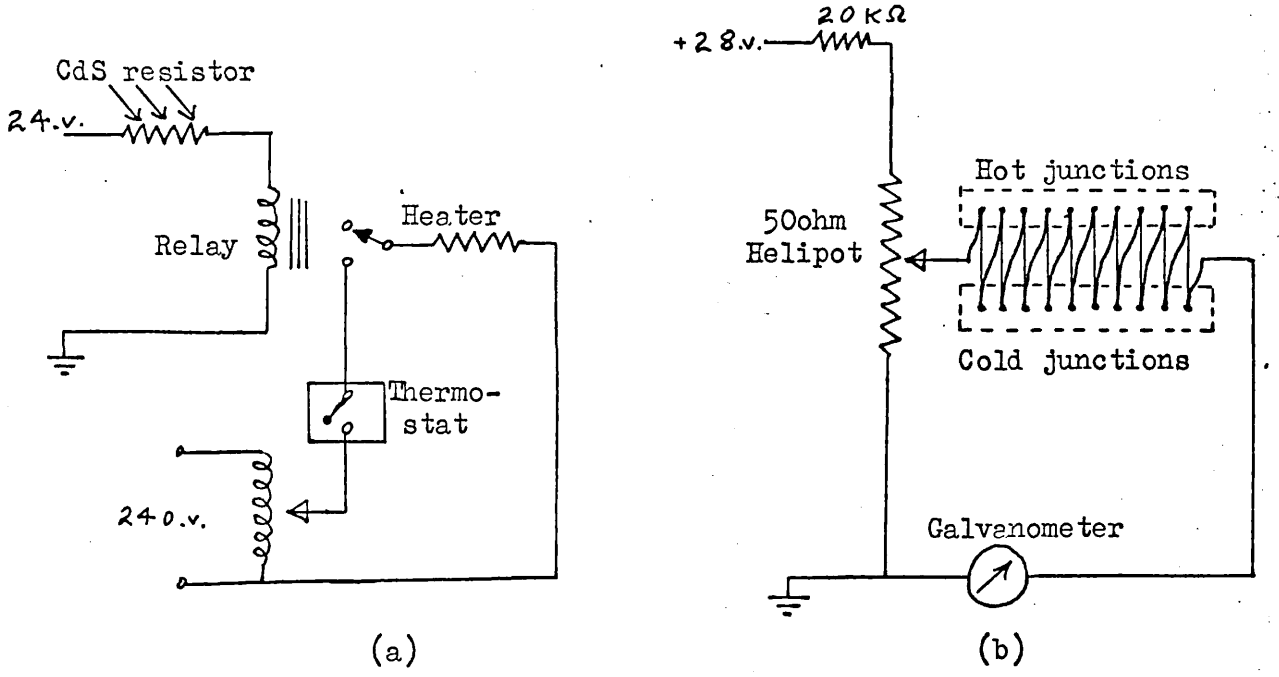

Fig. 5.7. The circuitry used in the constant temperature enclosure.

the specimen. Tensile stresses were obtained by suspending the specimen vertically and adding weights to a pan attached to the lower end of the specimen, as indicated in Fig.5.5. Compressive stresses were obtained by supporting the lower end of a specimen and attaching the weight pan to the upper end of the specimen. Care was taken to ensure that specimens were always stressed axially.

A Hounsfield Tensometer was used to apply forces greater than 15×10^6 dynes. This machine could apply forces of up to 2×10^9 dynes in tension or compression.

5.7 The Constant Temperature Enclosure.

In order to make measurements on specimens at various temperatures a constant temperature enclosure was constructed. A specimen in this enclosure could be subjected to bias stresses while ultrasonic measurements were simultaneously being made. Temperatures between $77^{\circ}K$ and $425^{\circ}K$ were possible. Fig.5.6 shows diagrammatically the apparatus which was constructed.

A recirculating system was used in which air was continuously withdrawn from one side of the specimen chamber, passed through a temperature controlling system and returned to the chamber. The specimen chamber measured 10" x 6" x 6" and the channel for circulating air had a square cross-section of 2" x 2". Construction was of polyurethane foam, all interior parts of the system being insulated from the outside by at least a $1\frac{1}{2}$" thickness of this material. The whole apparatus was encased

in sheet aluminium. The temperature of the specimen chamber was recorded with a thermometer. Transducer leads passed through the chamber walls. A small hole in the bottom of the chamber allowed bias stresses to be applied to specimens enclosed in the chamber. Air was circulated in the sense of the arrows marked on Fig.5.6 by means of an electrically driven fan. A heating element next to the fan was used to raise the air temperature, and cold nitrogen gas could be pumped in on the low pressure side of the fan to lower the air temperature. The temperature was detected by ten copper-constantan thermocouple junctions placed between the heater and the specimen chamber. A mechanical thermostat was placed after the thermocouples. Figs. 5.7(a) and (b) show the circuitry which was used to control the temperature.

The e.m.f. across ten thermocouples connected in series was applied to the sliding contact of a 50Ω Helipot across which a constant voltage was maintained using a stabilised d.c. power pack. The sliding contact of the Helipot was adjusted so that the Scalamp galvanometer gave zero deflection. The cold thermocouple junctions were kept in liquid nitrogen to provide a sufficiently constant low temperature reference. A change in air temperature in the enclosure resulted in a galvanometer deflection of about 3 cm. per ^{o}C. The motion of the galvanometer light spot was detected using a light sensitive Cd.S. resistor attached to the inside of the galvanometer scale. Operation at temperatures above room temperature will be considered first. When the resistor was not illuminated the relay of

Fig.5.8(a) was inactivated and power was supplied to the heater from a variac causing the temperature in the enclosure to rise. This caused the light spot to move towards the resistor. When a certain fraction of the light spot became incident on the resistor, the resistance fell from about 100KΩ to about 500Ω, when sufficient current passed through the relay to operate it and cut off the heater current. The temperature in the enclosure then fell, the thermocouple e.m.f. dropped, the light spot moved away from the resistor and the relay was inactivated again completing the heater current circuit. The light spot then moved back to the resistor and the cycle repeated. In this way temperature fluctuations over short periods in the specimen chamber were kept less than $0.1^{\circ}C$, while long term fluctuations were less than $1^{\circ}C$. To achieve the same stability at temperatures widely different from room temperature it was necessary to have two heaters, one of which was on continually to partially counteract heat losses. Ten thermocouple junctions were used instead of one to reduce the effect of stray thermal e.m.f.'s generated in other parts of the circuit on the temperature stability of the system. The operating temperature could be changed by adjusting the Helipot. Since a failure of the galvanometer bulb would result in the heater current flowing permanently, a mechanical thermostat was included in the heater circuit and set to cut out a few degrees above the operating temperature. This thermostat required a temperature change of $2^{\circ}C$ to operate it.

Temperatures below room temperature were achieved by evaporating liquid nitrogen in a storage dewar by

dissipating heat in a 10 W. resistor and circulating the cold nitrogen gas into the enclosure. To prevent a build-up of gas pressure, a small tube open to the atmosphere was incorporated between the specimen chamber and gas inlet tube. Cold gas was produced at a rate to keep the chamber temperature somewhat below that required and the heating system described above was then used to raise the temperature and control it.

CHAPTER 6

Some Measurements on Aluminium Crystals

6.0 Introduction

In order to establish that the experimental set-up described in Chapter 4 could be successfully used to investigate the generation of harmonics of an ultrasonic wave, an attempt was made to repeat some of the measurements already published in the literature. Hikata, Chick and Elbaum (1965) have investigated the dislocation contribution to the second harmonic of a 10 MHz compressional wave in aluminium, and Hikata, Sewell and Elbaum (1966) have made similar measurements in aluminium on the third harmonic. The aluminium crystals used in both references measured 127 mm x 9.7 mm x 9.7 mm, had purities from 99.99% aluminium upwards and the 127 mm axis lying in either the <100>, <110> or <111> crystal direction.

A crystal of 99.99% aluminium 50 mm long, with a circular cross-section 12 mm in diameter and with the cylindrical axis lying in the <100> crystal direction was obtained. The dimensions correspond to one of the suppliers standard crystal sizes. This crystal was used initially for second harmonic measurements. Subsequently, two further crystals were purchased, differing from the above crystal only in purity, one being 99.999%pure and the other 99.9999% pure. Henceforth these two crystals will be referred to respectively

as the 5N and 6N crystals. The 99.99% crystal will be referred to as the 4N crystal. The ratio of electrical resistivity at room temperature to that at liquid helium temperature, $\frac{\rho_{300}}{\rho_{4\cdot2}}$, was measured for the 4N and 6N crystals and found to be respectively 450 and 2,250. The crystals used by Hikata, Sewell and Elbaum (1966) had values of $\frac{\rho_{300}}{\rho_{4\cdot2}}$ lying between 270 and 3,100.

In Chapter 3 expressions were given for the second and third harmonic amplitudes. These were of the form

$$A_2 = \frac{\rho_o \omega^2}{k} \left[X^2 + Y^2 - 2XY \cos 2(\delta_{10} + \delta_{20}) \right]^{\frac{1}{2}} A_{10}^2, \quad (6.1)$$

where X represents the lattice contribution and Y is given by

$$Y = \frac{48 N b^4 R^3 q C' A_o}{\pi^2 A^3 S_o M_o^{\frac{1}{2}} L_o^2}, \quad (3.15)$$

and

$$A_3 = \frac{12 \rho \omega^2 N b^4 q R^3 C C'}{k A^4 S_o^{3/2} T_o^{1/2} L_o^4} A_{10}^3 . \quad (6.2)$$

It is seen that A_2 is a function of static bias stress A_o, loop length L_o, dislocation density N and the fundamental wave amplitude A_{10}, while A_3 is a function of loop length L_o, dislocation density N and the fundamental wave amplitude A_{10}, but not directly of static bias stress (only through L_o). Hikata, Chick and Elbaum (1965) and Hikata, Sewell and Elbaum (1966) investigated the dependence of A_2 and A_3 on these parameters. Similar

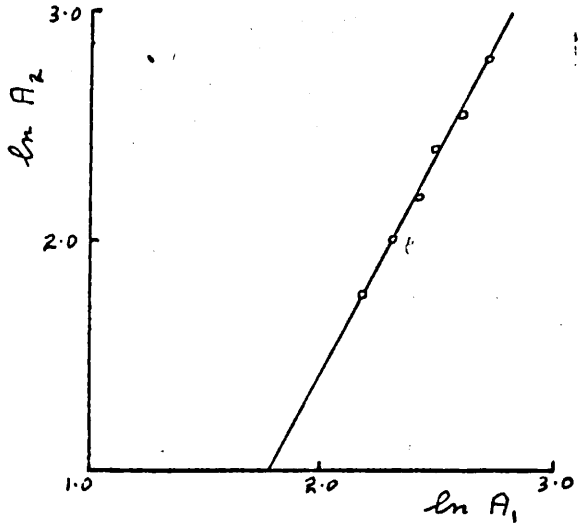

Fig. 6.1. The relation between the fundamental wave amplitude A_1 and the second harmonic wave amplitude A_2 in the 4N aluminium crystal, (arbitrary units of amplitude).

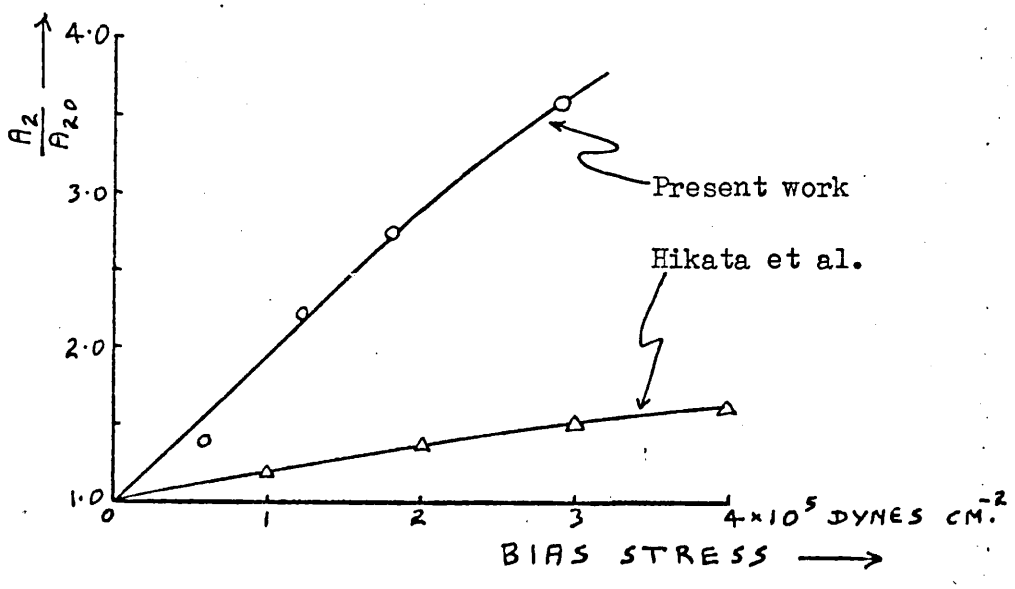

Fig. 6.2. The second harmonic amplitude change with bias stress in the 5N crystal, normalised to the amplitude at zero bias stress A_{20}. For comparison the measurements of Hikata, Chick and Elbaum (1965) are also shown.

experiments performed in the present work are discussed below and compared with those of Hikata et al.(1965) and (1966). In addition some further experiments are noted which show a time dependence of both A_2 and A_3. This effect has been studied in some detail, and the results of the investigation are given in Chapter 9.

6.1 An Investigation of Second Harmonic Behaviour

(a) Measurements with the 4N crystal.

Using the 4N aluminium crystal described above second harmonic echoes were obtained, and Fig.6.1 shows the dependence of the second harmonic wave amplitude on the fundamental wave amplitude. Provided the attenuation of the fundamental wave due to the generation of higher harmonics is small, the second harmonic wave amplitude is expected to vary as the square of the fundamental wave amplitude [see equation (6.1)], and this is seen to be true to a good approximation. Similar behaviour was observed with a polycrystalline rod of commercial aluminium. These results are consistent with those of Hikata, Chick and Elbaum (1965).

A difference between the present measurements and those reported by Hikata et al.(1965) is that no maximum in the harmonic echo pattern after the first received harmonic pulse was observed in the present case. However, this may be attributed to differences in the attenuation of the two samples.

The second power relation suggested that the

harmonic signals were not spurious but were coming from the aluminium crystal. However, a more positive proof of this would be given by a dependence of harmonic wave amplitude on bias stress, since this could be related to dislocations in the crystal.

Attempts to find a dependence of second harmonic wave amplitude on a static tensile bias stress at stresses up to 10^7 dynes cm^{-2} were unsuccessful however. This stress should have been sufficient to alter the dislocation configuration in the crystal. It was concluded that any contribution of the dislocations in the crystal to the second harmonic generation was masked by a much larger lattice contribution. Equation (6.1) indicates that the dislocation contribution increases linearly with bias stress and dislocation density and with the fourth power of dislocation loop length, while the lattice contribution is independent of bias stress (for the values of stress used in these experiments). When a dislocation loop length of 2.10^{-4} cm is assumed and a dislocation density of 10^6 cm^{-2} (typical values), the bias stress required for the two contributions to become equal in magnitude is found to be about 10^6 dynes cm^{-2}. However, if the dislocation loop length is instead taken as 10^{-4} cm, then the bias stress necessary for equality of the two contributions is increased by a factor of 16. A smaller dislocation density likewise increases this bias stress. The failure to observe a bias stress dependence of the second harmonic amplitude is not therefore surprising, since the crystal was relatively impure and dislocation loop lengths are not expected to have been large.

The 'as grown' crystal is also expected to be in a fairly annealed state, with a low dislocation density.

Plastic deformation is expected to increase the dislocation density and may also increase the dislocation loop length. The static bias stress needed to alter the second harmonic amplitude might therefore be smaller after the crystal has been plastically deformed. However, experiments showed that even after plastic deformation, there was no detectable dependence of the second harmonic amplitude upon bias stress.

(b) Measurements with the 5N crystal.

Following the unsuccessful attempts to find a bias stress dependence of the second harmonic amplitude in the 4N crystal, measurements were made on the more pure 5N aluminium crystal.

Dislocation loop lengths in this specimen are expected to be appreciably longer than in the less pure 4N crystal. A bias stress dependence of the second harmonic was indeed found in this crystal. In Fig.6.2 some measurements of this dependence are shown, together with some similar measurements of Hikata, Chick and Elbaum (1965). Both sets of measurements indicate a second harmonic amplitude increasing with bias stress. At a given bias stress the increase in second harmonic amplitude is seen to be greater in the present measurements, probably because a more pure crystal with correspondingly longer loop lengths was used in this work. The crystal used by Hikata et al.(1965) was of

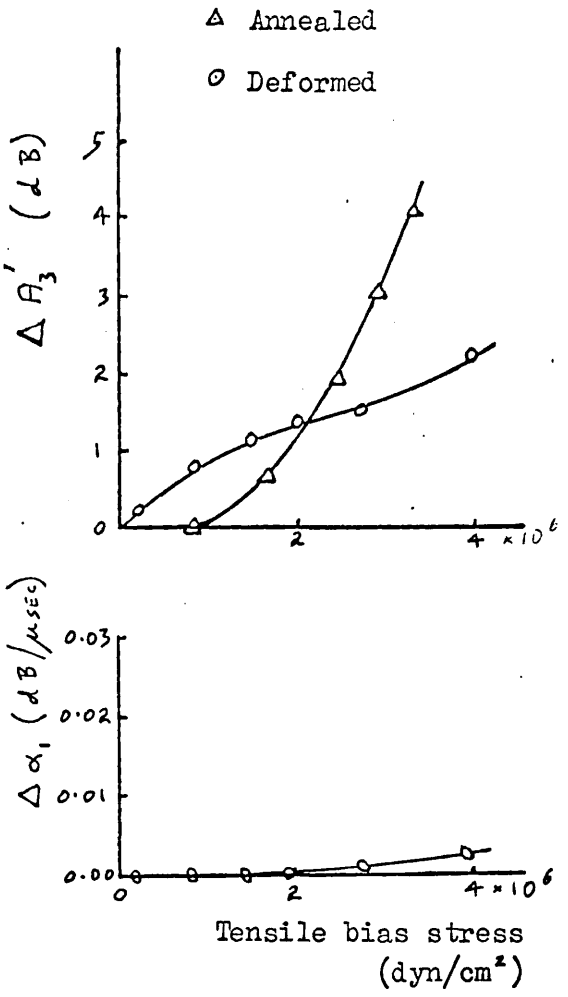

Fig. 6.3. The bias stress dependence of $\Delta A_3'$ in an aluminium crystal for which $\frac{\rho_{300}}{\rho_{4.2}} = 450$ (present work). The deformation was to 10^7 dyn/cm².

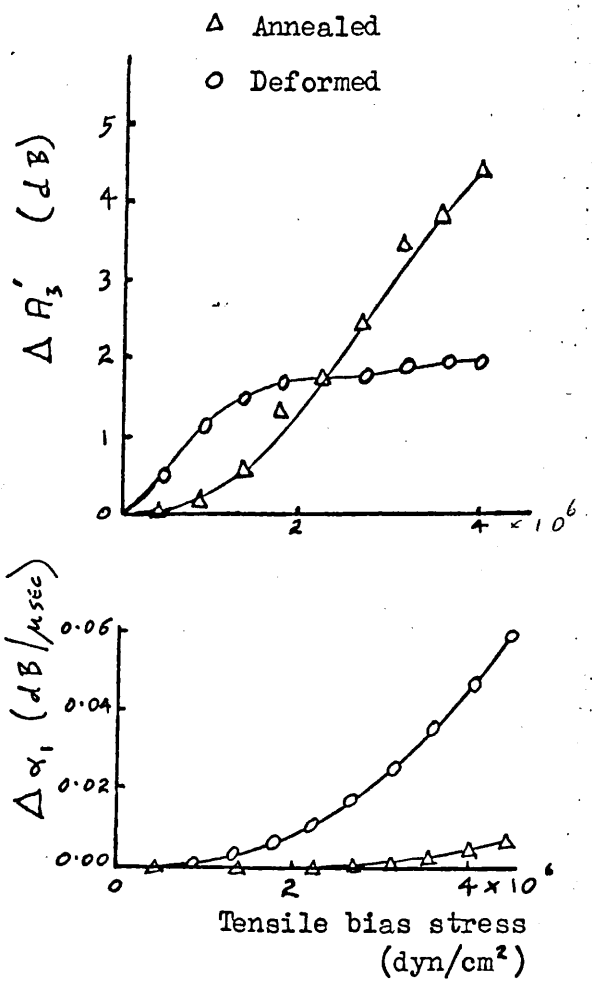

Fig. 6.4. The bias stress dependence of $\Delta A_3'$ in an aluminium crystal for which $\frac{\rho_{300}}{\rho_{4.2}} = 300$, as reported by Hikata, Sewell and Elbaum (1966). The deformation was to 6.7×10^7 dyn/cm².

99.99+% purity.

In the present measurements a time dependent behaviour was found which was not reported by Hikata, Chick and Elbaum (1965). The increase in second harmonic amplitude upon application of a bias stress was found to decay slowly with time while the bias stress remained constant. This behaviour was investigated in some detail and the results of this investigation are given in Chapter 9.

6.2(a) Third Harmonic Measurements in the 4N Aluminium Crystal.

Third harmonic measurements were made using the same 4N aluminium crystal as was used for the second harmonic experiments discussed in section 6.1(a) above. These third harmonic measurements were made, however, before the crystal was plastically deformed.

(i) The Effect of a Tensile Bias Stress.

Third harmonic echoes were observed in the 4N aluminium crystal and a dependence of the amplitude of these echoes on a tensile bias stress was observed. Fig.6.3 shows the observed bias stress dependence of the third harmonic, which is plotted in the form $\Delta A_3'$ as discussed in Chapter 3.2(e). The attenuation change of the fundamental wave is less than 0.001 db/μsec. Also shown are measurements made on this sample some weeks later when it had been reannealed under vacuum at

550^0C for three hours and then plastically deformed at 10^7 dynes cm^{-2} for $5\frac{1}{2}$ hours. The curves of Fig.6.3 are to be compared with those of Fig.6.4 which are the measurements of Hikata, Sewell and Elbaum (1966) on an annealed specimen before and after a prestress of 6.7×10^7 dynes cm^{-2}. The crystals are seen to have similar values of $\frac{\rho_{300}}{\rho_{4.2}}$, and hence similar purities.

Both the annealed specimen of Hikata, Sewell and Elbaum (1966) and the as grown crystal used in the present measurements show an initial slow increase in harmonic wave amplitude with bias stress followed by a more rapid increase. After prestressing, both crystals show a more rapid increase in harmonic amplitude at low bias stresses. The results of Hikata et al.(1966), however, show a saturation effect at larger bias stresses, whereas in the present measurements $\Delta A_3'$ continues to increase. The attenuation changes are also seen to be much greater in the crystal of Hikata et al.(1966).

The difference in the behaviour shown in Figs.6.3 and 6.4 can probably be attributed to the larger prestress given to Hikata et al.'s (1966) crystal, the slight difference in purity of the two crystals and to possible differences in the state of anneal.

An interpretation of the behaviour is given by Hikata et al.(1966) in terms of the distribution of point defects in an annealed crystal, which determine the dislocation loop length. It is expected that in the annealed state the distribution of defects between the bulk material and dislocation lines will be near equilibrium, with a higher concentration at the

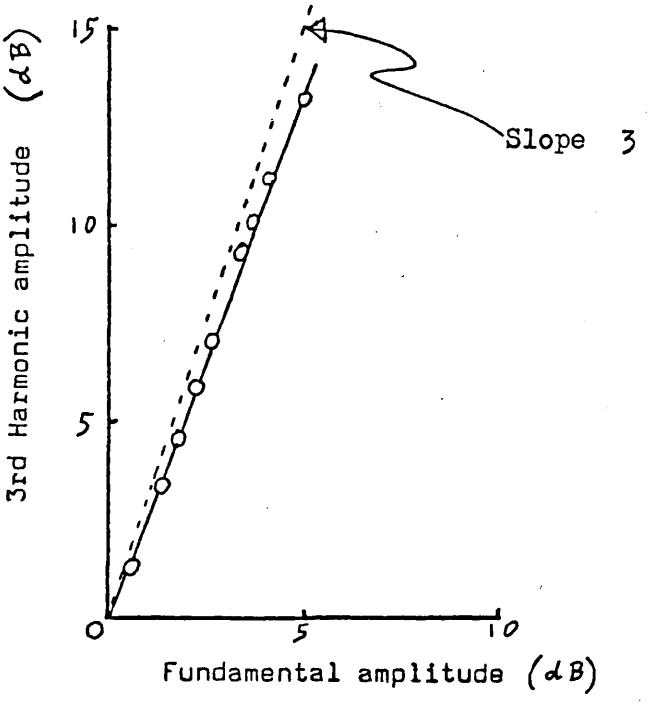

Fig. 6.5. The relation between the fundamental wave amplitude and the third harmonic wave amplitude in the 4N aluminium crystal.

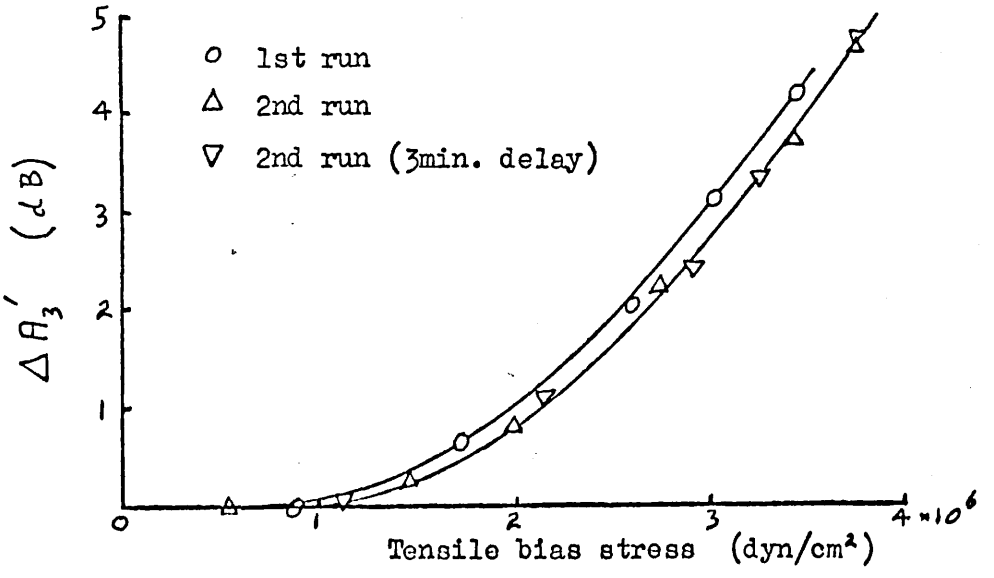

Fig. 6.6. Two measurements of the bias stress dependence of $\Delta A_3'$, in the 4N crystal. The results show (i) good reproducibility, (ii) the absence of any time dependence of $\Delta A_3'$.

dislocations than in the bulk material. After plastic deformation new dislocations will therefore lie in regions of relatively more pure material, assuming that the room temperature redistribution of impurities is slow. Dislocation loop lengths will therefore be longer than was the case in the annealed crystal. This increase in dislocation loop length would lead to the behaviour observed in Fig.6.4 according to the theory of third harmonic generation developed by Hikata and Elbaum (1966). This may be seen by referring to Fig.3.3. Suppose the dislocation loop length in the annealed crystal corresponds to a point to the left of the maximum in $\Delta A_3'$ and the loop length in the deformed crystal to a point much nearer to the maximum in $\Delta A_3'$. Then, since the change in $\Delta A_3'$ with loop length is smaller near the maximum in Fig.3.3, the deformed crystal is expected to show a smaller change in $\Delta A_3'$ with bias stress (ie:- increasing loop length) than is the annealed crystal. A saturation effect is expected if the loop length becomes actually equal to L_m.

(ii) The Effect of the Fundamental Driving Wave Amplitude.

The amplitude of the third harmonic is expected to vary as the third power of the fundamental driving amplitude, providing there is no change in dislocation loop length [see equation (6.2)]. Fig.6.5 shows the observed relation between the fundamental and third harmonic amplitudes. These measurements were made after the plastic deformation and there is seen to be a slight deviation from the slope of 3 condition, a slope of 2.7 being measured. Hikata, Sewell and Elbaum

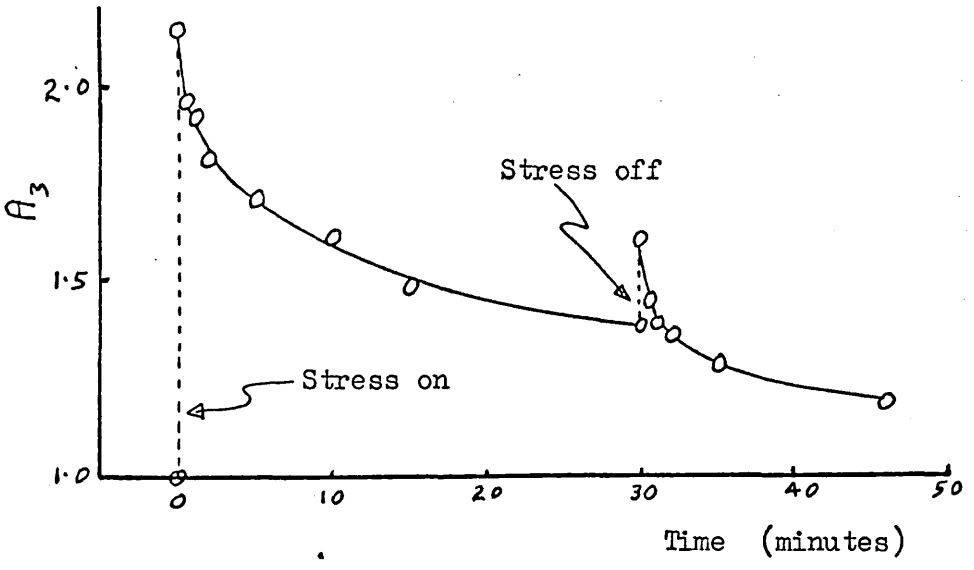

Fig. 6.7. The third harmonic amplitude A_3, normalised to its value under zero bias stress, as a function of time in the 4N crystal. A stress of 3.47×10^6 dyn/cm^2 was applied for a $\frac{1}{2}$hour.

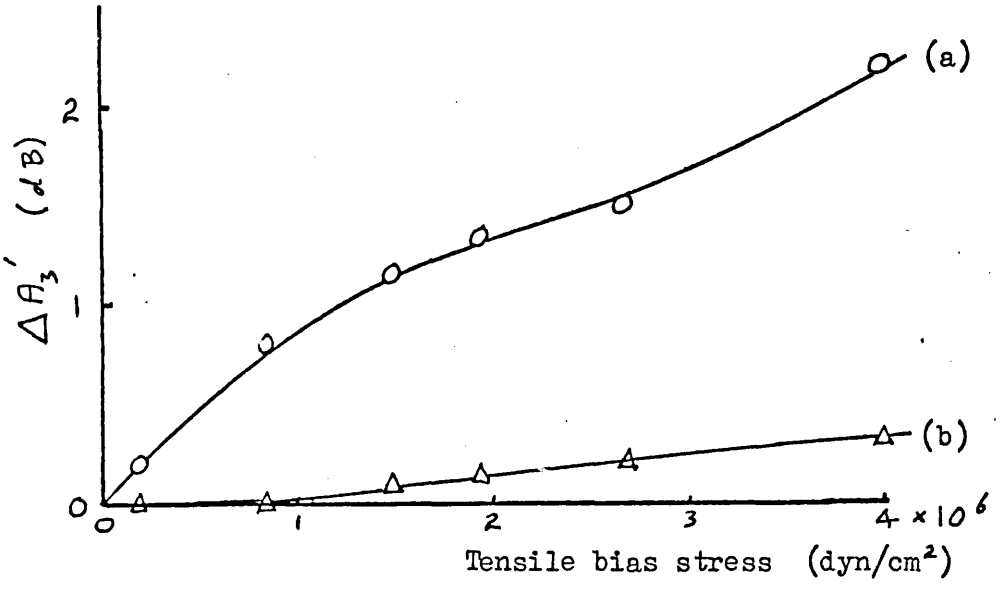

Fig. 6.8. Curve (a) shows the bias stress dependence of $\Delta A_3'$ in the 4N crystal after a deformation to 10^7 dyn/cm^2. Curve (b) shows the remaining change in third harmonic amplitude at zero bias stress after each measurement shown in curve (a).

(1966) noted a similar deviation, a slope of 2.66 being measured with a plastically deformed crystal. Further measurements of the 3rd power relation in the 6N crystal are contained in section 6.2(b) below.

(iii) The Reproducibility of the Third Harmonic Measurements.

The bias stress tests on the 'as grown' crystal were repeated a second time to establish whether they were reproducible or not. In the second experiment measurements of harmonic amplitude were made (i) as soon as a bias stress was applied, and (ii) after the stress had been applied for three minutes. Fig.6.6 shows the results of both experiments. It is seen that the three minute delay had, within the limits of experimental error, no effect on the measurements, ie: there was no time dependent effect present, and the results of the first and second experiments are seen to agree quite well.

A time dependent behaviour was noted however after the crystal was annealed at 550°C for 3 hours and subsequently plastically deformed at a prestress of 10^7 dynes cm^{-2} for $5\frac{1}{2}$ hours. The effect was similar to that already noted with second harmonic experiments in the 5N crystal, [see section 6.1(b)]. Fig.6.7 shows the third harmonic amplitude while a constant bias stress was applied for 30 minutes and then removed. The harmonic amplitude is seen to decay after an initial instantaneous increase when the bias stress was applied. The harmonic amplitude is seen to increase again upon removal of the bias stress, and then to decay again.

Such a time dependence was not reported by Hikata, Sewell and Elbaum (1966).

As a result of the appreciable changes in harmonic amplitude over relatively short times shown by Fig.6.7, bias stresses in subsequent investigations were applied only long enough for a single measurement to be made and then removed before the next bias stress was applied. In Fig.6.8, curve (a) shows the results of a test carried out in this way. Curve (b) shows the value the harmonic amplitude fell to under zero bias stress between each measurement. The harmonic amplitude under zero bias stress is seen to increase slightly during the experiment.

6.2(b) Third Harmonic Measurements on the 6N Aluminium Crystal

Third harmonic measurements were also made using the 6N aluminium crystal for which the resistivity ratio $\frac{\rho_{300}}{\rho_{4.2}}$ had the value 2,250. This was the purest crystal with which harmonic measurements were made. The dependence of the third harmonic amplitude on a tensile bias stress after successive plastic deformations of the crystal will be discussed first.

(i) The Effect of a Tensile Bias Stress

The change in third harmonic amplitude $\Delta A_3'$ and the change in attenuation of the fundamental wave $\Delta\alpha_1$ were measured as a function of tensile bias stress after varying degrees of plastic deformation.

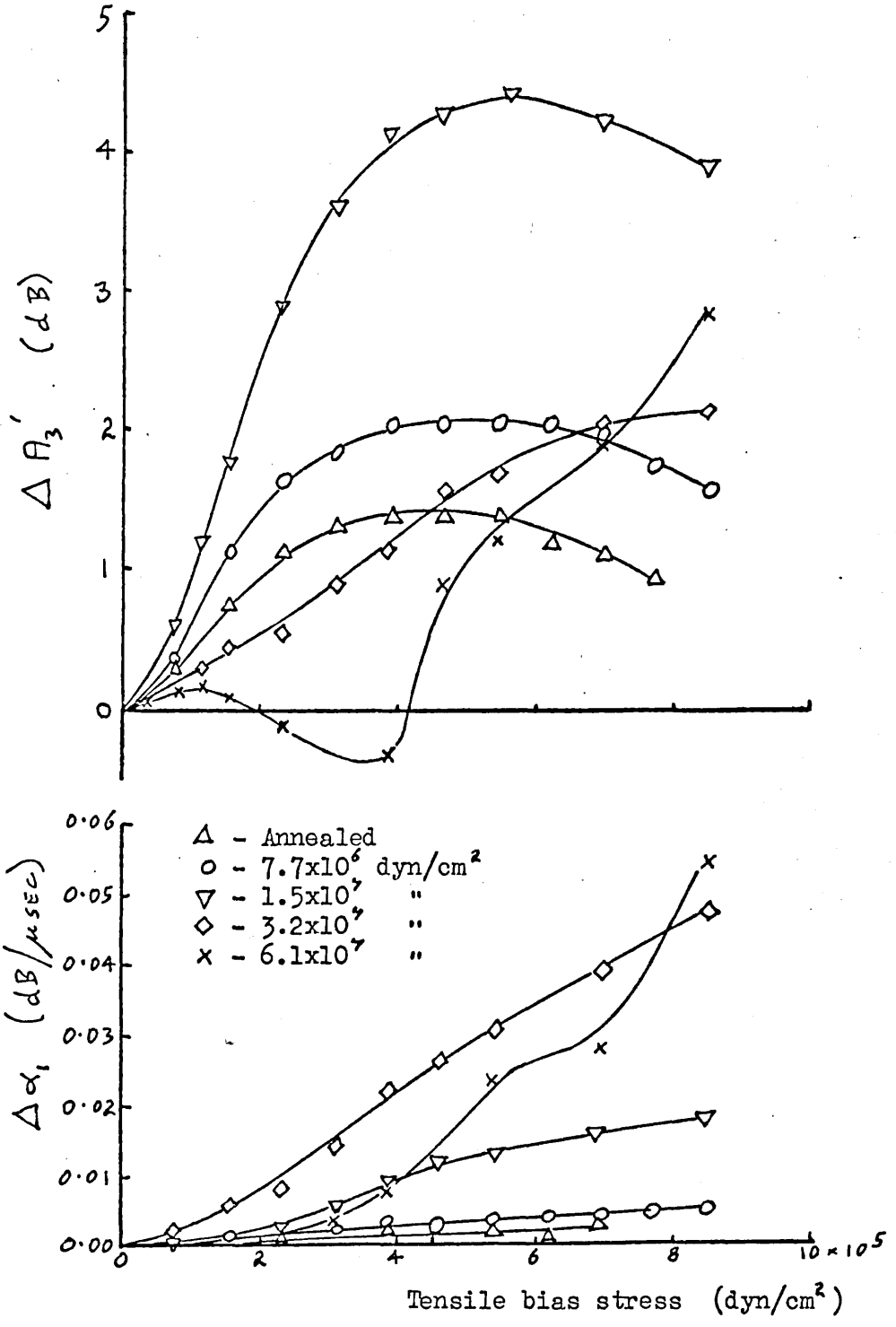

Fig. 6.9. The bias stress dependence of $\Delta A_3'$ in the 6N crystal is shown after successive prestresses in tension. The measurements were all made using the same fundamental wave amplitude.

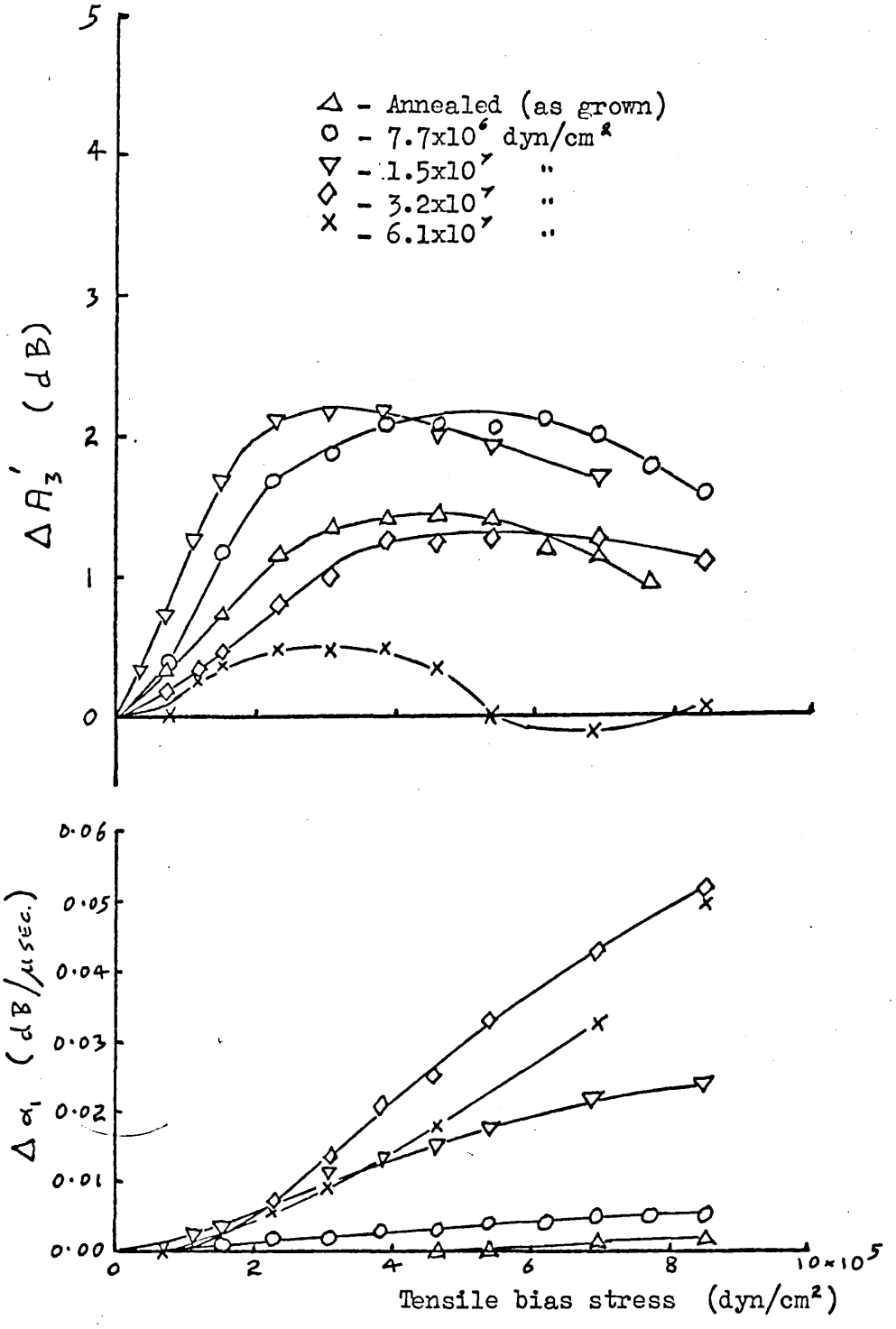

Fig. 6.10. The bias stress dependence of $\Delta A_3'$ in the 6N crystal is shown after successive prestresses in tension. The measurements were made in each case using the minimum possible fundamental wave amplitude.

Fig.6.9 shows measurements made at a constant fundamental driving wave amplitude, while Fig.6.10 shows similar measurements for which the fundamental wave amplitude was adjusted after each plastic deformation to give the same third harmonic amplitude at zero bias stress. Measurements were made on the first received 3rd harmonic pulse. The plastic deformation was found in fact always to increase the third harmonic amplitude at zero bias stress. This is expected from a consideration of expression (6.2) if the plastic deformation increases the dislocation density.

In both Fig.6.9 and Fig.6.10 $\Delta A_3'$ is seen to show a maximum as a function of bias stress after plastic deformation at stresses up to 1.5×10^7 dynes cm^{-2}. The dependence of $\Delta A_3'$ on bias stress after such deformation is seen to be much greater in Fig.6.9. For plastic deformation at stresses greater than 1.5×10^7 dynes cm^{-2} the increase in $\Delta A_3'$ with bias stress is seen to be reduced in both cases. However, in Fig.6.10 a maximum still appears whereas in Fig.6.9 the maximum disappears after the deformation at 3.2×10^7 dynes cm^{-2} and reappears as a very small peak at a bias stress of 1×10^5 dynes cm^{-2} after the final plastic deformation. After the final and greatest plastic deformation both Fig.6.9 and Fig.6.10 show $\Delta A_3'$ to pass through a minimum after the initial maximum. This minimum occurs at a lower bias stress in Fig.6.9 than in Fig.6.10. The changes in $\Delta\alpha_1$ with bias stress increase in both cases after plastic deformation at up to 3.2×10^7 dynes cm^{-2}. After the final plastic deformation however $\Delta\alpha_1$ shows a reduced dependence on bias stress.

The dependence of $\Delta A_3'$ upon the amplitude of the fundamental wave as illustrated by the differences between the curves of Figs.6.9 and 6.10 is investigated in more detail below. Such a dependence was observed by Hikata, Sewell and Elbaum (1966) who attributed it to unpinning of dislocations by the fundamental stress wave. The theory of dislocation third harmonic generation proposed by Hikata and Elbaum (1966), and discussed in Chapter 3, considers the harmonic generation to arise from non-linearities in the simple oscillation of dislocation loop lengths about a mean position. This is the behaviour expected when the attenuation of the fundamental wave is independent of the fundamental wave amplitude, i.e: in the region of the Granato and Lücke (1956) dynamic loss theory. The relation between stress and dislocation strain when the fundamental wave amplitude is large enough to produce unpinning in the first quarter of each stress cycle is also expected to be non-linear, [c.f. the Granato and Lücke (1956) hysteresis loss.] but no analytical theory has yet been devised to include this contribution to the third harmonic generation.

The measurements shown in Fig.6.10 were made using the minimum possible fundamental wave amplitude for which harmonic signals could be measured. These results are therefore more likely to be described by the theory of Hikata and Elbaum (1966) than those of Fig.6.9. Both of these sets of results will however be discussed as far as possible in terms of the equivalent measurements of Hikata, Sewell and Elbaum (1966) and the theory of Hikata and Elbaum (1966).

Comparing the curve of Fig.6.10 for the 'as grown' crystal with the theoretical curve of Fig.3.3, it appears that the dislocation loop length in the crystal is slightly less than L_m. If the bias stress increases the mean loop length by unpinning to a value greater than L_m then the maximum in the curve of Fig.6.10 is explained. The position of the maximum in Fig.6.10 after successive plastic deformations appears to move slightly towards a lower bias stress. This implies that the plastic deformation has created new dislocations with longer loop lengths, ie: loop lengths nearer to L_m. This may be accounted for as follows. In the undeformed crystal the distribution of impurities between the bulk of the crystal and the dislocations is expected to be near equilibrium, with the concentration in the bulk crystal being smaller than at the dislocations. Thus after plastic deformation new dislocations lying in the bulk of the crystal will have a smaller concentration of impurities pinning them than the original dislocations, assuming the room temperature redistribution of defects is slow. The increased loop length after plastic deformation may therefore be accounted for.

The measurements of Fig.6.10 resemble most closely those made by Hikata, Sewell and Elbaum (1966) using an aluminium specimen of <111> axial orientation and of $\frac{\rho_{300}}{\rho_{4\cdot2}} = 1{,}200$. The greater purity of the crystal used in the present work, $\frac{\rho_{300}}{\rho_{4\cdot2}} = 2{,}250$, suggests that the maximum in $\Delta A_3'$ in the undeformed crystal should occur at a lower bias stress in the present measurements. A comparison shows this to be the case, the maxima occurring at bias stresses of about 4×10^5 dynes cm^{-2} and 6×10^5 dynes cm^{-2}. However the measurements of

Hikata, Sewell and Elbaum (1966) indicate a much greater increase in loop length after plastic deformation than is observed here; after a deformation at 3.2×10^7 dynes cm^{-2} $\Delta A_3'$ is found by Hikata, Sewell and Elbaum (1966) to decrease to about -3.0 at a bias stress of 1.0×10^6 dynes cm^{-2}.

There are at least two possible reasons why such a decrease is not observed in the present measurements. Firstly the crystals were left at room temperature for several days after plastic deformation, and this may have given defects sufficient time to diffuse to new dislocations (see Chapter 9). Secondly a larger driving wave amplitude may have been used in the present measurements, leading to a greater dynamic unpinning by the fundamental wave. Hikata, Sewell and Elbaum (1966) point out that harmonic generation due to simple dislocation oscillation (as discussed in Chapter 3) is expected for edge dislocations to be of opposite phase to that resulting from dynamic unpinning of dislocations. The smaller decrease in $\Delta A_3'$ observed in the present measurements is therefore consistent with a system in which both contributions to the third harmonic generation are present, and the operative dislocation system is of a predominantly edge nature. Further evidence of this is given by the results of Fig.6.9. The contribution to the third harmonic from dynamic unpinning is expected to be greater here, since the fundamental wave amplitudes are greater. The curve of Fig.6.9 plotted after a deformation to 6.1×10^7 dynes cm^{-2} shows a much more rapid increase in $\Delta A_3'$ after the initial minimum than does the equivalent curve of Fig.6.10.

The marked increase in the magnitude of $\Delta A_3'$ at a given bias stress after the first two plastic deformations which is observed in both Figs.6.9 and 6.10 was not reported by Hikata, Sewell and Elbaum (1966). An explanation of this behaviour in terms of changes in dislocation loop length and density appears unlikely. However, it is seen from Fig.3.2 that the magnitude of the change in harmonic amplitude with loop length is sensitive to the type of dislocation present. If the undeformed crystal contains a mixture of both edge and screw dislocations, and the plastic deformations tend to produce predominantly edge type, then the observed behaviour may be accounted for. Since the crystal of Hikata, Sewell and Elbaum (1966) has its axis in a <111> direction whereas the axis of the present crystal is in a <100> direction, the deforming stresses will not activate the slip planes of each crystal in the same way.

The primary slip planes in aluminium are {111} planes and the slip directions are <110>. For a crystal with a cylindrical axis in a <100> direction as in the present work, the resolved shear stress in a particular slip plane and slip direction is $\frac{A_o}{\sqrt{6}}$, where A_o is the axial shear stress. For a crystal with a <111> direction along the cylindrical axis as used by Hikata, Sewell and Elbaum (1966) the corresponding resolved shear stress is zero. The two crystals are not therefore expected to show exactly similar behaviour.

In the case of the attenuation changes, the magnitude of $\Delta\alpha_1$ for a given change in loop length increases with dislocation density [Granato and Lücke (1956)]. Thus for a given static bias stress $\Delta\alpha_1$ is

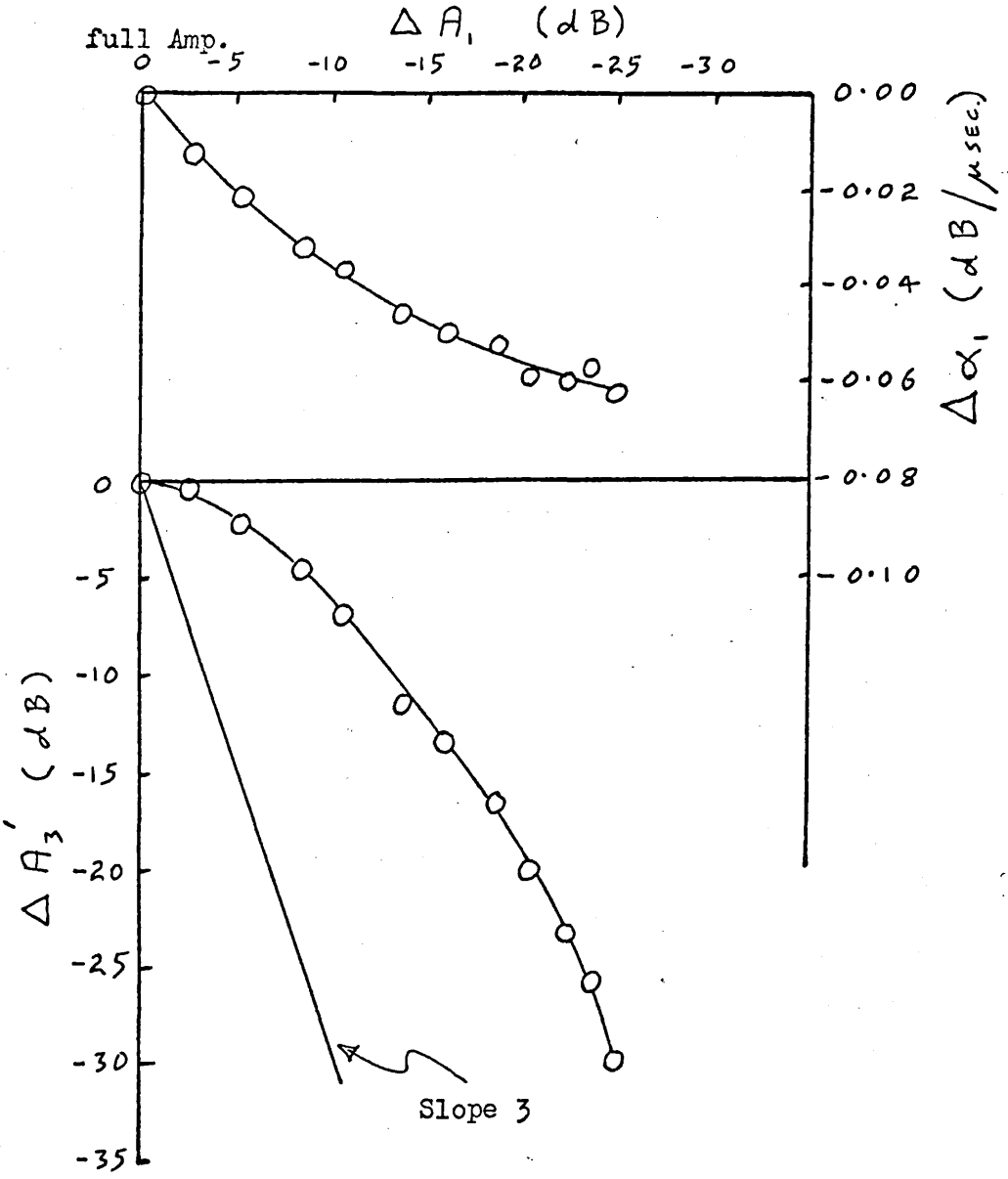

Fig. 6.11. The amplitude of the third harmonic $\Delta A_3'$ and the attenuation of the fundamental wave $\Delta\alpha_1$ as a function of the amplitude of the fundamental wave ΔA_1 for the 6N specimen after a deformation to 1.5×10^7 dyn/cm^2.

expected to be greater in a deformed crystal than in an undeformed one. In fact the magnitude of $\Delta\alpha_1$ for a given bias stress depends not only on dislocation density but also on the loop length before the bias stress is applied. This may be seen from Fig.3.3, which shows that the gradient of the curve of α_1 plotted against loop length decreases as L_o increases beyond L_m.

The results in Figs.6.9 and 6.10 may be interpreted in terms of these two effects. The increases in $\Delta\alpha_1$ at a given bias stress in the curves plotted before plastic deformation and after the first three plastic deformations indicate that the effect of increasing dislocation density after deformation dominates any effect due to loop length changes with bias stress. The corresponding decrease in $\Delta\alpha_1$ after the final plastic deformation indicates that the loop length effect is becoming dominant.

(ii) The Effect of the Driving Wave Amplitude on the Third Harmonic Amplitude.

In Fig.6.11 is shown the change in third harmonic amplitude with increasing fundamental wave amplitude. The change in attenuation of the fundamental wave is also shown. The crystal had first been prestressed to 1.5×10^7 dynes cm^{-2}. At the lowest driving amplitudes the third power relation is seen to hold. At higher amplitudes the third harmonic amplitude is seen to increase very much more slowly than the third power relation predicts. The attenuation of the fundamental

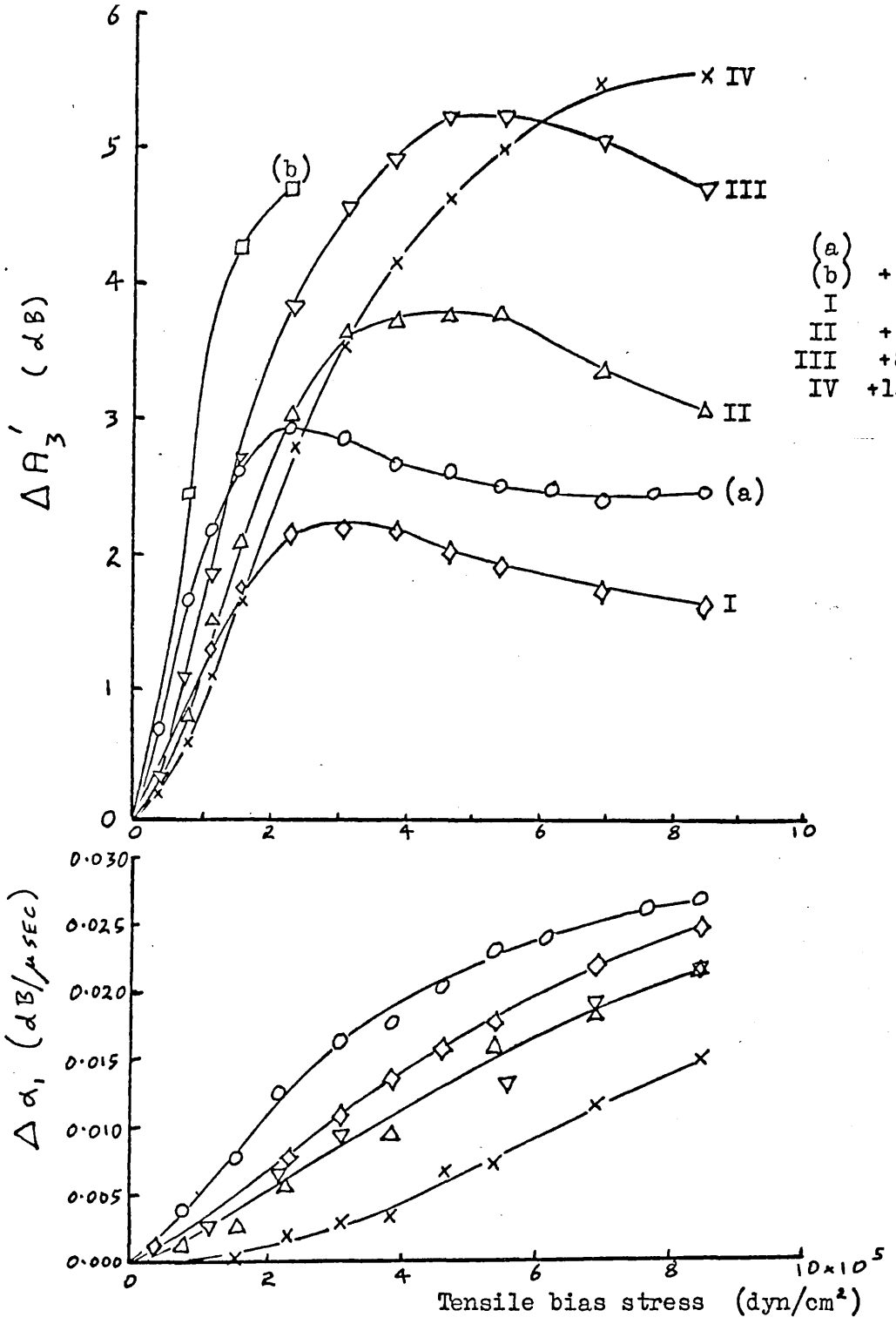

Fig. 6.12. The bias stress dependence of $\Delta A_3'$ in the 6N crystal after deformation at 1.5×10^7 dyn/cm^2, measured at different fundamental wave amplitudes. Curves (a) and (b) were obtained immediately after the deformation, curves I,II,III,IV were obtained some time later.

wave is also seen to depend on the amplitude of the fundamental wave. Thus it appears that the fundamental wave amplitudes used in the present experiments are indeed sufficient to cause dynamic unpinning of dislocations, as postulated in the previous section. A similar deviation from the third power relation in plastically deformed crystals was also noted by Hikata, Sewell and Elbaum (1966).

(iii) The Effect of the Driving Amplitude on the Bias Stress Dependence of $\Delta A_3'$.

A dependence of $\Delta A_3'$ at a given bias stress upon the driving wave amplitude has already been noted from the differences between Figs.6.9 and 6.10. The results of a more detailed investigation of this dependence are shown in Fig.6.12 for the 6N crystal after a plastic deformation to 1.5×10^7 dynes cm^{-2}. Considering first only the curves numbered I,II,III and IV it is seen that at a given bias stress the value of $\Delta A_3'$ increases with the amplitude of the fundamental wave, a behaviour opposite to that noted by Hikata, Sewell and Elbaum(1966) in similar experiments. The maximum in $\Delta A_3'$ also moves to a larger bias stress as the amplitude of the fundamental wave increases, which again is a behaviour opposite to that noted by Hikata, Sewell and Elbaum (1966). If the driving wave amplitude is sufficient to unpin dislocations, a smaller bias stress should be needed to increase the mean dislocation loop length to the value L_m of Fig.3.3. The maximum in $\Delta A_3'$ is therefore expected to move to a smaller bias stress, as observed by Hikata, Sewell and Elbaum (1966), and not as is observed here.

The failure of the theory of Hikata and Elbaum (1966) to account for the present measurements of $\Delta A_3'$ is thought to be most probably due to a contribution to the third harmonic from the non-linear nature of the driving wave induced unpinning of dislocations. Differences between the present measurements and those of Hikata, Sewell and Elbaum (1966) may be due to a different nature of pinning point in the two crystals; the pinning points in the present crystal may for example be weaker. Also as pointed out above the different resolved shear stresses in the slip systems of crystals with <111> and <100> axial directions may account for some difference of behaviour.

The behaviour of the change in fundamental wave attenuation shown in Fig.6.12 does however agree with that reported by Hikata, Sewell and Elbaum (1966). If increasing the fundamental wave amplitude increases the dislocation loop length beyond the value L_m of Fig.3.3, then the slope of the corresponding point on the curve of α_1 against loop length in Fig.3.3 decreases. Hikata, Sewell and Elbaum (1966) attribute the observed decrease in $\Delta\alpha_1$ with increasing fundamental wave amplitude at constant bias stress to this effect.

Each of the curves I,II,III and IV in Fig.6.12 was obtained some days after the initial plastic deformation. Also shown in Fig.6.12 are two curves labelled (a) and (b) which were plotted only six hours after the deformation. In this case $\Delta A_3'$ is seen to show a greater dependence upon bias stress, and the maximum in $\Delta A_3'$ shown by curve (a) occurs at a smaller bias stress than in Curve I.

If the point defects are diffusing to new dislocations after the plastic deformation the initially increased loop lengths will be reduced, and the observed movement of the maximum in $\Delta A_3'$ is accounted for. It therefore appears that the redistribution of point defects after plastic deformation may be faster in the present case than it was for the crystal of Hikata, Sewell and Elbaum (1966). This is a possible explanation for the relatively small movement of the maximum in $\Delta A_3'$ observed in Fig.6.10.

6.3 Conclusions

It will be remembered that the primary purpose of the experiments reported above was to check whether the present experimental set-up was working correctly. From the general agreement between the results obtained with this set-up and those reported by Hikata, Chick and Elbaum (1965) and Hikata, Sewell and Elbaum (1966) it is concluded that the experimental set-up was indeed working satisfactorily.

An effect not reported by Hikata et al.(1965) and (1966) has also been noted. This is a time dependence of both the second and third harmonic amplitude. In the case of the second harmonic this time dependence was not present in an undeformed crystal, but appeared only when the crystal had been subjected to plastic deformation, suggesting that the effect is somehow related to plastic deformation. The time dependence of both the second and third harmonic amplitude is investigated further in Chapter 9.

In the experiments with the third harmonic which were similar to those carried out by Hikata, Sewell and Elbaum (1966) serious disagreement appears only in the measurements of the dependence of $\Delta A_3'$ upon the driving wave amplitude at a given bias stress. Factors which might account for this disagreement are a difference in purity, nature of pinning point, the different crystal orientation used in the present experiments (<100> instead of <111>) and fundamental stress wave induced u_k^n pinning of dislocations. The latter effect may play a more important part in the present measurements if the experimental system used is of lower sensitivity, thus requiring a greater fundamental wave amplitude to give a detectable harmonic signal. In any event, fundamental stress wave induced unpinning of dislocations is considered an important reason for some failure of the Hikata and Elbaum (1966) theory of third harmonic generation to describe the experimental results. An analytical theory of third harmonic generation due to stress wave induced unpinning of dislocations is clearly required. It would also be useful to increase the sensitivity of the present third harmonic experimental system so that measurements might be made with lower driving stress amplitudes, i.e: in the stress amplitude independent damping region.

CHAPTER 7.

A Preliminary Investigation of Harmonic Generation in Sodium Chloride

7.0 Introduction

Experiments first carried out were aimed at detecting a second harmonic wave generated in a sodium chloride crystal. Second harmonic echoes with amplitudes proportional to the square of the fundamental wave amplitudes were observed, but no dependence of harmonic amplitude on tensile bias stresses for values up to 1.5×10^7 dynes cm^{-2} was found. The maxiumum fundamental-wave stress-amplitude which was applied was about 10^5 dynes cm^{-2}. With a fundamental-wave stress-amplitude of 0.5×10^5 dynes cm^{-2} at the driving transducer, typical voltages at the receiving transducer for the harmonic and fundamental waves respectively were 15 mv and 1.5 volt.

Correct operation of the experimental set-up was confirmed by inserting the 5N aluminium crystal and checking that the second harmonic echoes showed a dependence on bias stress (see Section 6.1). It was concluded that the harmonic signal from the NaCl crystal arose predominantly from the anharmonicity of the lattice, the dislocations present having no detectable effect. It will be remembered that the absence of a bias stress dependence of the second harmonic in a 4N aluminium crystal was explained in this way also (see Section 6.1).

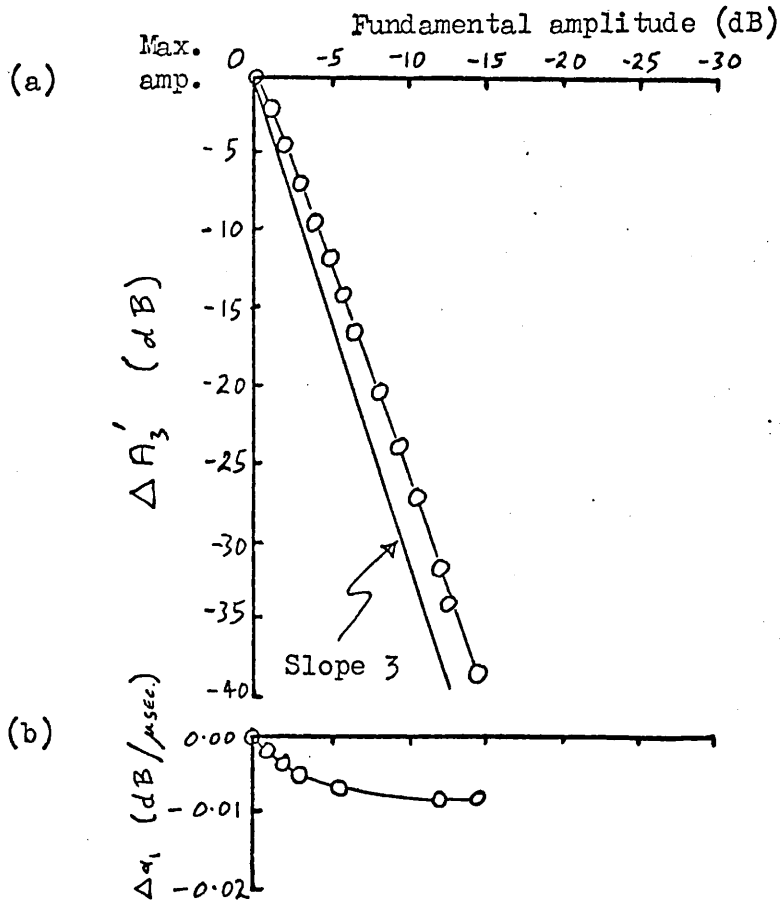

Fig. 7.1. The 3rd harmonic amplitude and the attenuation of the fundamental wave as a function of the fundamental wave amplitude in an NaCl crystal.

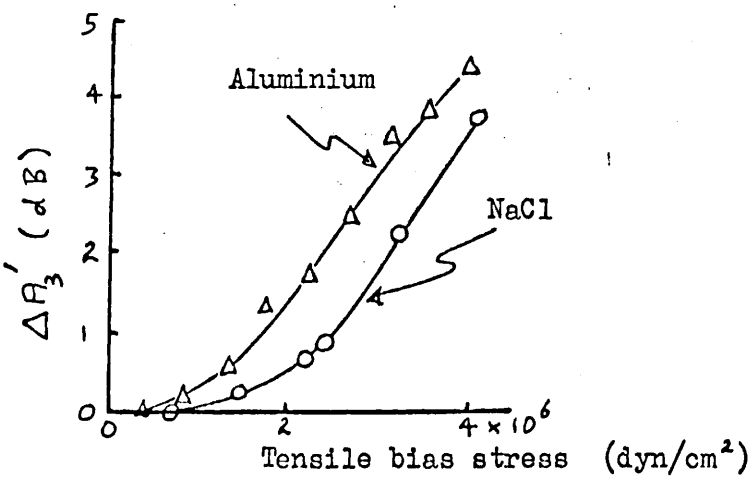

Fig. 7.2. A comparison of the bias stress dependence of $\Delta A_3'$ in NaCl & Al.

Since, for the third harmonic, the lattice contribution is expected to be appreciably smaller than the dislocation contribution (see Section 3.2), measurements to detect a dislocation contribution to the third harmonic were made.

Third harmonic echoes were observed in an NaCl specimen, and in Fig.7.1(a) is shown the relation between the fundamental wave amplitude and the third harmonic wave amplitude. The measurements were made on the first received harmonic pulse. The corresponding change in attenuation of the fundamental wave is shown in Fig.7.1(b). Equation (3.22) predicts a third harmonic amplitude increasing with the third power of the fundamental wave amplitude, but a slight deviation from this third power relation is shown by the measurements of Fig.7.1. Such a deviation has been noted also by Hikata, Sewell and Elbaum (1966) in measurements with an aluminium crystal, and in the present work with aluminium crystals (see Section 6.2). It will be noted that the attenuation of the fundamental wave appears to be dependent on the strain amplitude of the fundamental wave, as was the case with the measurements on aluminium.

With a fundamental stress wave amplitude of 0.5×10^5 dynes cm^{-2} at the driving face of the specimen, the third harmonic signal at the other end of the crystal amounted to 1/3% of the fundamental wave amplitude; these figures correspond to voltages at the receiving transducer for the harmonic and fundamental waves respectively of 5 mv and 1.5 volt.

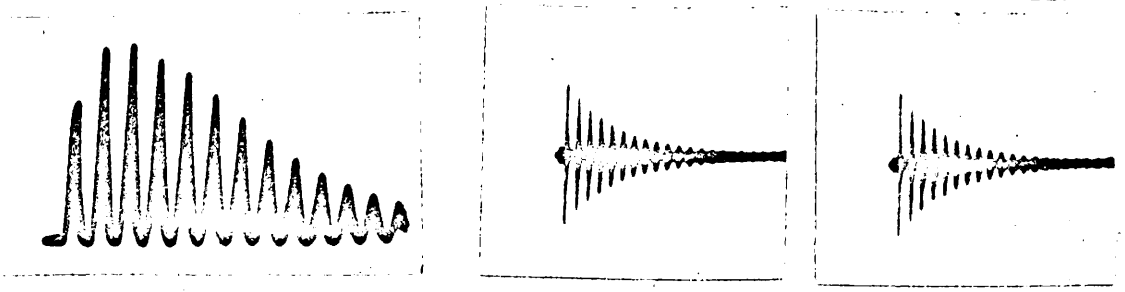

(a) (b) (c)

Fig. 7.3. Measurements in an NaCl crystal 2.4 cm long, using quartz transducers to generate the fundamental wave and to receive the harmonic echoes. The trace (a) shows the 3rd harmonic echoes. Traces (b) and (c) show 30MHz echoes of a 30MHz fundamental wave applied respectively to the harmonic receiving transducer and the 10MHz driving transducer.

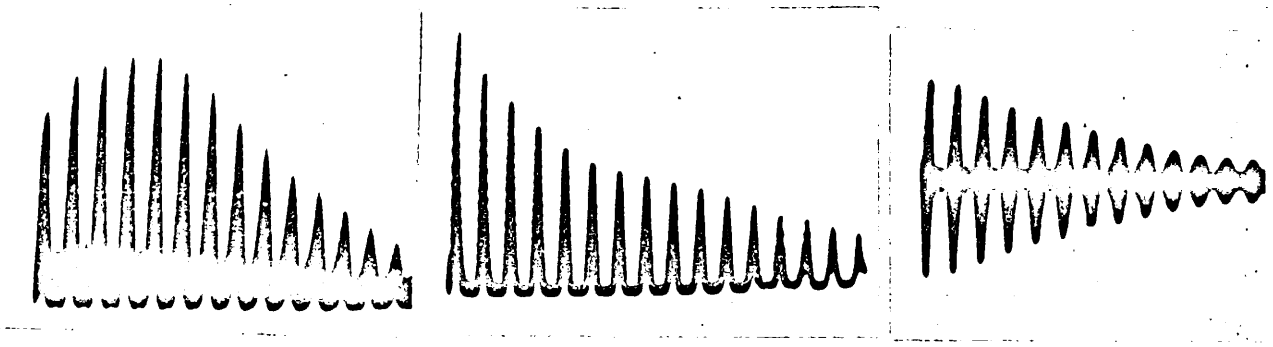

Trace I Trace II Trace III

Fig. 7.4. Third harmonic measurements using the capacitative detector. Trace I shows the 3rd harmonic echoes, trace II shows 10MHz echoes received at the capacitative detector, and trace III shows 30MHz echoes received at the capacitative detector when a 30MHz signal was applied to the driving transducer.

A dependence of the third harmonic amplitude on bias stress was found in this crystal, as shown in Fig.7.2. Also shown in Fig.7.2 are measurements made with the 4N aluminium crystal, and the behaviour of both crystals is seen to be similar.

7.1. The Dependence of the Third Harmonic Amplitude upon Distance

The third harmonic echo patterns in some annealed NaCl specimens were found to display a maximum between the second and third received pulses, as illustrated in Fig.7.3(a). In Figs.7.3(b) and (c) are shown the echo patterns obtained when respectively the harmonic receiving transducer and the fundamental transducer were driven directly with a signal of exactly the frequency of the third harmonic. These echo patterns do not show any maximum after the first received pulse. It is concluded that the echo pattern shown in Fig.7.3(a) does not result from the transducer bonds on the geometry of the sample.

There appear to be no other published experimental results of third harmonic measurements in which this maximum is observed, although a maximum has been observed with second harmonic echoes [Hikata, Chick and Elbaum (1965)]. Hikata and Elbaum (1966) have predicted theoretically a maximum in both second and third harmonic amplitude with distance, as was discussed in Section 3.2.

However, Gauster and Breazeale (1967) have disputed that the theory of Hikata and Elbaum (1966) can be applied

to measurements in a pulse-echo system where both the fundamental and harmonic waves are undergoing reflections. The effect of a reflection at a stress-free boundary upon second harmonic generation has been considered by Buck and Thompson (1966), who show that, after the reflection, energy flow from the fundamental to a second harmonic wave is reversed. In this case no maximum in second harmonic amplitude after the first received pulse is expected (see Section 2.1). This reversal of energy flow from the fundamental to the second harmonic is a well known feature of finite amplitude wave propagation in liquids [Breazeale and Lester (1961)] . Measurements consistent with a decrease in second harmonic amplitude after reflection from a stress-free boundary in a solid have been reported by Gauster and Breazeale (1967), in accordance with the theory developed by Buck and Thompson (1966). A further and more detailed theoretical analysis of the reflection of fundamental and harmonic waves has been given by Van Buren and Breazeale (1968), who consider also the reflection of third harmonic waves. The effect of reflection at a stress-free boundary upon a third harmonic wave is similar to that upon a second harmonic wave, namely that the third harmonic amplitude decreases to zero after reflection before increasing again.

The maximum appearing in Fig.7.3(a) and that reported by Hikata, Chick and Elbaum (1965) are therefore in conflict with these theoretical calculations and other reported observations supporting this theory.

Gauster and Breazeale (1967) have suggested that

Hikata, Chick and Elbaum (1965) observed a maximum because quartz transducers were attached at each end of the specimen and that therefore stress-free boundaries were not used. In fact, when reflection takes place from a rigid boundary, the reversal of energy flow from the fundamental wave to the harmonics is not expected theoretically to take place [Fay (1957)]. Since quartz transducers were used to obtain the results shown in Fig.7.3(a), it was decided to carry out a second experiment using a capacitative detector (see Section 4.40) to detect the third harmonic signal. This detector provides a good stress-free boundary for the reflection of ultrasonic waves. Fig.7.4 shows the echo patterns obtained in this way. The third harmonic echoes (trace I) still show a maximum after the first received pulse. The experimental procedure used in this experiment is identical to that of Gauster and Breazeale (1967), who made measurements on a second harmonic. However, whereas Gauster and Breazeale (1967) obtained results which supported the theory of Buck and Thompson (1966), the results shown in Fig.7.4 clearly do not.

It is interesting to compare the position of the maximum in third harmonic amplitude with that predicted by the theory of Hikata and Elbaum (1966) which neglects reflection altogether. The attenuation of the fundamental wave α_1 was found experimentally to be 0.1 ± 0.05 db/cm which, when inserted in equation (3.24), leads to a maximum in the third harmonic amplitude after a distance of about 33 cm. The maximum in Fig.7.3(a) which was obtained using a quartz transducer occurs at about 10 cm, while that in Fig.7.4(a) which was obtained using a

capacitative detector occurs after about 20 cm, i.e: nearer to the value predicted by equation (3.24). It will be noted that one effect of replacing a quartz transducer by a capacitative detector is to reduce the reflection loss at the specimen surface, and therefore in this respect the experimental situation is more consistent with the assumptions of Hikata and Elbaum (1966). The reflection loss with a quartz transducer was estimated for the fundamental wave in the present work to be about 0.2 db/reflection.

It is concluded that there must be some further factor which has not yet been taken into account. This factor apparently leads to a behaviour more nearly described by the theory of Hikata and Elbaum (1966) for wave propagation in an infinitely long solid than to the behaviour expected of waves undergoing reflection at a stress-free boundary.

One difference between the measurements of Gauster and Breazeale (1967) and those described above using the capacitative detector is that, in the present case, the harmonic wave is expected to be generated mainly by dislocations, and not by the lattice itself, since we are dealing with the third harmonic. Two experiments were carried out to help determine the effect of dislocations upon the maximum in the third harmonic echoes. The first experiment involved reducing the dislocation loop lengths by X-irradiation. The second experiment involved applying a bias stress to the crystal and observing the effect upon α_1 and $\Delta A_3'$.

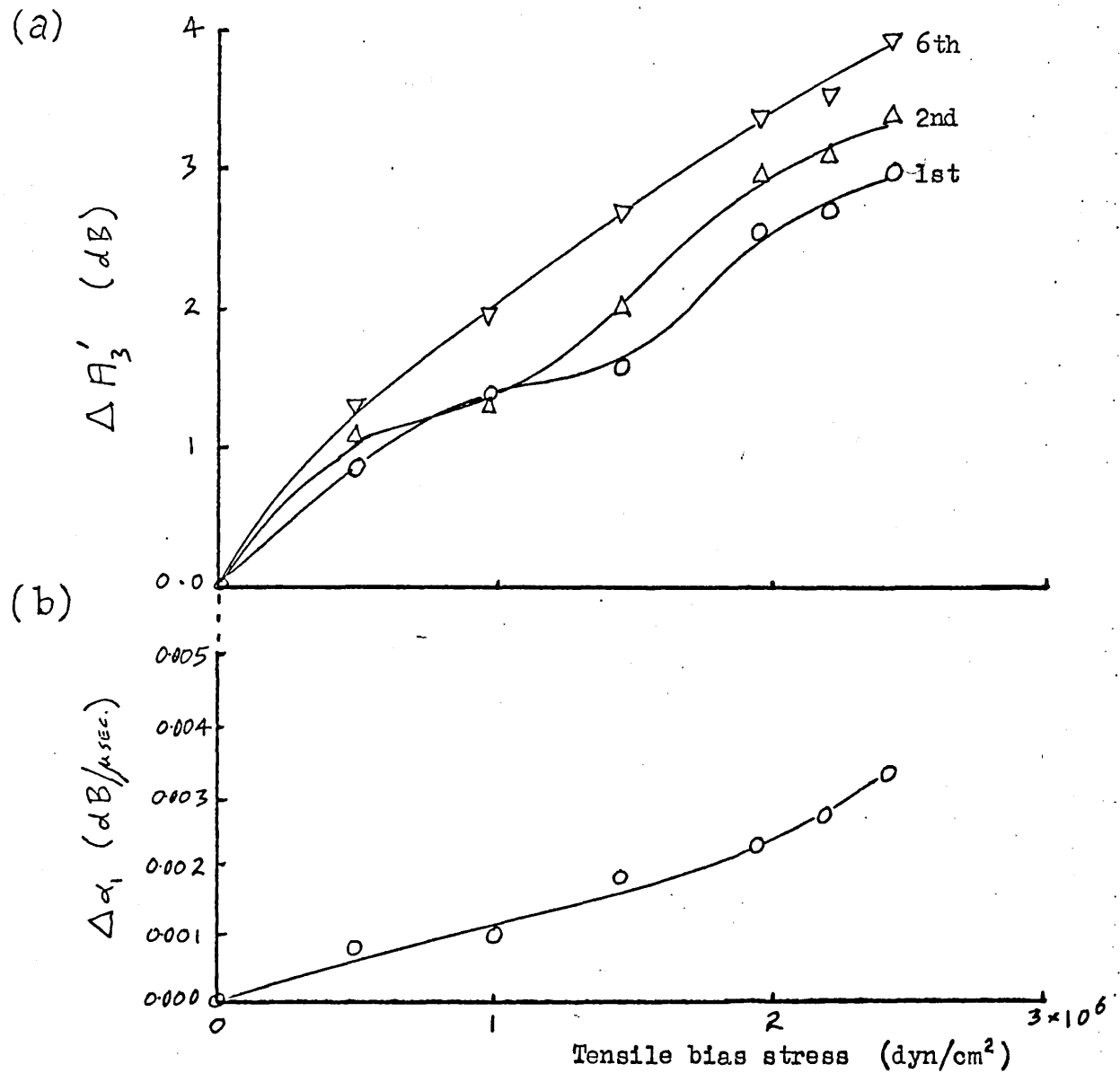

Fig. 7.5. The change in third harmonic amplitude with bias stress in an NaCl crystal. Measurements were made on the 1st received pulse, the 2nd received pulse and the 6th received pulse in a specimen 2.4cm long.

(a) The effect of X-irradiation.

The maximum in third harmonic amplitude after the first received pulse was found to be removed by X-irradiation, the first received pulse being the largest after X-irradiation. Since X-irradiation introduces colour centres which are expected to reduce dislocation loop lengths (see Section 8.3), it is concluded that the maximum observed in Fig.7.3 is related to the generation of the third harmonic wave by dislocations.

(b) The Effect of a Bias Stress.

When a tensile bias stress was applied to the crystal, an increase in the amplitude of the third harmonic echoes was observed.

The measurements of $\Delta A_3'$ which were made when the bias stress was applied are shown in Fig.7.5(a). Measurements were made on the first, second and sixth received pulse. The measurements show that $\Delta A_3'$ increases with bias stress. This may be accounted for in terms of the Hikata and Elbaum (1966) theory if the

bias stress is considered to increase dislocation loop lengths and these loop lengths correspond to a value of approximately L_1 in Fig.3.3. However, according to equation (3.29) $\Delta A_3'$ is independent of propagation distance, while Fig.7.5(a) shows that, for a given bias stress, $\Delta A_3'$ increases with distance of propagation, ie: $\Delta A_3'$ is not the same for each echo. The values of $\Delta A_3'$ plotted in Fig.7.5 have been corrected for attenuation changes, but these corrections are small. The apparent dependence of $\Delta A_3'$ upon distance (ie: echo number) does not therefore arise from an incorrect measurement of $\Delta\alpha_1$. Geometrical distortion of the sample by the bias stress was also ruled out as a cause of this behaviour since measurements on higher order fundamental echoes showed no signs of corresponding changes in pulse amplitude.

In conclusion, it is noted that there is agreement between some of the results noted above and the theory of Hikata and Elbaum (1966). In particular, the increase in $\Delta A_3'$ with bias stress is in agreement with this theory although the dependence of this increase upon distance of propagation is not. The behaviour of the third harmonic generation after reflection at a stress-free boundary does not appear to be in agreement with theoretical calculations of Buck and Thompson (1966), but instead appears better described by the theory of Hikata and Elbaum (1966) which neglects reflection altogether.

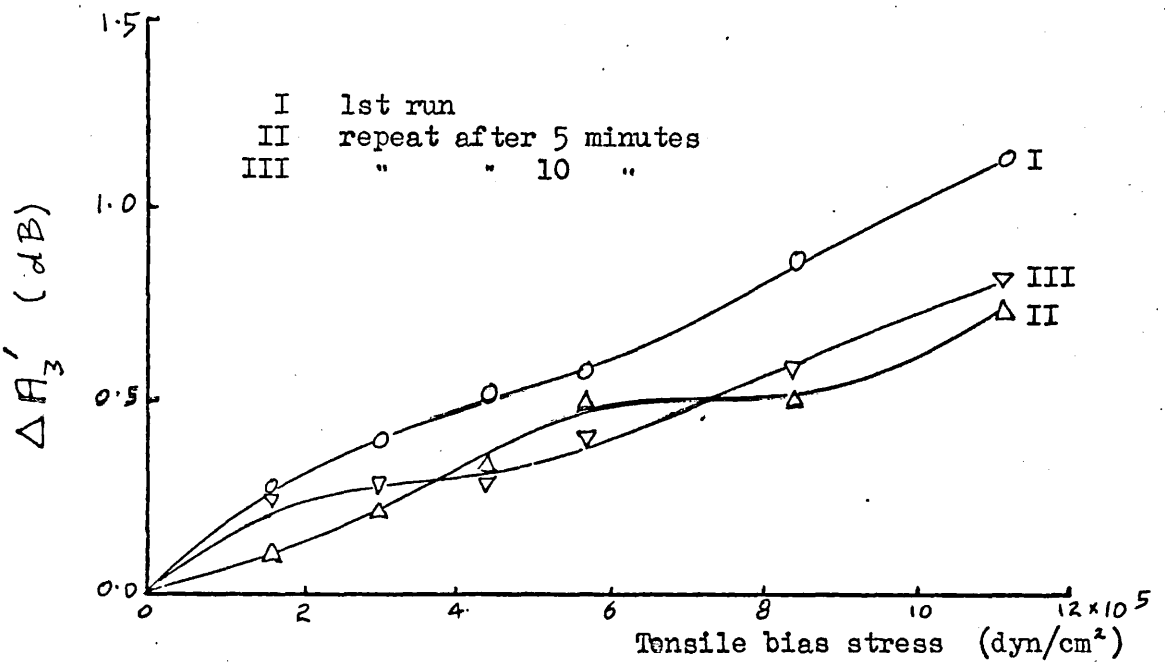

Fig. 7.6. Measurements of $\Delta A_3'$ as a function of bias stress in an NaCl crystal. The measurements were repeated after an interval of 5 minutes and 10 minutes, and show a lack of reproducibility.

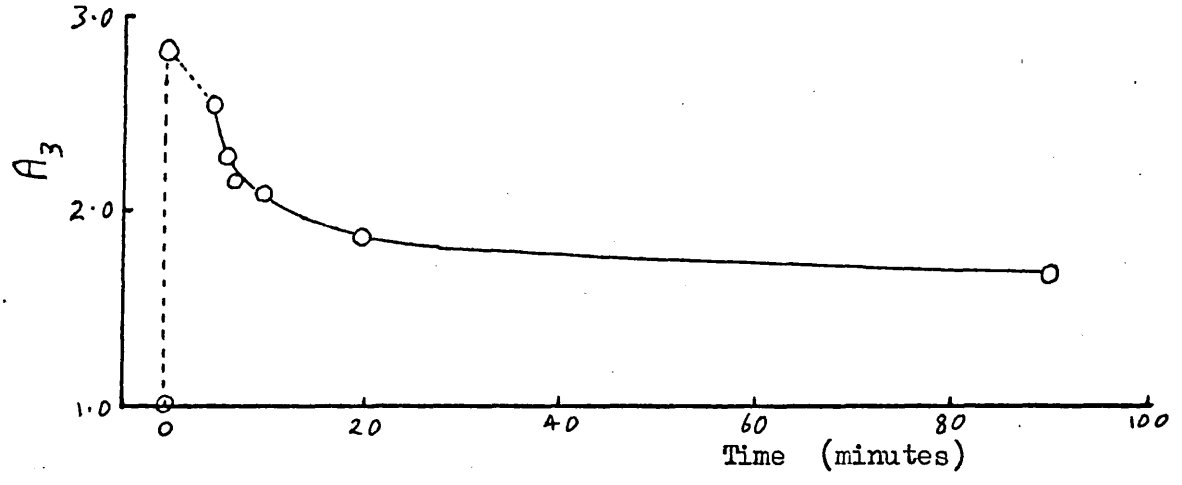

Fig. 7.7. The decay in the 3rd harmonic amplitude A_3 in an NaCl crystal during and after stressing to 0.75×10^7 dyn/cm .

Further work should be done to discover the reasons for this discrepancy. It may be noted that there is some discrepancy between the theory which allows for reflection and the experiment in the case of finite amplitude waves propagating in liquids. After reflection at a stress-free boundary the energy flow from the fundamental to the second harmonic is reversed but it has been found that the wave returns to its undistorted form more quickly than theory predicts [Mellen and Browning (1968)]. There is also found to be considerable distortion of the fundamental 2 MHz wave which is attributed to diffraction.

7.2. The Reproducibility of the Measurements in NaCl

An experiment was carried out in which measurements of the change in harmonic amplitude with bias stress were repeated after time intervals of five and ten minutes. The results are shown in Fig.7.6. The change in attenuation of the fundamental wave was less than 0.001 db/μsec. Detailed reproducibility is seen to be not very good. The stability of the gain of the harmonic amplifying system with time was measured. The gain was found to fluctuate by only about 1% over a 30 minute period, which is insufficient to account for the differences seen in Fig.7.6.

The lack of reproducibility was found to be due, in part at least, to a time dependence of the third harmonic amplitude after the application of a bias stress.

In Fig.7.7 are shown measurements made on an NaCl crystal to which a bias stress of 7.5×10^6 dynes cm^{-2} was applied for five minutes and then removed. The harmonic amplitude is shown both during and after application of the bias stress.

A large increase in harmonic amplitude occurs when the bias stress is first applied, followed by a slow decrease while the crystal remains stressed. When the stress is removed, the harmonic amplitude falls and approaches a value greater than that before the stress was applied. Since the stress of 7.5×10^6 dynes cm^{-2} is sufficient to produce plastic deformation in sodium chloride, the dislocation density after deformation will be increased and a larger value of harmonic amplitude is therefore expected.

7.3. Factors affecting Reproducibility

From the preliminary investigation described above it was clear that the poor reproducibility of many of the measurements was likely to make a detailed study of the dislocation contribution to the third harmonic difficult. An investigation into the reasons for this poor reproducibility and ways of improving it was therefore carried out and is reported in Chapter 8. This approach also led to some other significant third harmonic measurements being made (see Chapter 8).

Three factors were considered to have a possible

influence on the reproducibility of the measurements. These were (i) the time dependence of the third harmonic amplitude after application of a bias stress, (ii) unpinning of dislocations by the fundamental stress wave, and (iii) plastic deformation produced by bias stresses.

The time dependent nature of the third harmonic amplitude after the application of a bias stress illustrated in Fig.7.7 can clearly influence the reproducibility of any experimental results. The nature of this time dependent behaviour is discussed further in Section 9.2. To improve reproducibility in any experiments where time dependence was not being investigated, measurements of $\Delta A_3'$ as a function of bias stress were made in the following way. Bias stresses were applied only for a short time while a photograph of the oscilloscope screen (see Section 4.6) was actually being taken.

The dependence of the fundamental wave attenuation upon the stress amplitude of the wave noted in Fig.7.1(b) suggests, according to the Granato-Lucke (1956) hysteresis theory of dislocation damping, that unpinning of dislocations is taking place. The extent of the dislocation unpinning produced by a bias stress may therefore be influenced by the stress amplitude of the fundamental wave, and if this is not the same in each experiment different results might be expected. The use of longer specimens should be advantageous in this connection. If the length is chosen so that the harmonic amplitude of the first received pulse is a maximum, then smaller driving wave amplitudes will be required to produce a detectable harmonic signal, (see Section 8.2).

Bias stresses of the order of 10^6 dynes cm^{-2} are sufficient to produce plastic deformation of the sodium chloride crystals, so that in subsequent measurements the crystals are not expected to have the same dislocation configuration. This may clearly lead to poor reproducibility of experimental measurements. Of course, the plastic deformation may itself be investigated with the aid of third harmonic measurements.

If the magnitude of the bias stresses needed to produce changes in $\Delta A_3'$ could be reduced, then the plastic deformation would also be reduced and the reproducibility of the measurements should be improved. Three ways of reducing the magnitude of the bias stresses needed to produce unpinning of dislocations may be considered. These are (i) increasing the dislocation loop lengths, (ii) introducing weaker pinning points into the specimens, (iii) thermally assisting the unpinning of dislocations.

Taking (i) first, two methods of increasing dislocation loop lengths are considered in Chapter 8. Firstly, a more pure crystal is used. Secondly, the effect of plastic deformation upon loop lengths is investigated. It has already been noted in experiments with aluminium crystals (see Section 6.2) that in an annealed crystal impurity concentrations may be greater at dislocation sites than in the bulk of the crystal. Plastic deformation may then generate new dislocations in relatively more pure material with correspondingly longer loop lengths.

The possibility (ii) of introducing weaker pinning

points is investigated by introducing colour centres into sodium chloride crystals by X-irradiation. Unfortunately, however, this also reduces the loop lengths in the crystal.

Finally, (iii) above suggests experiments at elevated temperatures where thermal activation may make dislocations easier to unpin.

CHAPTER 8.

Further Measurements with Sodium Chloride

This chapter is concerned with the investigations which were carried out following the preliminary measurements discussed in Chapter 7. These investigations all involve third harmonic amplitude measurements.

8.1. The Effect of an Anneal

In Chapter 6 it was suggested that dislocation loop lengths were shorter in an annealed crystal than in the same crystal after plastic deformation. This was attributed to impurities diffusing to dislocation sites during the anneal, thus leaving regions of relatively defect-free crystal. New dislocations generated in these regions are then expected to have longer loop lengths. Hikata, Sewell and Elbaum (1966) have previously found evidence of this effect in third harmonic measurements with aluminium crystals. Some experiments were carried out using NaCl crystals in an attempt to investigate further the effect of annealing.

An experiment was first performed to detect whether the dislocation density in a crystal may be reduced during an anneal. Using an etch-pit technique (see Section 5.5), estimates of the dislocation density in several unannealed crystals were obtained. These crystals

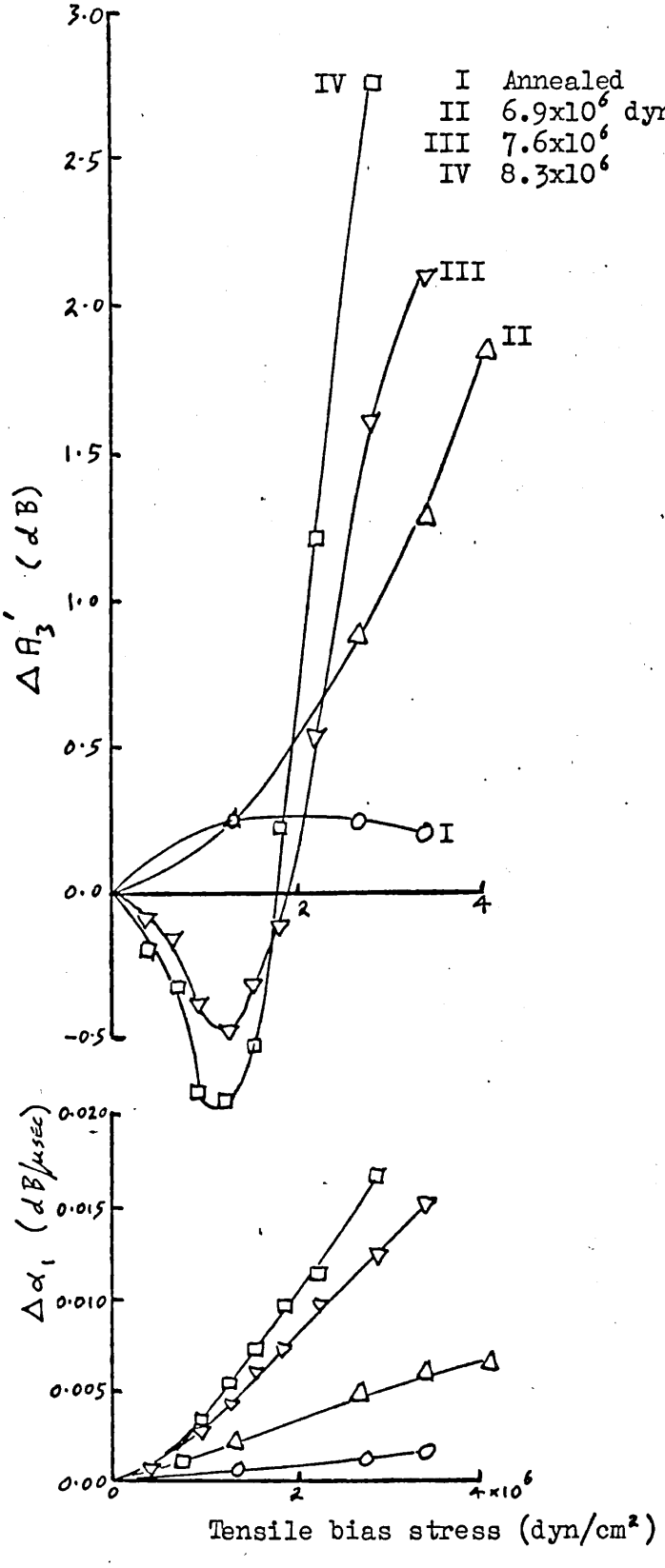

Fig. 8.1. A tensile bias stress after deformation in tension.

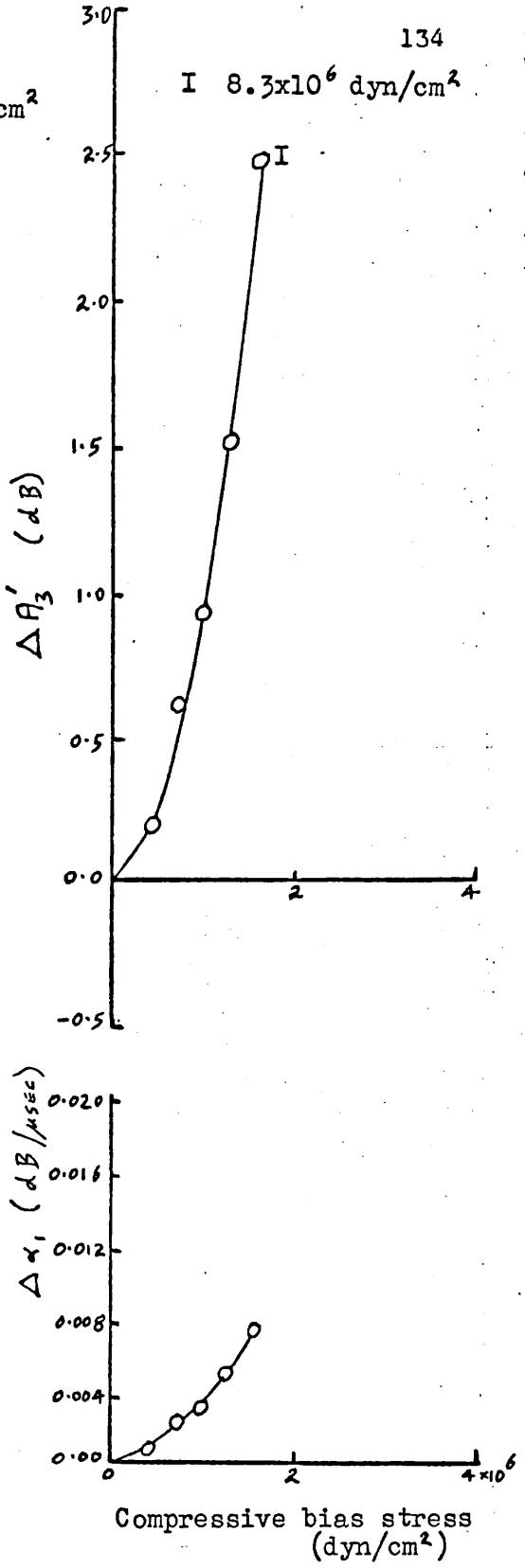

Fig. 8.2. A compressive bias stress after deformation in tension.

were then annealed at about 750°C [M.P. = 801°C] for some hours and later etched a second time. No significant change in dislocation density was detected. However, the results of the following experiment indicate that some dislocation properties are indeed altered by an anneal.

An NaCl specimen, measuring 1.3 x 1.3 x 8.0 cm^3, was cut from an 'as grown' crystal. This specimen was chosen to be of greater length than those previously used so that smaller fundamental wave amplitudes could be used, as discussed in Section 7.3. A third harmonic was observed in this crystal and was found to be independent of bias stresses up to 10^7 dynes cm^{-2}. However, after the crystal was annealed, a small dependence of $\Delta A_3'$ upon bias stress was noted, as shown in Fig.8.1 (curve I). After a deformation at 6.9×10^6 dynes cm^{-2}, an appreciable dependence of $\Delta A_3'$ upon bias stress was noted (curve II). Only curves I and II of Fig.8.1 will be considered here (see Section 8.2).

The absence of any dependence of $\Delta A_3'$ upon bias stress before annealing may be attributed to the dislocation loop lengths being too short for any significant unpinning to take place. If there is a diffusion of impurities to dislocations during an anneal, then a reduction in loop length will occur. Consequently, no dependence of $\Delta A_3'$ upon bias stress is expected after the anneal. In fact, curve I of Fig.8.1 shows a small dependence of $\Delta A_3'$ upon bias stress in the annealed crystal. This is attributed to dislocations in the crystal which were unpinned by thermal stresses existing

in the crystal during the cooling down following the high temperature anneal (see also Section 9.2). These dislocations are expected to have an increased loop length since they will have been generated in regions of the crystal made relatively more pure by the anneal. The greater dependence of $\Delta A_3'$ upon bias stress after a plastic deformation (curve II) may be attributed to the plastic deformation generating even more dislocations in the relatively more pure regions of the crystal. .

These measurements of dislocation density before and after an anneal, the dependence of $\Delta A_3'$ upon bias stress before and after an anneal and after plastic deformation are seen to be consistent with the idea that plastically deforming an annealed crystal may give rise to longer dislocation loop lengths than would be expected from a consideration of the crystal purity.

8.2. Internal Stresses remaining after Plastic Deformation

The presence of residual internal stresses after the plastic deformation of an aluminium crystal has been observed by Hikata, Chick and Elbaum (1965) during an investigation of second harmonic generation. The results to be described below are concerned with residual stresses in an NaCl crystal as revealed by third harmonic measurements. The NaCl crystal used in this investigation was the one described in Section 8.1 above.

Fig.8.1 shows the dependence of $\Delta A_3'$ and $\Delta\alpha_1$ upon a tensile bias stress before and after successive plastic

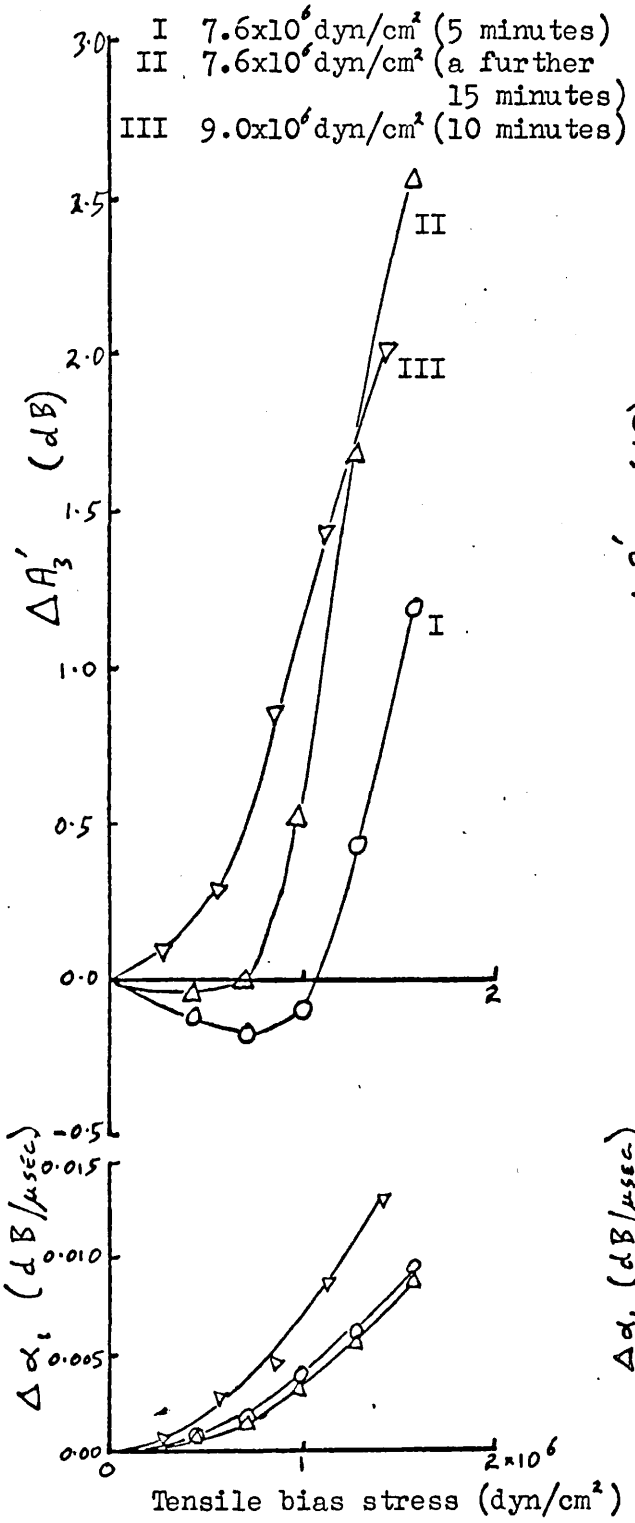

Fig. 8.3. A tensile bias stress after deformation in compression.

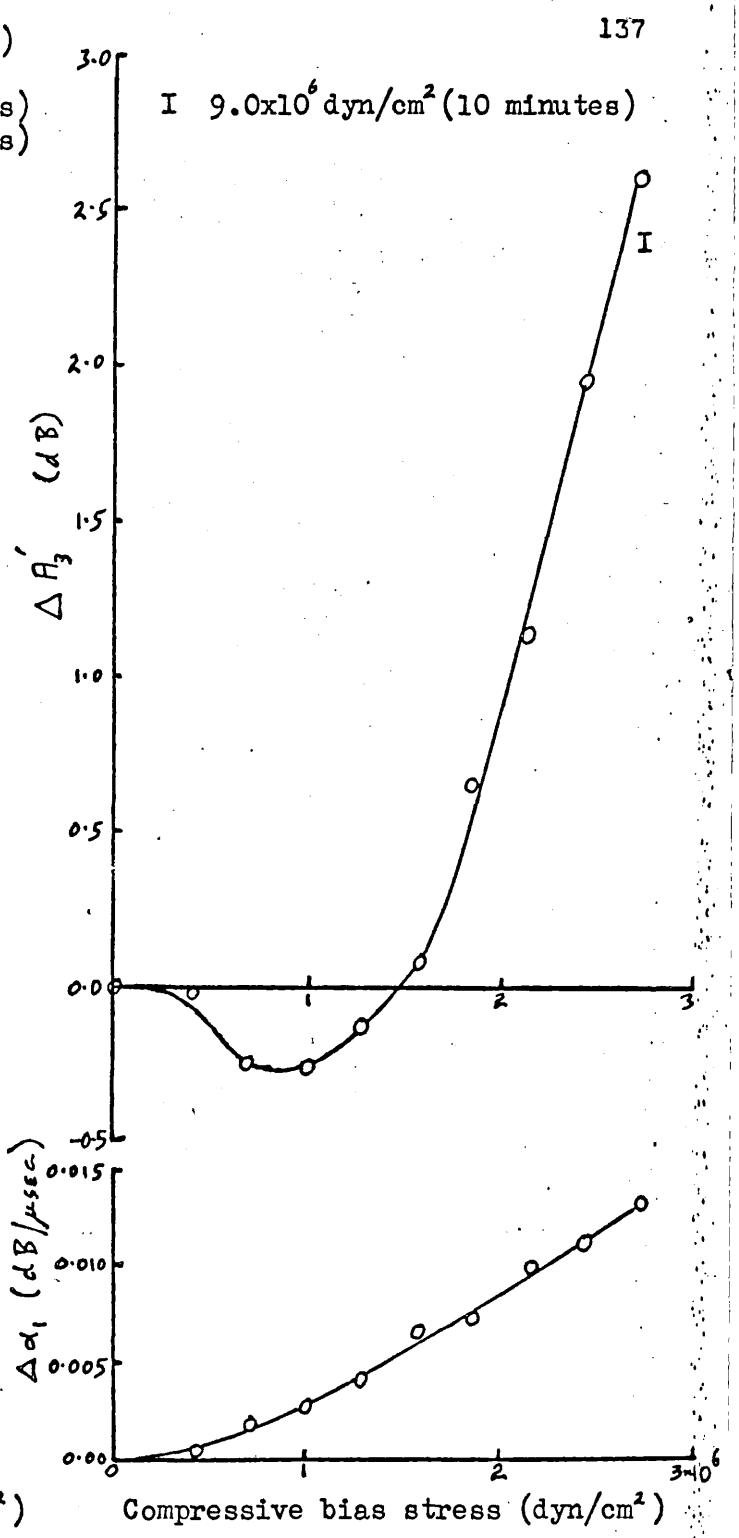

Fig. 8.4. A compressive bias stress after deformation in compression.

deformations in tension. Each deforming stress was applied for ten minutes (except where otherwise indicated) and twenty four hours was allowed to pass before any further measurements were made. This was to allow the time dependence of the third harmonic amplitude to become negligible (see Chapter 9). The large increase in $\Delta A_3'$ at a given bias stress after the first plastic deformation has been considered in Section 8.1. The fact that $\Delta A_3'$ increases with bias stress suggests according to Fig.3.3 that the effective dislocation loop length is less than L_m. After further plastic deformation in tension, $\Delta A_3'$ is seen (curve III) to pass through a minimum before increasing, and this minimum becomes more marked with further deformation (curve IV).

It is possible to account for a decrease in $\Delta A_3'$ with bias stress if, as a result of plastic deformation, the effective loop length has become greater than that corresponding to L_m of Fig.3.3. The curve of Fig.3.3 shows that a further increase in loop length when a bias stress is applied will then result in a decrease in $\Delta A_3'$. The subsequent increase in $\Delta A_3'$ at higher bias stresses might then be due to dislocation multiplication.

Fig.8.2, however, shows that a compressive bias stress does not produce a minimum in $\Delta A_3'$. [After the results of Fig.8.2 were obtained, tests showed that a tensile bias stress still produced a minimum in $\Delta A_3'$.] Since a compressive bias stress is expected to increase loop lengths in the same way as a tensile bias stress,

the results of Fig.8.2 indicate a loop length less than L_m, in contradiction to the results of Fig.8.1.

An alternative interpretation of the results is proposed according to which the minimum in $\Delta A_3'$ is attributed to internal stresses in the crystal remaining after plastic deformation. Small compressive internal stresses are considered to remain in the crystal after plastic deformation in tension. These internal stresses may lead to unpinning of some dislocations which may however be repinned by a subsequent tensile bias stress. A decrease in the effective dislocation loop length at small tensile bias stresses will then result. According to Fig.3.3, this would lead to a decrease in $\Delta A_3'$ for an effective dislocation loop length less than L_m.

The internal stresses observed by Hikata, Chick and Elbaum (1965) during second harmonic measurements in aluminium crystals were considered to influence the curvature of dislocations only, whereas here the internal stresses are considered to cause actual unpinning of dislocations.

The bias stress dependence of the third harmonic has been further investigated by subjecting the crystal to successive prestresses in compression instead of tension. This treatment is expected to produce tensile internal stresses which may compensate or replace the compressive internal stresses. In Fig.8.3 are shown the effects of a tensile bias stress on the third harmonic amplitude after three successive compressive prestresses

of increasing magnitude. The minimum is seen to gradually disappear, as expected. After the final prestress in compression which is seen in Fig.8.3 to have removed the minimum completely, a compressive bias stress was applied to the crystal. Fig.8.4 shows a minimum appearing in $\Delta A_3'$ at small compressive bias stresses. This is expected if the internal stresses are now mainly tensile, ie: the results are in agreement with the above interpretation.

The changes in $\Delta\alpha_1$ with bias stress after successive plastic deformations are interpreted in terms of two effects. Firstly, a change in loop length with bias stress leads to a change in α_1. The magnitude of this change is given by the slope of the curve of α_1 plotted against loop length as in Fig.3.3. Secondly, an increase in dislocation density brought about by plastic deformation is expected to increase the value of $\Delta\alpha_1$ [Granato and Lücke (1956)]. The observed changes in $\Delta\alpha_1$ are consistent with both an increased dislocation density and with loop lengths of less than L_m which are increased by plastic deformation. After the final plastic deformation, the change in α_1 at a given compressive bias stress is less than at a tensile bias stress of the same magnitude. This is attributed to the smaller degree of unpinning produced by the compressive bias stress, as indicated by the corresponding changes of third harmonic amplitude shown in Figs.8.3 and 8.4.

It is worth noting that the crystal used in these measurements in fact contained ten or twenty sub-crystals. The small angle grain boundaries associated with these

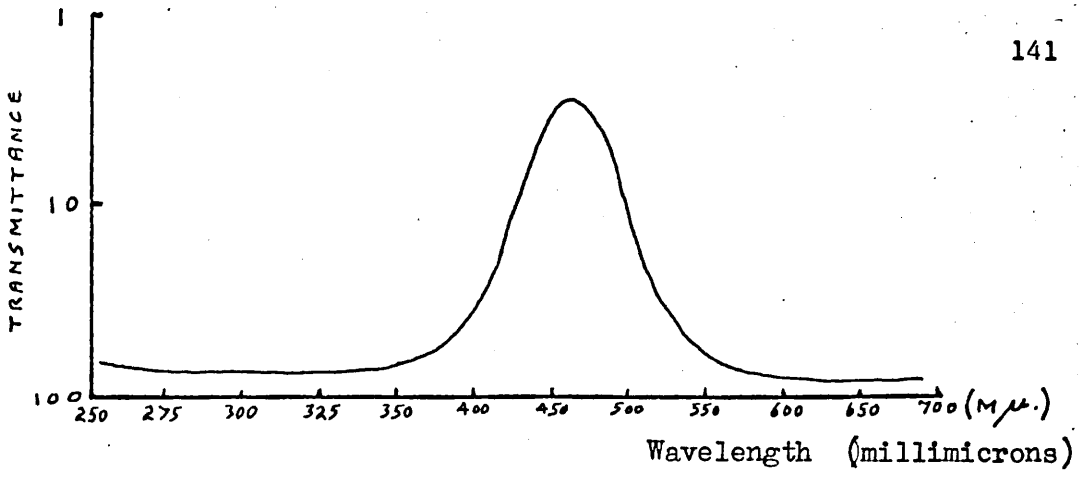

Fig. 8.5. The transmittance of an X-irradiated NaCl crystal.

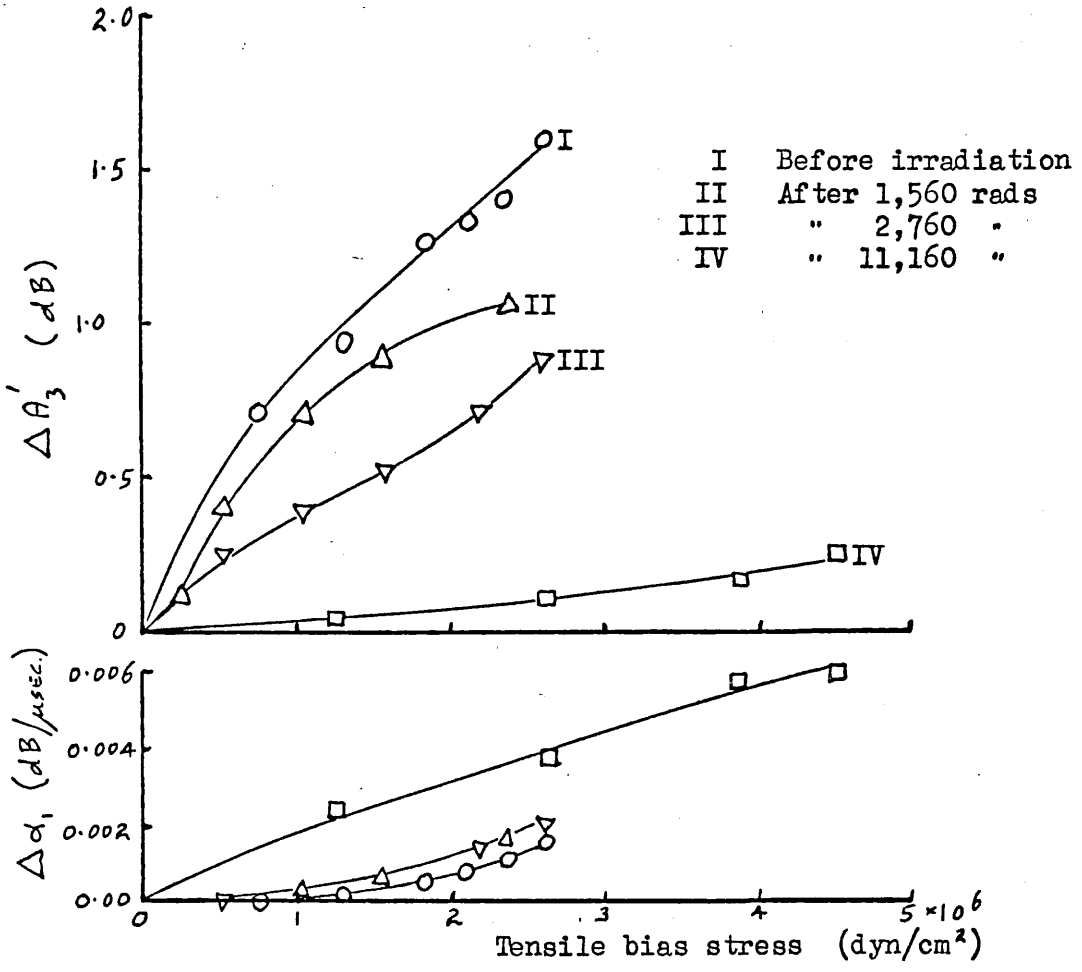

Fig. 8.6. The effect of X-irradiation on the bias stress dependence of $\Delta A_3'$.

may have played some part in the formation of the residual internal stresses.

8.3 The Effect of X-irradiation

Some NaCl crystals were X-irradiated to produce colour centres in order that the effect of both the concentration and the nature of dislocation pinning points upon the stress dependence of third harmonic generation might be investigated.

In Fig.8.5 the transmittance of an X-irradiated crystal is shown plotted against optical wavelength. The peak is centred at about 462 mμ and is attributed to F-centres.

An NaCl crystal was subjected to repeated X-irradiations and after each dose the variation of third harmonic amplitude with bias stress was measured. Fig.8.6 shows the results of these measurements. The successive irradiations are seen to have decreased the value of $\Delta A_3'$ at a given bias stress. This behaviour is attributed to a reduction in dislocation loop length owing to pinning of dislocations by colour centres. Shorter dislocation loop lengths will become unpinned at a larger bias stress, ie: a given bias stress will produce less unpinning in an irradiated crystal. This is seen from Fig.3.3 to result in a smaller increase in $\Delta A_3'$ for initial loop lengths less than L_m, as is observed.

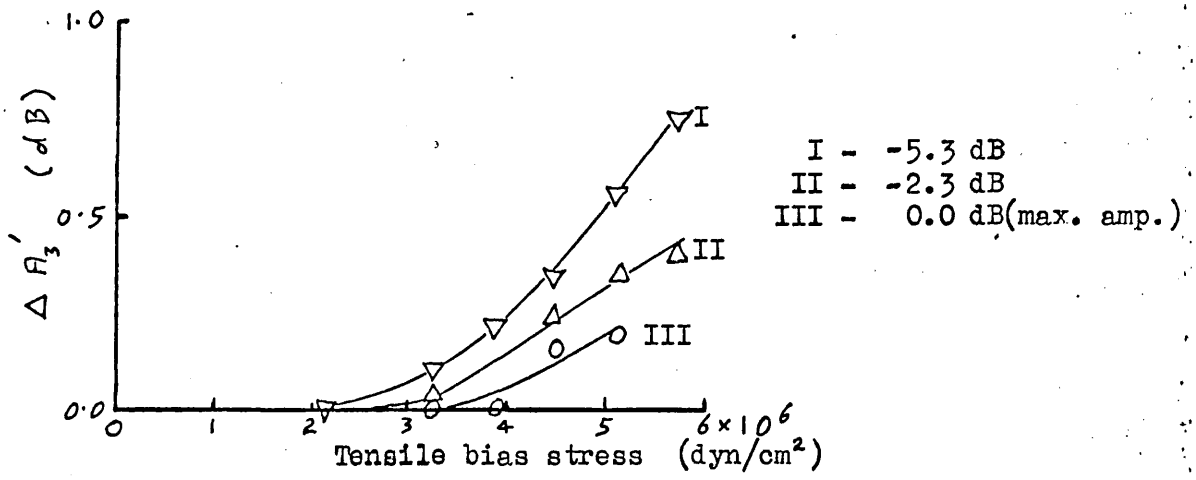

Fig. 8.7. The effect of the fundamental wave amplitude on the bias stress dependence of $\Delta A_3'$ in an X-irradiated NaCl crystal.

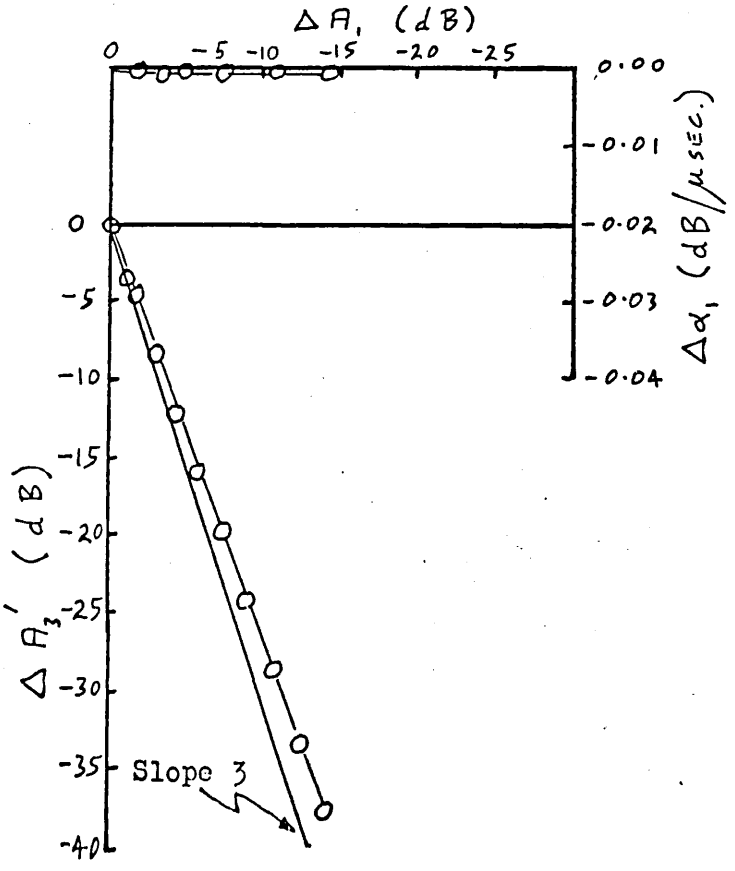

Fig. 8.8. The amplitude of the third harmonic $\Delta A_3'$ and the attenuation of the fundamental wave $\Delta\alpha_1$ as a function of the amplitude of the fundamental wave ΔA_1 in an X-irradiated crystal.

Three types of investigation were carried out using irradiated crystals. Firstly, the dependence of the fundamental wave amplitude on changes in $\Delta A_3'$ with bias stress was investigated. Secondly, the temperature dependence of the increase in $\Delta A_3'$ with bias stress was investigated. Thirdly, an investigation was carried out into the time dependent behaviour of $\Delta A_3'$ in an irradiated crystal when a large bias stress was applied. The first two of these investigations are discussed in Section 8.5 and the third is discussed in Chapter 9.

8.4 The Effect of the Fundamental Wave Amplitude in an Irradiated Crystal.

The bias stress dependence of the third harmonic amplitude in a non-irradiated NaCl specimen was measured in several experiments, for each of which a different fundamental driving pulse amplitude was used. A comparison of the results of each experiment revealed no behaviour which could be related to the different fundamental pulse amplitudes.

Similar experiments with an X-irradiated crystal did however reveal a dependence upon the driving pulse amplitude. Fig.8.7 shows the results of three experiments; one using the minimum possible fundamental wave amplitude (curve I), one with the maximum possible amplitude (curve III) and one with an intermediate amplitude (curve II). As the driving pulse amplitude increases the value of $\Delta A_3'$ at a given bias stress is

seen to decrease.

A dependence of $\Delta A_3'$ at a given bias stress upon the amplitude of the fundamental wave suggests that the fundamental wave is causing unpinning as well as the bias stress.

In an attempt to obtain further evidence of unpinning by the fundamental wave, the attenuation α_1 at zero bias stress was measured at different fundamental wave amplitudes. The results are shown in Fig.8.8 together with the dependence of $\Delta A_3'$ upon the fundamental wave amplitude. The attenuation is seen to be independent of the fundamental wave amplitude within the limits of experimental error. Thus, according to the Granato-Lücke (1956) hysteresis theory of dislocation damping, no appreciable unpinning is being caused by the fundamental wave. The third harmonic amplitude change with the fundamental wave amplitude at zero bias stress is also seen to depart only slightly from the third power relation predicted by a theory (see Chapter 3) which assumes no unpinning by the fundamental wave to take place. It therefore appears that, if the fundamental wave is responsible for any unpinning, then this unpinning must be of small extent.

It is possible to reconcile these apparently conflicting results, namely the evidence of stress wave induced unpinning of dislocations from measurements of $\Delta A_3'$ but not from measurements of α_1, by considering the behaviour expected of a crystal in which loop lengths are small. This may be seen by

referring to Fig.3.3. After X-irradiation loop lengths may have been reduced to a value below that of L_1. An increase in such a loop length brought about by the combined effect of the bias stress and the fundamental stress wave is seen still to result in an increase in $\Delta A_3'$. However, the change in α_1 with loop length in this region is small; the slope of the curve of α_1 in Fig.3.3 is seen to approach zero at very small loop lengths.

Of course the value of α_1 for a given loop length shown in Fig.3.3 is calculated neglecting any additional hysteresis loss due to stress wave induced unpinning and repinning of dislocations in each stress cycle. However, this contribution to α_1 may be small if the extent of the unpinning due to the stress wave is small.

The relative magnitudes of the fundamental stress wave amplitude (see Section 7.0) and the bias stresses used also suggest that the stress wave will have little effect on the overall unpinning which is taking place; the bias stresses are about an order of magnitude greater.

8.5 The Effect of Temperature

Experiments were carried out in which the value of $\Delta A_3'$ at fixed values of bias stress was measured at different temperatures. This was done in order to investigate the temperature dependence of dislocation unpinning, a process which is expected to be thermally activated. It was found, however, that even changing

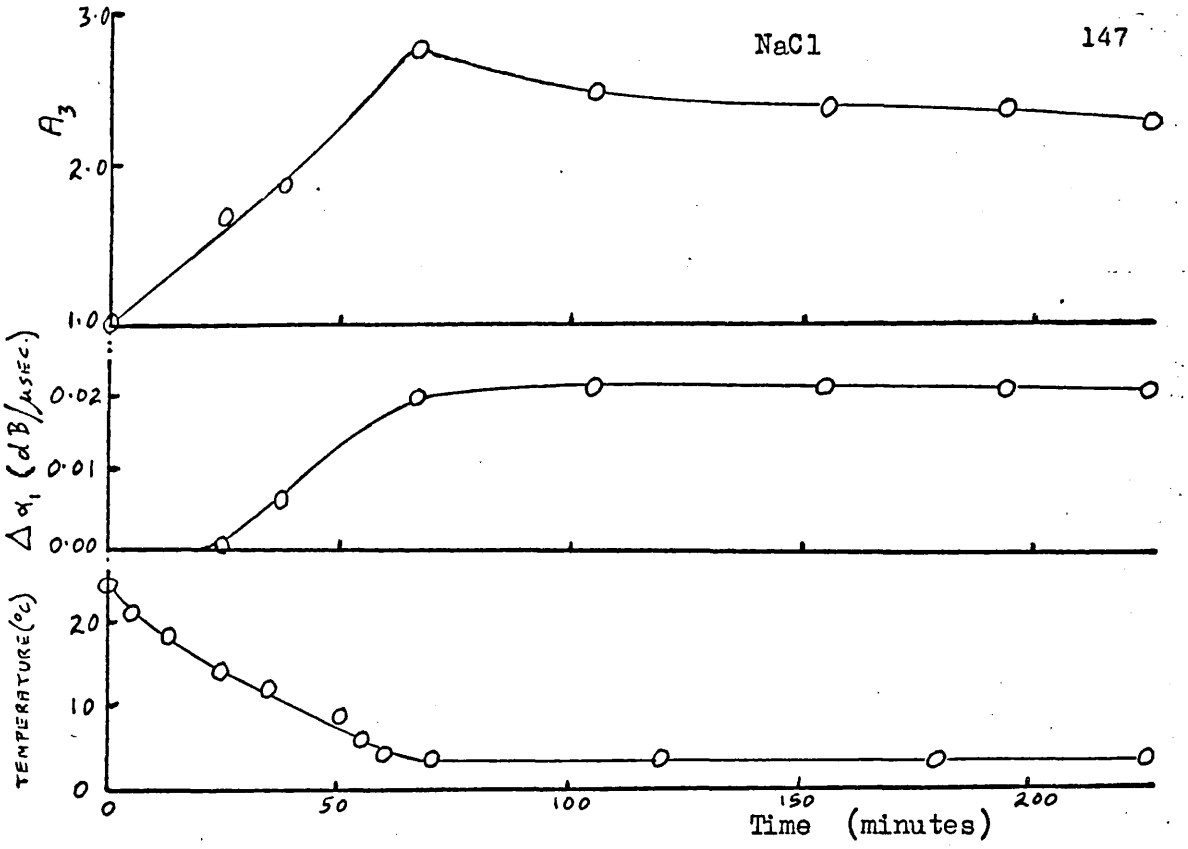

Fig. 8.9. The effect of decreasing temperature on the third harmonic amplitude A_3 and the attenuation of the fundamental wave $\Delta\alpha_1$.

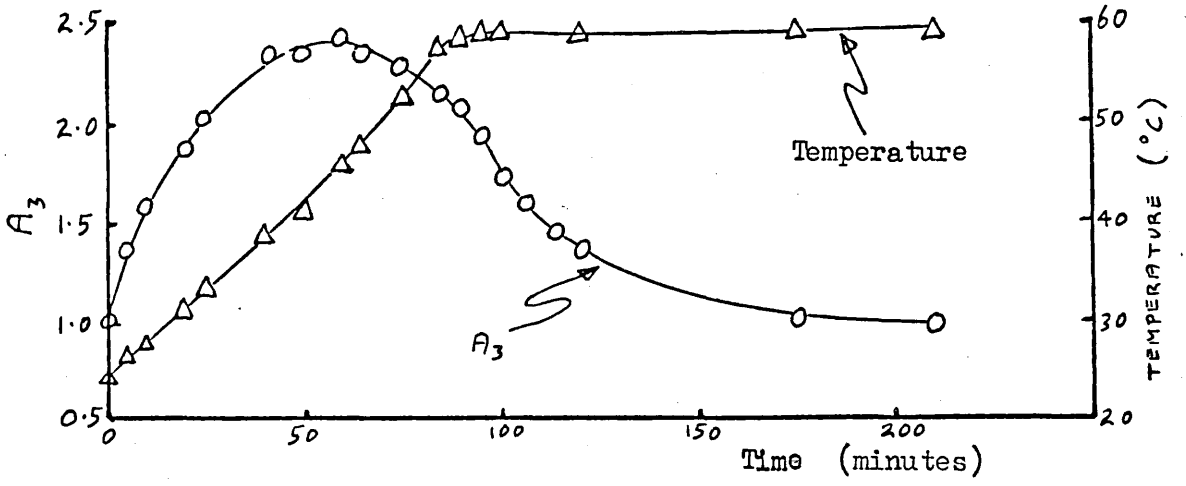

Fig. 8.10. The effect of increasing temperature on the 3rd harmonic A_3, in an NaCl crystal.

the temperature of a crystal at zero bias stress had a very considerable effect upon the third harmonic amplitude. Consequently, this effect will be described first.

(a) The Effect of Temperature Changes.

Fig.8.9 shows the effect of cooling from 26°C to 3.5°C on the third harmonic amplitude in NaCl at zero bias stress. The accompanying change in attenuation of the fundamental wave and the rate of cooling are also shown in Fig.8.9. The harmonic amplitude and the attenuation of the fundamental wave are seen to increase during cooling, with the harmonic amplitude showing a small recovery towards its initial value when constant temperature is attained. The change in third harmonic amplitude is seen to be very large compared with changes induced by external bias stresses at constant temperature (see Fig.7.2); to produce the same change by applying a tensile bias stress would mean subjecting the crystal to considerable plastic deformation.

In Fig.8.10 is shown the effect of an increase in temperature from 24°C to 59°C on the third harmonic amplitude at zero bias stress. An increase is again noted, which shows a much more rapid recovery towards its initial value than was observed at 3.5°C.

The magnitude of the change in third harmonic amplitude brought about by a slowly changing temperature (about 1/3°C per minute in Fig.8.10) suggests that

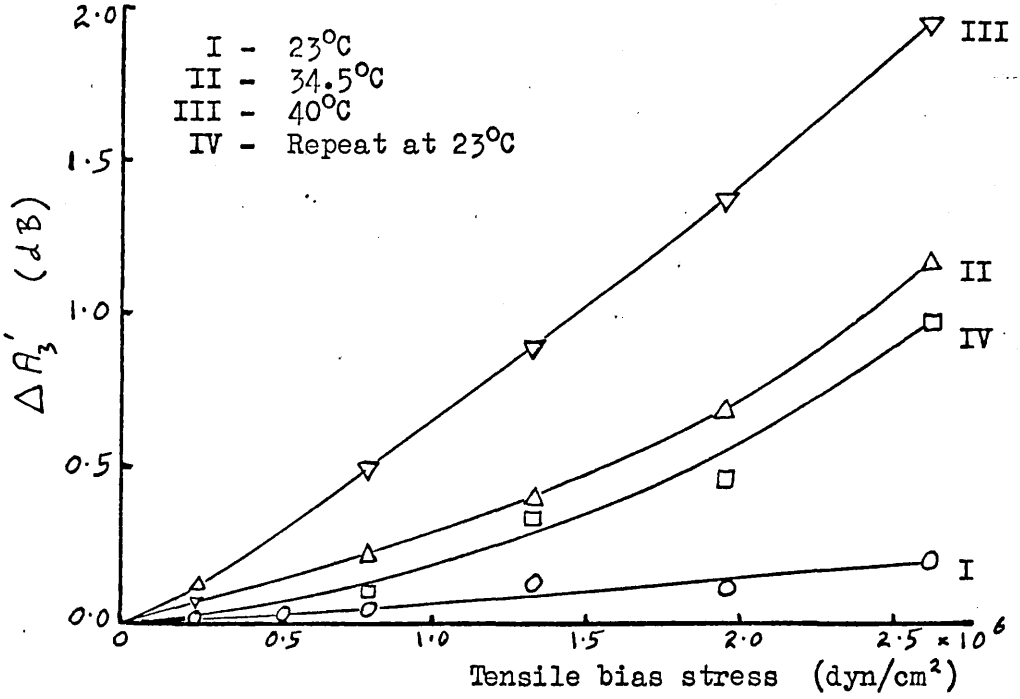

Fig. 8.11. The change in $\Delta A_3'$ with bias stress at different temperatures in an X-irradiated crystal. All attenuation changes of the fundamental wave were less than 0.004 dB/μsec.

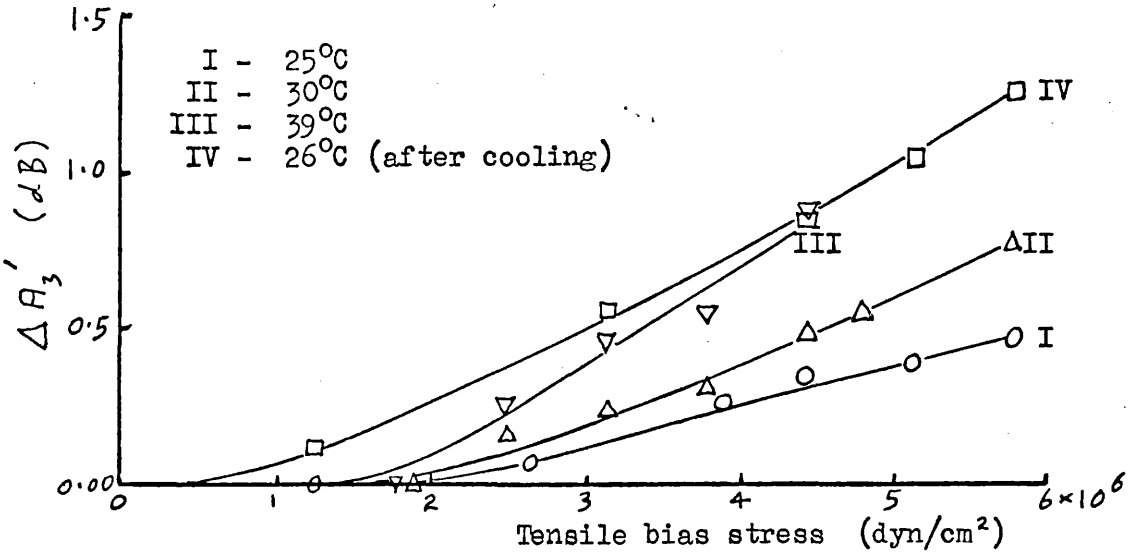

Fig. 8.12. The change in $\Delta A_3'$ with bias stress at different temperatures in the crystal used for the measurements of Fig. 8.11, but after a further X-irradiation (9,000 rads), and slower temperature changes.

temperature changes may be an important factor influencing the reproducibility of third harmonic measurements (see Section 7.2). Clearly care must be taken to avoid rapid changes in room temperature.

There are considered to be two reasons for the change in third harmonic amplitude with temperature. Firstly, stresses resulting from temperature gradients in the specimen may produce unpinning of dislocations. Secondly, changes in the lattice parameter may lead to a redistribution of dislocations in a crystal. For example, internal stresses may be relieved. However, a further discussion of these effects will be delayed until Chapter 9, when measurements of similar temperature effects in aluminium crystals and some further measurements in NaCl are reported.

(b) The Effect of Temperature on $\Delta A_3'$ at Different Bias Stresses in an Irradiated Crystal.

The dependence of $\Delta A_3'$ upon bias stress in an unirradiated crystal was not found to be greatly influenced by the temperature at which the experiment was carried out, providing the recovery of $\Delta A_3'$ with time following a temperature change was allowed time for completion.

Using an X-irradiated sample, however, a temperature dependence of $\Delta A_3'$ at a given bias stress was found. Fig.8.11 shows the results of an experiment in which measurements were made first at room temperature (curve I), then at 34.5°C (curve II), then at 40°C (curve III) and finally on returning to room temperature (curve IV).

The temperature change from room temperature to 34.5°C carried out after plotting curve I caused an increase in third harmonic amplitude, as expected from a consideration of Fig.8.10. This increase in harmonic amplitude was allowed to decay (see Fig.8.10) before the measurements at 34.5°C shown in curve II were made. A similar procedure was adopted after all the temperature changes. Thus the harmonic amplitude at zero bias stress was approximately the same in all the curves I, II, III and IV.

The following points are noted from a consideration of Fig.8.11.

(i) The value of $\Delta A_3'$ at a given bias stress increases as the temperature at which measurements are made is increased above room temperature.

(ii) When the temperature of the specimen is returned to room temperature, the specimen does not show the same behaviour as it did at room temperature before the high temperature measurements were made. At a given bias stress higher values of $\Delta A_3'$ are found.

It is considered that there may be two factors which might be giving rise to the behaviour observed here. These are:

(a) Thermally assisted unpinning of dislocations when a bias stress is applied. This will lead to greater unpinning at higher temperatures and therefore to a greater increase in dislocation loop length From Fig.3.3 it is seen that this will lead to a greater

increase in $\Delta A_3'$, as is observed.

(b) It was pointed out above that changes in temperature during the experiment resulted in changes in harmonic amplitude. Although no measurements were made until these changes were complete and the harmonic amplitude had returned to its initial value, it is still possible that the dislocation configuration was not the same before and after a temperature change.

To investigate this latter possibility further, a second experiment was carried out in which the rate of temperature change was much smaller. The harmonic amplitude was still affected by the temperature change but to a smaller extent; a change of the form shown in Fig.8.10 was observed, but the height of the peak was much smaller than in the first experiment. The specimen was also given a further dose of X-irradiation. Fig.8.12 shows the results of this second experiment. The following points are noted from these results.

(i) The further irradiation of the specimen is seen to have reduced the room temperature value of $\Delta A_3'$ at a given bias stress (see curve I in Fig.8.12) to approximately the value it had at room temperature before the first experiment (see curve I in Fig.8.11). This suggests that dislocation loop lengths are longer after the high temperature measurements than they were before.

(ii) The measurements made at 30°C and 38.8°C show an increase in $\Delta A_3'$ with temperature at a given bias stress in a way similar to that shown in Fig.8.11. Thus it appears that the slower rate of change in

temperature has not appreciably altered the results.

(iii) The measurements made at room temperature (curve IV) after completion of the high temperature measurements show a much greater dependence of $\Delta A_3'$ upon bias stress than was observed at room temperature before the temperature was increased (curve I). This behaviour has already been noted in Fig.8.11.

(iv) In view of the lack of reproducibility of the room temperature results noted above, it appears that the specimen cannot be assumed to have the same dislocation-pinning point configuration at the various temperatures at which measurements were made. It is not therefore possible to say what significance can be attached to the observed increase in $\Delta A_3'$ at a given bias stress with temperature. This may, for example, be due to thermally assisted unpinning or to unpinning as a result of thermal stresses (due to temperature gradients in the crystal). Further investigations are required to resolve this behaviour.

8.6 The Effect of Crystal Purity.

In order to investigate further the effect of loop length upon dislocation third harmonic generation, a specially pure NaCl crystal was obtained (see table 5.1). Unfortunately, the crystal supplied by the crystal growers contained several sub-crystals with widely different crystal orientations. This meant that the single crystal specimen which was eventually

cut from this material was small (2.6 x 2.3 x 1.7 cm^3). The crystal was annealed at 650°C for some hours.

A tensile bias stress was found to increase the third harmonic amplitude in a way similar to that already observed with normal crystals. See, for example, Fig.7.2. In particular, there was no evidence, even after plastic deformation, of a maximum in $\Delta A_3'$ as expected for long dislocation loop lengths (see Fig.3.3). It is concluded that the purity of this crystal is little different from that of the other crystals used in this work.

CHAPTER 9

Time Dependent Behaviour in Aluminium and NaCl

9.0. Introduction

Time dependent effects have been observed in both aluminium and sodium chloride single crystals. A time dependence of the second harmonic amplitude has been observed only in aluminium however, while a time dependence of the third harmonic amplitude has been observed in both aluminium and NaCl. It will be remembered that it was not possible to obtain NaCl crystals of sufficient purity for dislocation second harmonic measurements to be made. Measurements of the second harmonic effect will be discussed first and then measurements of the third harmonic effect.

9.1. The Time Dependence of the Second Harmonic Amplitude in Aluminium

(i) Measurements at Room Temperature.

A time dependence of the second harmonic amplitude in a 5N aluminium crystal after applying a bias stress has already been mentioned in chapter 6.1. In Fig. 9.1(a) the second harmonic amplitude in a 5N aluminium crystal is shown as a function of time after the application and subsequent removal of a tensile bias stress. The second harmonic amplitude is seen to increase instantaneously to a new value when the bias stress is applied. This new value then decays slowly with time until the bias stress is removed, when there is an instantaneous decrease in the second harmonic amplitude. The second harmonic

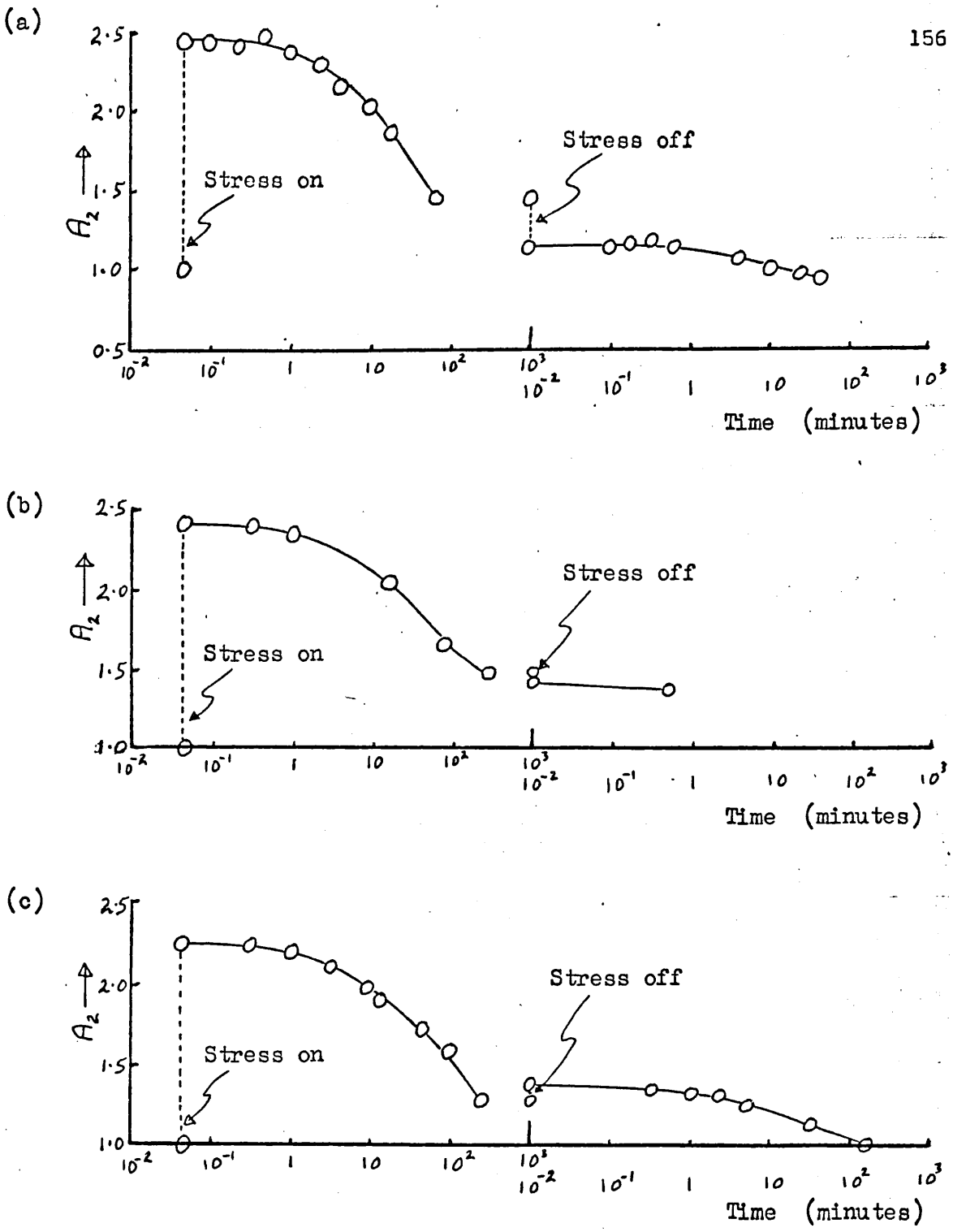

Fig. 9.1. The 2nd harmonic amplitude as a function of time when a stress of 1.8×10^5 dynes cm^{-2} is applied. In (a) the stress is applied for 75 minutes, in (b) for 133 minutes and in (c) for 250 minutes.

amplitude. The second harmonic amplitude then continues to decay slowly. In Fig. 9.1(b) a slightly different behaviour is shown when the bias stress is removed after a longer period of time. The instantaneous decrease in harmonic amplitude accompanying the removal of the bias stress is seen to be less than in Fig. 9.1(a). When the bias stress is applied for an even longer time the removal is seen in Fig. 9.1(c) to be accompanied by an instantaneous increase in second harmonic amplitude.

It was thought that the decay of the second harmonic amplitude might be the result of some thermally activated process, in which case the decay might be more rapid at elevated temperatures. An investigation of the effect of temperature was therefore carried out. However it was found that changes in temperature had a quite considerable effect upon the amplitude of the second harmonic at zero bias stress. It will be remembered that a similar effect was noted in section 8.6 with measurements on the third harmonic in NaCl. Before describing measurements of the time dependence at elevated temperatures the effect of temperature changes on the second harmonic in aluminium will be considered.

(ii) The Effect of Changes in Temperature.

It was found that with zero bias stress applied to the crystal the harmonic amplitude began to change as soon as the temperature started to rise or fall. To investigate the possibility of this behaviour being due to changes in the transducer bond properties or to geometrical distortion of the crystal with changing temperature the experiment was repeated using first a fused silica rod and then a polycrystalline impure (commercial) aluminium rod instead of the aluminium single

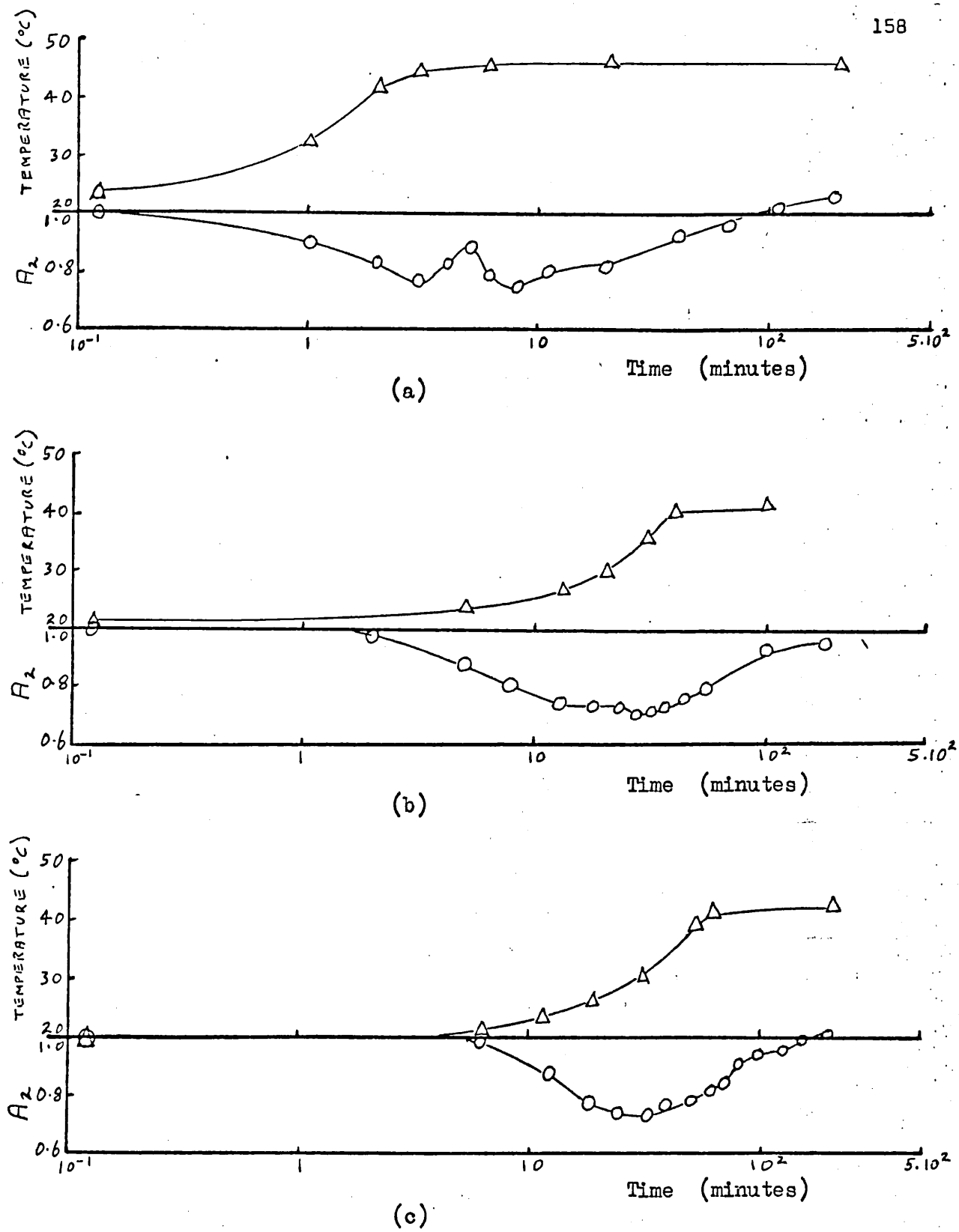

Fig. 9.2. The change in 2nd harmonic amplitude with three different rates of increasing temperature.

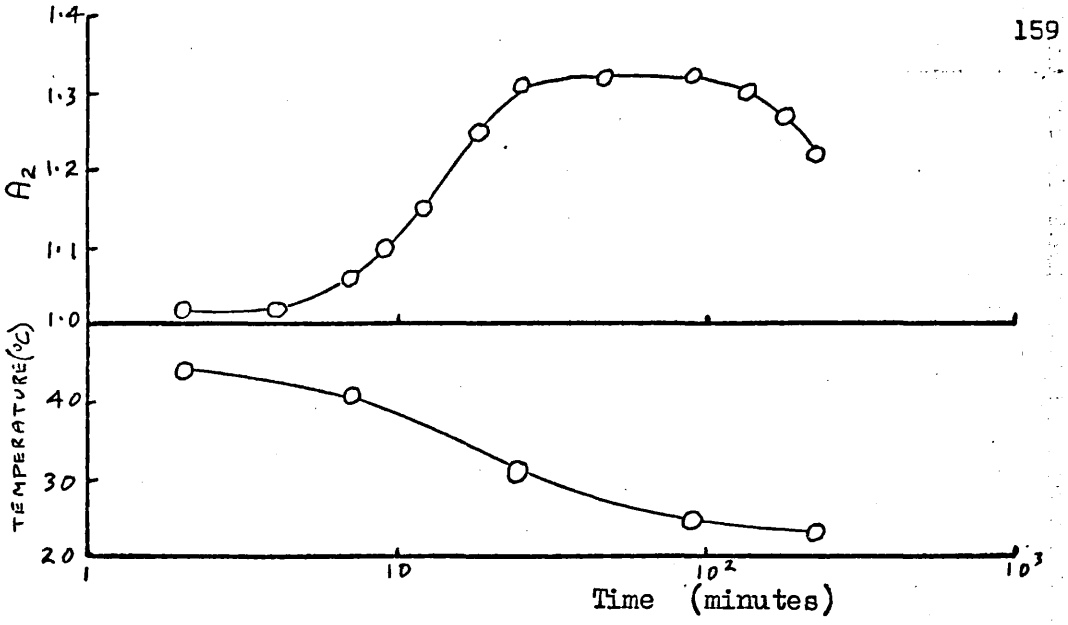

Fig. 9.3. The change in 2nd harmonic amplitude A_2 with decreasing temperature.

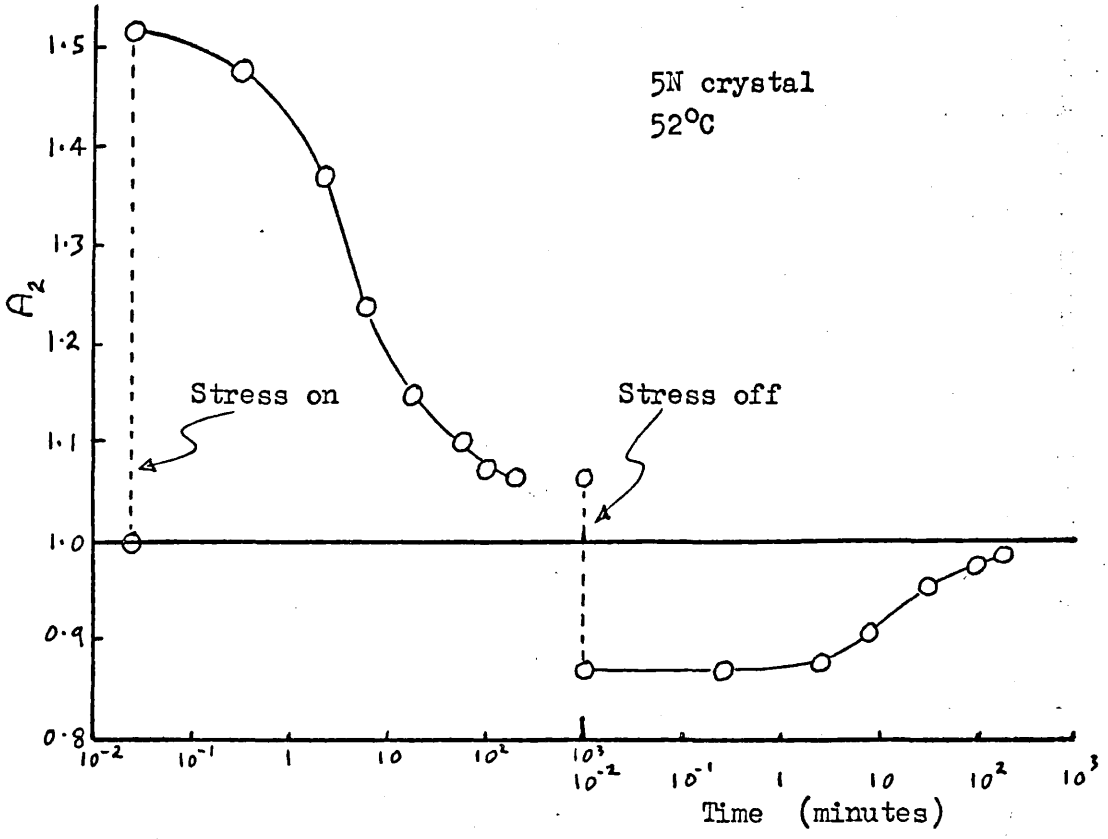

Fig. 9.4. The recovery of the 2nd harmonic amplitude A_2 at 52°C.

crystal. No dependence of harmonic amplitude on temperature was detected in either case. It was concluded that the effect was not due to the transducer bond or to distortion of the crystal.

In Figs. 9.2 (a), (b) and (c) are shown the harmonic amplitude changes when the temperature of the aluminium crystal was increased from room temperature to approximately 45°C at different rates. The harmonic amplitude is seen to decrease as the temperature rises. For the most rapid increase in temperature [Fig. 9.2(a)] the harmonic amplitude is seen to pass through two minima and then to rise slowly towards its initial value before the temperature change. For the least rapid increase in temperature [Fig. 9.2(c)] the harmonic amplitude is seen to pass through only one minimum before recovering towards its initial value. Fig. 9.2(b) shows an intermediate behaviour. The lowest value attained by the second harmonic amplitude is seen to be approximately independent of the rate of temperature change (the final temperatures are not exactly the same in the three cases). The curve of Fig. 9.2(a) was found to be well reproduced by a second identical experiment after the crystal had remained at room temperature for a few days.

The behaviour of the harmonic amplitude as the crystal was allowed to cool down to room temperature again is shown in Fig. 9.3. The harmonic amplitude is seen to increase to a single maximum value and then to decrease towards its initial value.

Two factors are considered important in giving rise to the behaviour shown in Fig. 9.2 and in Fig. 9.3. The first is thermal stresses resulting from temperature gradients in the crystal. The second is a modification of the dislocation configuration in the crystal brought about by changes in the

lattice parameter with temperature. For example, some internal stresses may be relieved at higher temperatures.

The effect of thermal stresses arising from temperature gradients will be considered first. These stresses are expected to be largest when the rate of change in temperature is the greatest. The first minimum in second harmonic amplitude shown in Fig. 9.2(a) is therefore attributed to these stresses, since this minimum disappears when the rate of temperature change is small [Fig. 9.2(c)]. When the temperature reaches a constant value the stresses disappear and the harmonic amplitude is expected to return to its initial value, assuming that the stresses were insufficient to alter the dislocation configuration appreciably.

The change in harmonic amplitude which occurs even when the temperature is changed very slowly [Fig. 9.2(c)] is attributed to changes in dislocation configuration associated with changes in the lattice parameter. Since it is the final temperature which determines the new dislocation configuration the rate at which this temperature is achieved is not expected to influence the second harmonic amplitude. The recovery which appears when constant temperature is attained and the recovery shown in Fig. 9.1 at constant temperature are attributed to some similar process. This recovery is considered further below.

It is seen that the harmonic amplitude increases with decreasing temperature and decreases with increasing temperature. Thermal stresses are expected to be of a tensile nature when the outside of the crystal is hotter than the inside, and compressive when the temperature gradient is reversed. Also an expansion of the lattice is expected, for example, to relieve a tensile internal stress while a contraction of the lattice is expected

to have the opposite effect. Thus it appears reasonable that heating and cooling can cause the second harmonic amplitude to change in opposite ways. It should be noted that thermal stresses due to temperature gradients in a cylindrical specimen can act in a radial direction while external bias stresses were always applied along the axis of the crystal.

(iii) Measurements at Constant Elevated Temperatures.

The decay of the second harmonic amplitude with time after applying a tensile bias stress of 0.8×10^5 dynes cm^{-2} was measured at several temperatures between room temperature and $60^{\circ}C$. Sufficient time was allowed after a change in temperature for the harmonic amplitude to attain a constant value. This time varied from about 10 hours at $30^{\circ}C$ to 2 hours at $60^{\circ}C$. That the specimen in fact recovered to near its initial state after each experimental run at a particular temperature was shown by the fact that the harmonic amplitude change on initial application of the bias stress was always of about the same magnitude.

As the temperature at which recovery took place increased, the recovery time decreased rapidly. It was therefore possible to observe the later stages of the recovery which at room temperature would have involved measuring over extremely long times. In Fig. 9.4 is shown the recovery of the harmonic amplitude at $52^{\circ}C$ after applying a bias stress of 0.8×10^5 dynes cm^{-2}. The harmonic amplitude is seen to approach the value which it had before application of the bias stress. When the bias stress is removed the harmonic amplitude decreases instantaneously to below its initial value and then recovers back towards its initial value. The decrease in harmonic amplitude on removal of the bias stress is to be contrasted

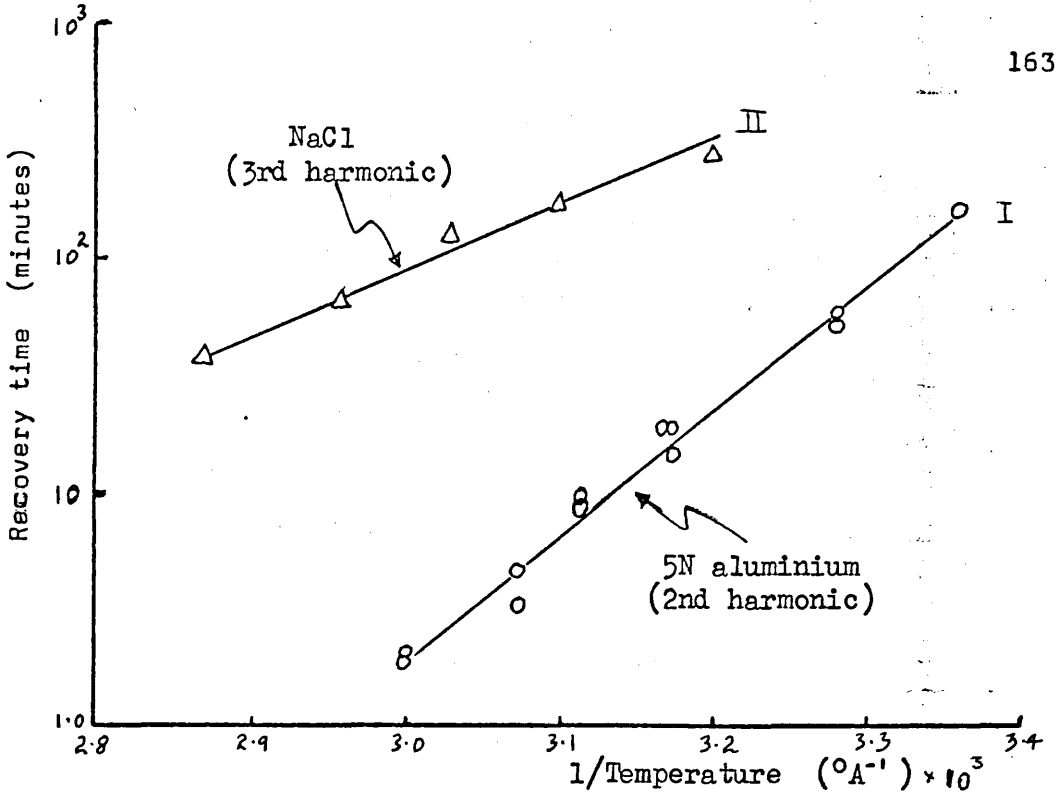

Fig. 9.5. The recovery time plotted against reciprocal temperature.

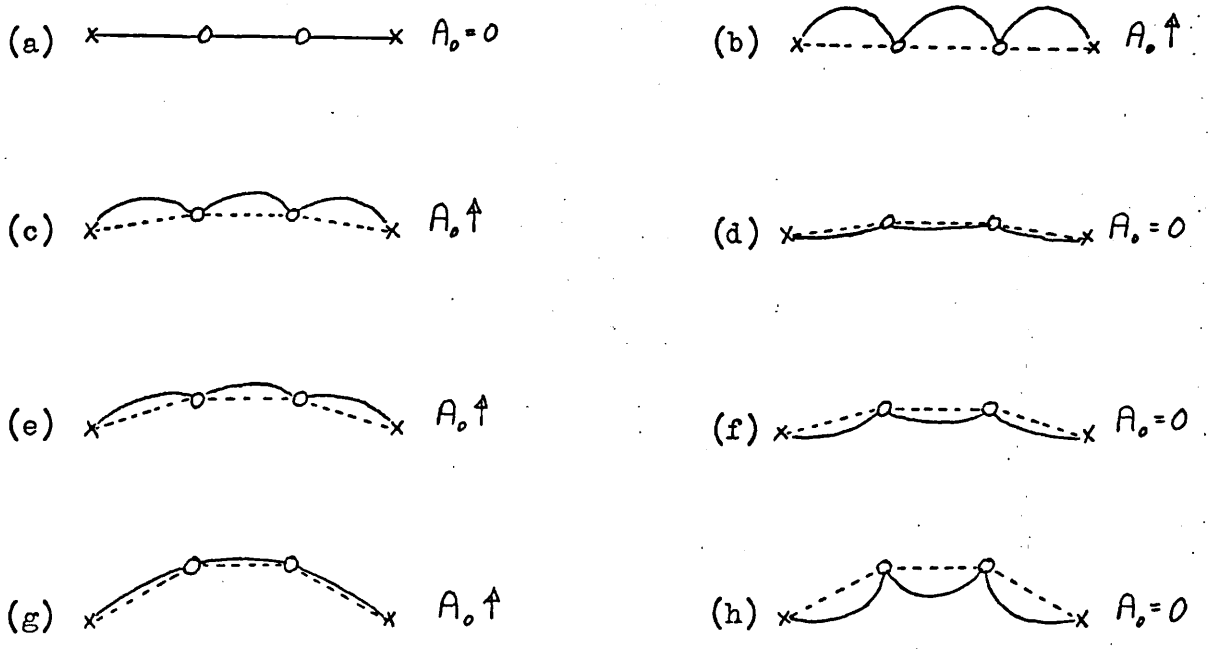

Fig. 9.6. The model of dislocation-point defect behaviour after application of a bias stress A_0 for certain periods of time.

with the behaviour shown in Fig. 9.2(c) when a bias stress was removed after a long period at room temperature producing an increase in harmonic amplitude. In order to discover whether the recovery process was thermally activated, the results of measurements at different temperatures were represented graphically by plotting the $(\ell n_e \tau, \frac{1}{T})$ curve, where τ is the time in which the harmonic amplitude recovered by half the instantaneous increase associated with the bias stress, and T represents temperature. In Fig. 9.5 curve I shows the measurements plotted in this way. The experimental points are seen to lie fairly well on a straight line which is of the form of the Arrhenius equation

$$\tau = \tau_o \exp(\frac{Q}{kT}) , \qquad (9.1)$$

where τ_o is a constant, Q is an activation energy and k is Boltzmann's constant. The recovery process thus appears to be thermally activated with an activation energy calculated from the results of Fig. 9.5 to be 1.07 ev.

(iv) Discussion.

According to the Hikata and Elbaum (1966) theory of dislocation second harmonic generation the harmonic amplitude increases with bias stress [see equation (3.15)]. This is attributed physically to the curvature of dislocations as a result of the bias stress, i.e: the dislocation motion must be asymmetric as well as non-linear for a dislocation second harmonic to be generated. The decay in second harmonic amplitude following the instantaneous increase in amplitude brought about by a bias stress as observed in the present measurements is attributed to a reduction with time in the curvature of dislocations. The mechanism for this is thought to be the

diffusion of dislocation pinning points, and the activation energy measured above may then be associated with this diffusion process.

The proposed model for this mechanism is illustrated in Fig. 9.6. In Fig. 9.6(a) is shown diagrammatically the position of a pinned dislocation before the application of a bias stress, After the bias stress is applied the dislocation loop lengths are bowed out, as shown in Fig. 9.6(b), with a resultant increase in harmonic amplitude. There is now a net force acting upon the pinning points which may lead to them diffusing through the lattice. Suppose that after a certain time the dislocation has moved to the position shown in Fig. 9.6(c). The outer two pinning points are considered fixed; they may for example be cross-over points in the dislocation network. The curvature of the dislocation loop lengths is seen to be reduced. If the bias stress is removed at this point the curvature of the dislocation may be reversed and become smaller, as shown in Fig. 9.6(d).

The model is now able to account qualitatively for the behaviour shown in Fig. 9.1(a). Removal of the bias stress will be accompanied by a decrease in harmonic amplitude, since the curvature of the loop lengths is reduced. The force on the pinning points will now return them to the original positions, and the harmonic amplitude will continue to decay towards its initial value, as observed.

Suppose now that the bias stress is applied for a longer period so that the dislocation moves to the position shown in Fig. 9.6(e). Let this position be such that when the bias stress is removed the curvature of the loop lengths is reversed but remains of the same magnitude, as shown in Fig. 9.6(f). In this case the second harmonic amplitude will be unchanged. In

this way it is possible to account for the results shown in in Fig. 9.1(b), where the removal of the bias stress is accompanied by only a small change in harmonic amplitude.

Finally, consider the situation shown in Fig. 9.6(g) where the pinning points have diffused even further. The bowing out of the loop lengths when the bias stress is removed is seen in Fig. 9.6(h) to be much increased. The behaviour noted in Fig. 9.1(c), namely an increase in harmonic amplitude upon removal of the bias stress, may therefore be understood.

However the model described above does not account for the behaviour shown in Fig. 9.4. These measurements were made at a much higher temperature than those of Fig. 9.1, and the recovery shown in Fig. 9.4 is expected to be much more complete than that of Fig. 9.1(c). It is seen that the harmonic amplitude decreases when the bias stress is removed, instead of increasing as the above model predicts and as shown in Fig. 9.1(c). Further investigation is needed to resolve this difficulty. For example, unpinning of dislocations may be important, in which case experiments with smaller bias stresses would be worthwhile.

9.2. The Time Dependence of the Third Harmonic Amplitude

(a) Measurements in Sodium Chloride.

A time dependence of the third harmonic amplitude in a NaCl crystal after the application of a bias stress has already been noted in section 7.2, (see Fig. 7.). The effect of temperature on this time dependence has been investigated in the same way as for the second harmonic in aluminium.

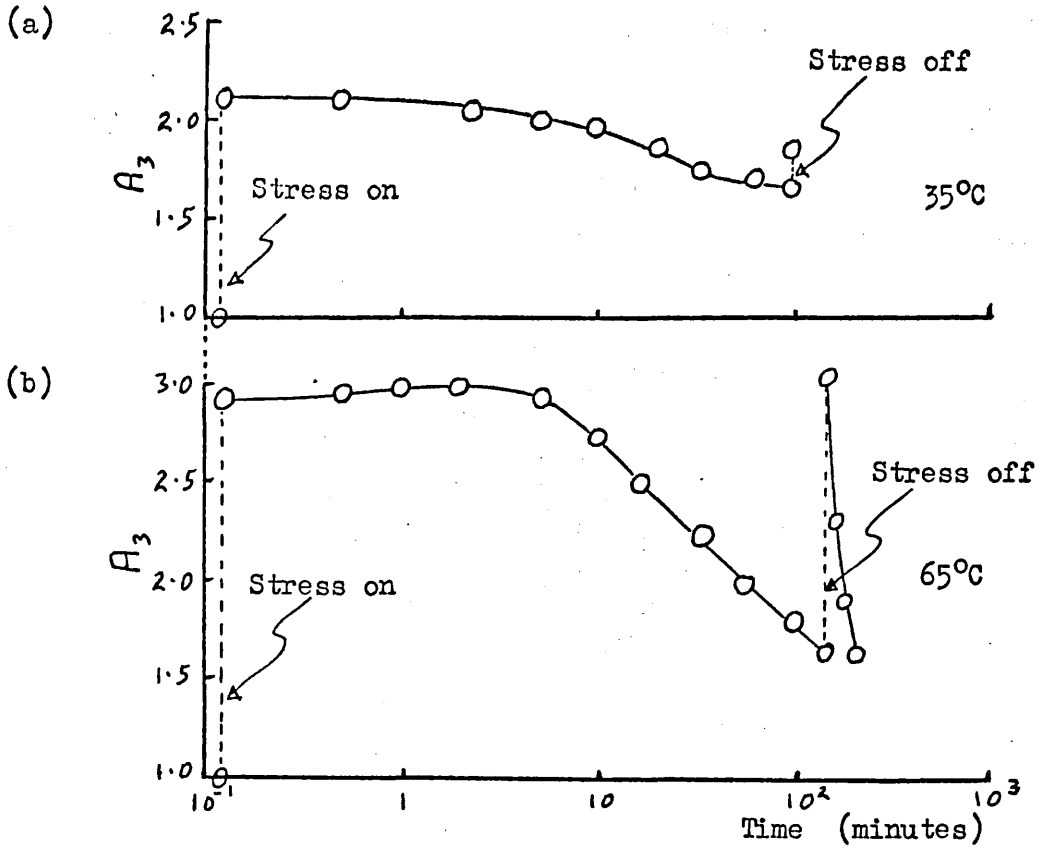

Fig. 9.7. The recovery of the 3rd harmonic amplitude in an NaCl crystal after stressing to 5×10^6 dyn/cm^2 at (a) 35°C and (b) 65°C.

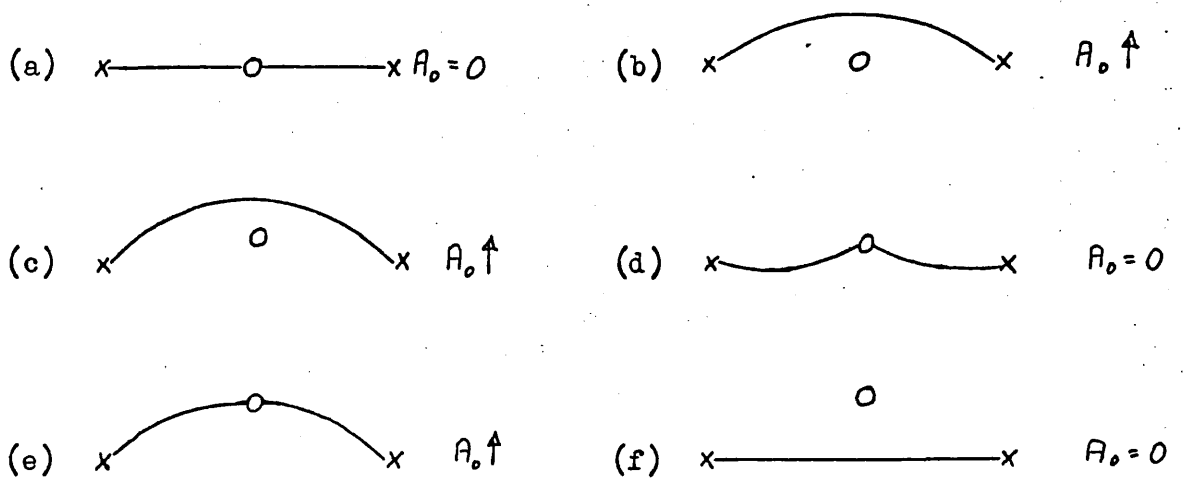

Fig. 9.8. The model of dislocation-point defect behaviour which is proposed to account for the recovery of the 3rd harmonic amplitude after the application of a bias stress A_0. The effect of removing A_0 after different time intervals is shown.

(i) The Effect of Temperature Changes.

The effect of a decreasing temperature upon the third harmonic amplitude in NaCl is shown in Fig. 8.9 while Fig. 8.10 shows the effect of an increasing temperature. It is seen that the magnitude of the changes in third harmonic amplitude with temperature are much greater than were observed with the second harmonic in aluminium for equivalent temperature changes [see section 9.1(ii)]. This may be due in part to the lower thermal conductivity of NaCl (0.096 Joules $cm^{-1}\ {}^{o}K^{-1}\ sec^{-1}$) compared with that of aluminium (2.38 Joules $cm^{-1}\ {}^{o}K^{-1}\ sec^{-1}$). This means that temperature gradients and therefore thermal stresses will be greater in NaCl than in aluminium.

(ii) Measurements at Constant Elevated Temperatures.

The decay in third harmonic amplitude at room temperature after applying a bias stress was very slow, so measurements were normally made at much higher temperatures. Fig. 9.7(a) and (b) show the behaviour of the third harmonic amplitude at $35^{o}C$ and $65^{o}C$ respectively when a bias stress was applied and then removed after a time interval. When the stress was applied there was an instantaneous increase in third harmonic amplitude the magnitude of which is seen to depend on the temperature (see section 8.6). The third harmonic amplitude is seen to decrease with time towards its initial value while the bias stress remains applied. The rate of this decrease is seen to be greater at the higher temperature. The removal of the bias stress is seen to be accompanied by an instantaneous increase in harmonic amplitude, the magnitude of which is greater when the recovery has proceeded further (i.e: at $65^{o}C$). Measurements were made at various temperatures and curve II of Fig. 9.5 shows that the measurements are again described by expression (9.1), with an

case removal of the bias stress is seen to result in a second unpinning of the dislocation.

The behaviour of the third harmonic when the bias stress is removed after different periods of time may now be understood. If the stress is removed immediately an instantaneous decrease in harmonic amplitude is expected, according to the situation shown in Fig. 9.8(a) and (b). When the stress is removed after a long period, i.e: when the recovery is complete, then an increase in harmonic amplitude is expected according to Fig. 9.8(e) and (f). This increase is expected to be of similar magnitude to that which accompanies the application of the bias stress. This is the behaviour seen in Fig. 9.7(b). When the bias stress is removed before the recovery is complete there may be a small decrease, a small increase or no change in harmonic amplitude depending upon the relative number of dislocations showing the behaviour of Fig. 9.8(d) and Fig. 9.8(f). The results of Fig. 9.7(a) are consistent with a more than half complete recovery.

The model of dislocation behaviour discussed above is similar to one proposed by Carpenter (1968) in connection with some measurements of the recovery with time of an ultrasonic attenuation in LiF.

In the present measurements with NaCl further investigations are suggested in which (i) the magnitude of the bias stress is altered, and (ii) different amplitudes of the fundamental wave are used. If the model proposed here is correct, then larger bias stresses should increase recovery times since point defects will have farther to diffuse. The activation energy may or may not be changed, depending upon the nature of the stress field surrounding the dislocations. An increased fundamental

wave amplitude is expected to reduce the recovery time if the amplitude of dislocation oscillation is comparable with the separation of pinning points and dislocations after pinning.

(b) Measurements in Irradiated Sodium Chloride.

Some measurements were attempted with X-irradiated crystals, in order to determine the effect of colour centres on the recovery process. A time dependent behaviour was observed, similar to that shown in Fig. 9.7(a) for an unirradiated crystal. However the increases in harmonic amplitude produced by bias stresses were much smaller than those found in unirradiated crystals (see Fig. 8.6) and were too small to allow accurate measurement over long periods of time. It was not therefore possible to investigate the temperature dependence of the recovery as was done in unirradiated NaCl.

(c) Third Harmonic Measurements in Aluminium.

Measurements of the time dependence of the third harmonic amplitude in the 4N aluminium crystal at room temperature have already been shown in Fig. 6.7. The behaviour is seen to be similar to that observed with the third harmonic in NaCl [see for example Fig. 9.7(b)] in the following respects:

(i) The instantaneous increase in harmonic amplitude when a bias stress is applied is followed by a decrease in harmonic amplitude with time.

(ii) When the bias stress is removed, the harmonic amplitude increases instantaneously and then decreases again with time.

The effect of temperature changes upon the third harmonic

amplitude in the aluminium crystal was also found to be much the same as that in the NaCl crystal. However no experiments to determine an activation energy have yet been carried out.

CHAPTER 10.

Conclusion

The aim of this work has been to investigate ultrasonic second and third harmonic generation due to dislocation This chapter contains a brief summary of the results of the experimental work which has been carried out.

The initial experiments with aluminium crystals revealed a dislocation second harmonic generation in a 5N crystal similar to that observed by Hikata, Chick and Elbaum (1965). The absence of a dislocation effect in a 4N crystal was attributed to shorter dislocation loop lengths in this lower purity crystal.

During the course of these measurements an interesting time dependent effect was observed which has not been reported previously. It is proposed that this effect is due to the thermally activated diffusion of dislocations and point defects through the lattice, and an activation energy of 1.1 ev has been measured for this process. A similar time dependence of the third harmonic amplitude in NaCl was also found. A model to account for this behaviour is proposed in which point defects diffuse to dislocation lines, thereby reducing the dislocation loop lengths. An activation energy of 0.58 ev for this diffusion process has been measured. A significant difference between the models proposed to account for the second harmonic effect and the third harmonic effect should be noted. In the case

of the second harmonic it is proposed that the thermally activated motion of both dislocations and pinning points leads to a reduction in the curvature of dislocations and therefore to a reduction in harmonic amplitude. However, in the case of the third harmonic point defects alone are considered to diffuse through the lattice to dislocations and thus reduce the dislocation loop length. These measurements have provided useful information on the strain-ageing properties of aluminium and NaCl crystals, and future investigations of this effect would be worthwhile.

A dependence of the second and third harmonic amplitudes on temperature changes has been attributed to two effects. These are (i) thermal stresses due to temperature gradients in the specimens, and (ii) a change in the lattice parameter with temperature leading to a change in the dislocation configuration in the crystal. It is worth noting that a temperature change of $35^{\circ}C$ in 90 minutes led to a $2\frac{1}{2}$ fold increase in third harmonic amplitude in an NaCl crystal.

Although the third harmonic measurements in aluminium crystals were in good general agreement with the work of Hikata, Sewell and Elbaum (1966) and with the theoretical predictions of Hikata and Elbaum (1966), a different dependence of $\Delta A_3'$ at a given bias stress upon the amplitude of the fundamental wave has been noted. Two proposed reasons for this are (i) the different crystal orientation used in this work and in the work of Hikata, Sewell and Elbaum (1966) which leads to different resolved shear stresses in the

dislocation slip planes, and (ii) the unpinning of dislocations by the fundamental stress wave as well as by a bias stress.

The deviation from the third power relation between the fundamental and third harmonic wave amplitudes noted in a 6N aluminium crystal is also attributed to the unpinning of dislocations by the fundamental stress wave. An analytical theory of harmonic generation due to stress-wave-induced unpinning of dislocations is required.

During the course of the investigation of third harmonic generation in NaCl some interesting effects have been observed which did not appear in the measurements on aluminium crystals. Evidence has been found for the presence of internal stresses remaining in an NaCl crystal after plastic deformation. It is shown that compressive internal stresses remain after a plastic deformation in tension, and that these stresses become tensile after a further plastic deformation in compression. It should be noted that the internal stresses observed here must be sufficient to cause actual unpinning of dislocations, whereas those reported by Hikata, Chick and Elbaum (1965) during an investigation of second harmonic generation in aluminium need only have influenced the curvature of dislocations.

A maximum in third harmonic amplitude with propagation distance when the harmonic wave is reflected from a stress free boundary at one end of the specimen has been observed in agreement with the results of a second harmonic investigation by Hikata, Chick and Elbaum

(1965) using two quartz transducers, but contrary to theoretical predictions. In fact the observed behaviour is found to be in better agreement with that expected of a harmonic wave travelling in an infinitely long solid. Further investigations are needed to resolve this difficulty.

Possible evidence of the thermally assisted unpinning of dislocations in an X-irradiated NaCl crystal has been found as a result of some measurements of the bias stress dependence of $\Delta A_3'$ at different temperatures. A difficulty in interpreting these measurements is that changes in temperature may have led to changes in the dislocation configuration in the crystal. These changes might themselves account for the results obtained at different temperatures.

Evidence has also been found to suggest that dislocation loop lengths in an NaCl crystal which has been first annealed and then slightly deformed are much longer than would be expected simply from a consideration of the crystal purity. Such an effect has been noted in aluminium by Hikata, Sewell and Elbaum(1966).

The absence of a dislocation second harmonic effect in NaCl is attributed to the dislocation loop lengths being too short. It is not of course possible to obtain NaCl crystals of the same degree of purity that is possible with zone refined aluminium crystals. It may be argued that there is some point in studying dislocation second as well as third harmonic generation, since the second harmonic amplitude is sensitive to the

curvature of dislocations while the third harmonic amplitude is sensitive to changes in loop length, due for example to unpinning. In order to detect changes in second harmonic amplitude due to changes in the curvature of dislocation loop lengths in NaCl, the lattice second harmonic generation must be reduced. This might be done by propagating shear waves instead of compressional waves. An alternative approach might be the use of Li F instead of NaCl, since the Li F lattice is expected to show a smaller degree of anharmonicity than NaCl [Kontorova (1968)].

REFERENCES

BARBER, D.J. (1962)	Journ. Appl. Phys. 33. 3141.
BEAN, C.P., DE BLOIS, R.W. and NESBITT, L.B. (1959)	Journ. Appl. Phys. 30. 1976.
BREAZEALE, M.A. and LESTER, W.W. (1961)	Journ. Acoust. Soc. Am. 33. 1803.
BREAZEALE, M.A. and FORD, J. (1965)	Journ. Appl. Phys. 36. 3486.
BRUGGER, K. (1964)	Phys. Rev. 133. A1611.
BUCK, O. and THOMPSON, D.O.(1966)	Matl. Science and Eng. 1. 117.
CARPENTER, S.H. (1968)	Acta. Metallurgica 16. 73.
CARR, P.H. (1968)	Phys. Rev. 169. 718.
COTTRELL, A.H. (1961)	Dislocations and Plastic Flow in Crystals (O.U.P.).
FAY, R.D. (1957)	Journ. Acoust. Soc. Am. 29. 1200
GAUSTER, W.B. and BREAZEALE, M.A. (1966)	Rev. Sci. Inst. 37. 1544.
GAUSTER, W.B. and BREAZEALE, M.A. (1967)	Journ. Acoust. Soc. Am. 41. 860.
GAUSTER, W.B. and BREAZEALE, M.A. (1968)	Phys. Rev. 168. 655.
GEDROITS, A.A. and KRASIL'NIKOV, V.A. (1963)	Sov. Phys.-JETP 16. 1122.
GIMPL, M.L., FUSCHILLO, N. and NELSON, C.E. (1965)	Journ. Appl. Phys. 36. 3946.
GRANATO, A.V. and LUCKE, K. (1956)	Journ. Appl. Phys. 27. 583.
HIKATA, A., CHICK, B. and ELBAUM, C. (1963)	Appl. Phys. Lett. 3. 195.
HIKATA, A., CHICK, B. and ELBAUM, C. (1965)	Journ. Appl. Phys. 36 229.
HIKATA, A. and ELBAUM, C. (1966)	Phys. Rev. 144. 469.
HIKATA, A., SEWELL, F.A. and ELBAUM, C. (1966)	Phys. Rev. 151, 442.
HOLT, A.C. and FORD, J. (1967)	Journ. Appl. Phys. 38. 42.
KOEHLER, J.S. (1952)	Imperfections in Nearly Perfect Crystals. (WILEY).
KONTOROVA, T.A. (1968)	Sov. Phys.-Solid State 10.389.

KRASIL'NIKOV, V.A. and ZAREMBO, L.K. (1967)	Trans. IEEE SU-14. 1.12.
LANDAU, L.D. and LIFSHITZ, E.M. (1959)	Theory of Elasticity. (Addison-Wesley).
MARKHAM, J.J. (1966)	Solid State Physics, Supp. 8. (A.P.).
MASON, W.P. (1958)	Physical Acoustics and Properties of Solids. (Van Nostrand).
MELLEN, R.H. and BROWNING, D.G. (1968)	Journ. Acoust. Soc. Am. 44. 646.
MELNGAILIS, J., MARADUDIN, A.A. and SEEGER, A. (1963)	Phys. Rev. 131. 1972.
PAPADAKIS, E.P. (1963)	Journ. Acoust. Soc. Am. 35. 490.
PETERS, R.D. and BREAZEALE, M.A. (1968)	Appl. Phys. Lett. 12. 106.
REDWOOD, M. (1964)	Ultrasonics Oct.-Dec. 174
STANFORD, A.L. and ZEHNER, S.P. (1967)	Phys. Rev. 153. 1025.
SUZUKI, T., HIKATA, A., and ELBAUM, C. (1964)	Journ. Appl. Phys. 35. 2761.
THMPSON, D.O., TENNISON, M.A. and BUCK, O. (1968)	Journ. Acoust. Soc. Am. 44. 435.
THURSTON, R.N. and SHAPIRO, M.J. (1967)	Journ. Acoust. Soc. Am. 41. 1112.
TRUELL, R. and OATES, W. (1963)	Journ. Acoust. Soc. Am. 35. 1382.
VAN BUREN, A.L. and BREAZEALE, M.A. (1968)	Journ. Acoust. Soc. Am. 44. 1014.
WILLIAMS, E. (1963)	Electric Filter Circuits. (PITMAN).